# Geology of the Southwestern San Mateo Mountains, Socorro County, New Mexico



by

Michael L. Hermann

Submitted in Partial Fulfillment
of the Requirements for the Degree of
Master of Science in Geology

New Mexico Institute of Mining and Technology
Socorro, New Mexico

October 1986

## TABLE OF CONTENTS

## PLATES



## TABLES



## FIGURES

## APPENDICES

Abstract

Approximately 39 square miles of the Nogal Canyon Caldera, southern San Mateo Mountains, Socorro County, New Mexico were mapped at a scale of 1:24000. Thick accumulations of Vicks Peak Tuff ( > 4000 feet) were partially delineated in a deep part of the cauldron, northwest of Rock Springs Canyon. Moderate accumulations (up to 2000 feet) occur to the east near Casa Grande. Cauldron-collapse breccias occur within the thick section of Vicks Peak Tuff northwest of Rock Spring. This confirms the Nogal Canyon Caldera as the eruption site for the Vicks Peak Tuff.

Detailed geologic mapping and lithologic studies of pre Vicks Peak Tuff units (Rock Spring and Red Rock Ranch Formations) suggest several periods of volcanic activity in the southern San Mateo Mountains during the Oligocene.

Geochemical sampling, in conjunction with mapping, has possibly linked intrusive activity with alteration and mineralization in the study area. Digital enhancement of Landsat data was done to detect limonitic areas. Paleomagnetic data from other studies aided in correlating ash-flow tuffs in the study area with tuffs exposed in the Mogollon-Datil Volcanic Field.

## BACKGROUND AND INTRODUCTION TO THESIS PROBLEM

The San Mateo Mountains of southern Socorro County, New Mexico are a north-south trending, fault-block range, consisting almost entirely of Oligocene lavas, ignimbrites, and intrusive rocks. These rocks range in composition from rhyolitic to basaltic. Minor alluvial and lacustrine sediments are interbedded with the various volcanic flows. Exposures of Paleozoic rocks have also been described by Farkas (1969) in the extreme southern portion of the range, and Atwood (1982) has described outcrops of Precambrian granitic rock in the central San Mateo Mountains.

Slopes surrounding the range consist of alluvial piedmont deposits (volcaniclastic) and low relief pedimented bedrock surfaces. Steep cliffs in the southern part of the range (near Vicks Peak) are predominantly Vicks Peak rhyolite, a thick welded ignimbrite.

In addition to the geologic study done by Lasky (1932), in the vicinity of the San Mateo Mountains, studies by Furlow (1965), Farkas (1969), Deal (1973), Maldonado (1974), Atwood (1982) and Foruria (1984) have been reported. Areas covered by earlier geologic studies are shown in Figure 1, which also shows the mapping scale, and purpose of investigation. The study area is also shown. Accessibility to the field area is by Cibola National Forest roads 225 and 377 via U.S. Highway 85 (Figure 2).

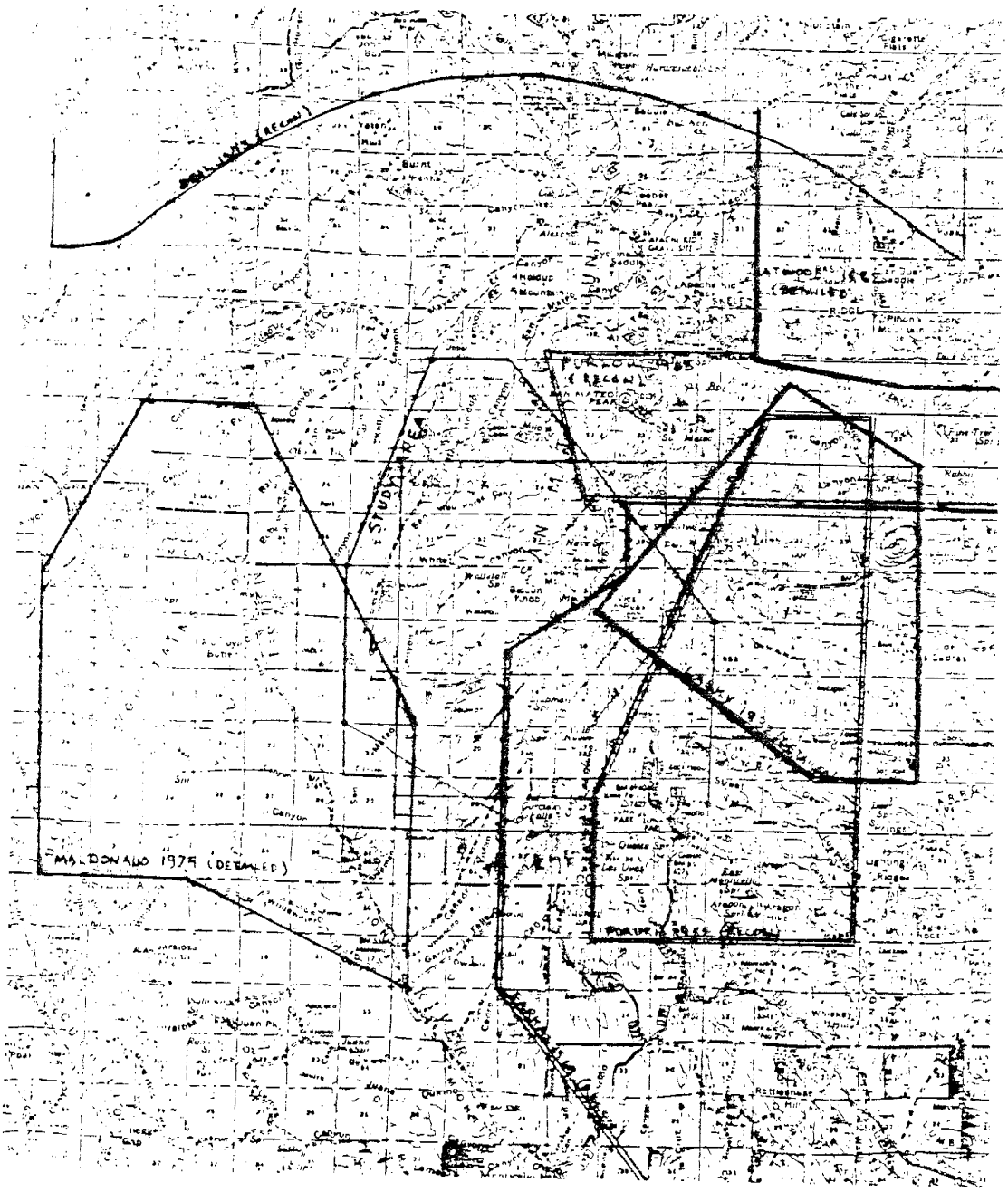


Figure 1. Locations of previous geological studies in the vicinity of the San Mateo Mountains.

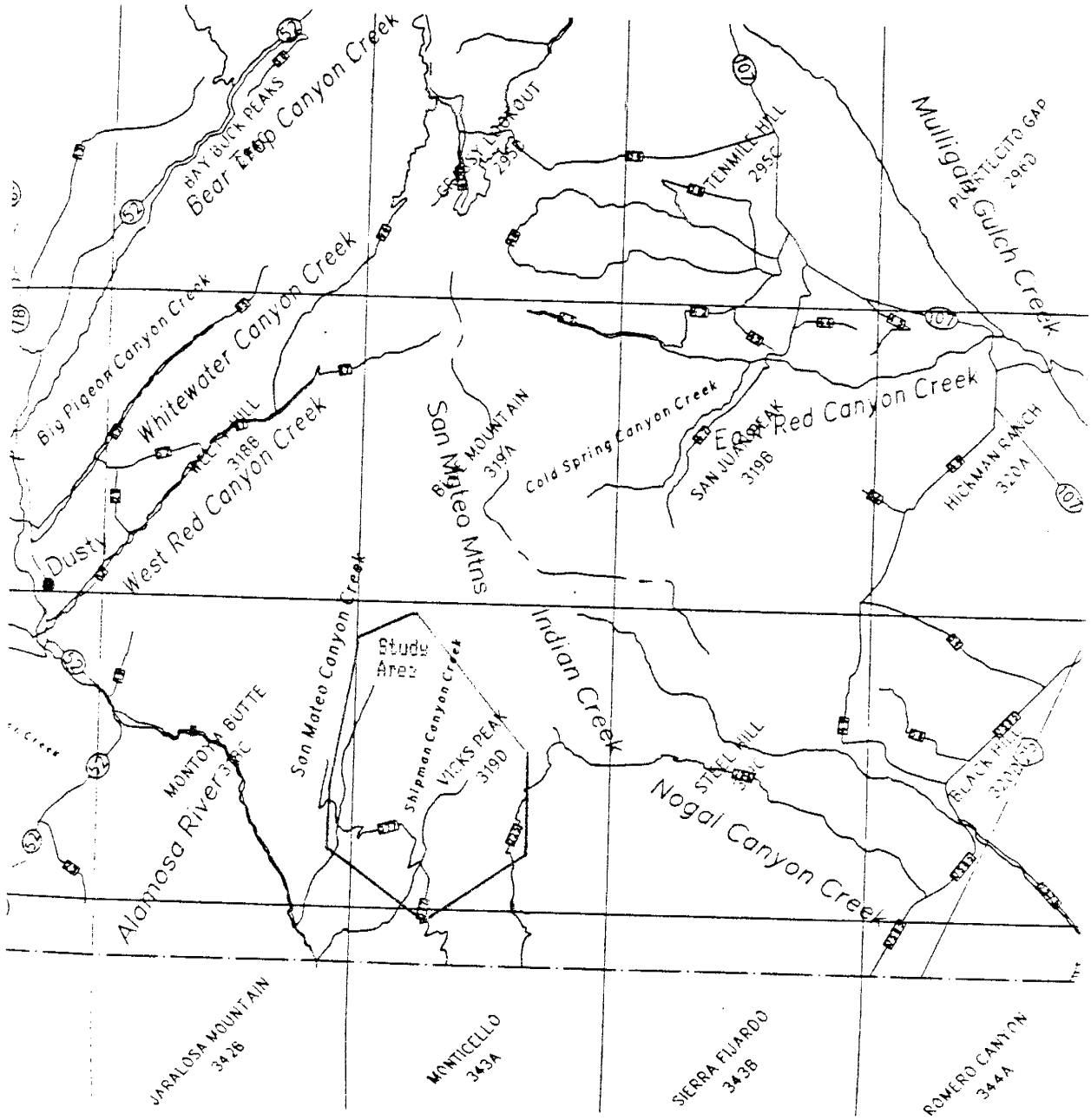


Figure 2. Major roads in the vicinity of the southern San Mateo Mountains. U.S.G.S 7.5' quadrangle boundaries are also shown (courtesy Larry Spear and the Office of Government Research).

Earlier geologic studies (especially Farkas, 1969) have delineated a complex stratigraphic sequence and tectonic history for the southern San Mateo Mountains. Initial reconnaissance of the southern San Mateo Mountains indicated that the stratigraphy of Farkas (1969) and Foruria (1984) was generalized and further subdivision of their volcanic units was possible, and necessary to understand the complex volcanic and structural history of the area. Stratigraphic nomenclature used by earlier workers is presented in Table 1.

Earlier workers (Farkas 1969 and Furlow 1965) were not able to locate or identify volcanic source vents for most of their units. Deal and Rhodes (1976) reinterpreted findings from earlier studies and proposed the southern San Mateo Mountains to be the source cauldron (Nogal Canyon Cauldron, see Figure 3) for the Vicks Peak Rhyolite.

Source areas for voluminous ignimbrite eruptions are commonly roughly circular volcano-tectonic depressions (calderas) tens of kilometers in diameter and hundreds to thousands of meters deep. They are often characterized by thick accumulations of ignimbrite (ash-flows) within the collapse depression with thinner wedge like outflow sheets of ignimbrite surrounding the caldera. The thick deposits of ignimbrite within some calderas are thought to accumulate during the simultaneous eruption and collapse of the area above the source magma chamber during eruption.

| Maldonado (1974) | Farkas (1969) | This Study | Atwood (1976) | Ferguson (1986) |
|---|---|---|---|---|
| tuff of Shipman canyon | Datil Group | post Rock Spring Formation rocks | peralkalic rhyolite of San Juan Peak | tuff of Turkey Springs |
| rhyolite of Alamosa Creek | Indian Creek rhyolite | upper volcaniclastic unit (Tv2) | Beartrap Canyon formation | unit of East Red Canyon |
| latite of Grapevine Canyon | Vicks Peak rhyolite | tuff of Turkey Springs (Tts) | upper tuff member | bedded ash-flow tuffs |
| Whitewater Canyon latite | Rock Spring Formation | lower volcaniclastic unit (Tvl) | upper rhyolite member | rhyolite lavas |
| Vicks Peak rhyolite | volcanic agglomerate | air-fall tuff (Taf) | pyroclastic member | South Canyon Tuff |
| Montoya Butte andesite-latite | upper andesite flows | Alamosa Creek rhyolite (Tac) | lower rhyolite member | Lemitar Tuff |
| | upper latite tuff | Vicks Peak Tuff (Tvp) | lower tuff member | rhyolite lavas |
| | variegated breccia | Rock Spring Formation | Potato Canyon rhyolite tuff | bedded ash-flow tuffs |
| | upper Luna Park tuff | La Jencia Tuff (Tlj) | Springtime Canyon quartz latite | Vicks Peak Tuff |
| | lower latite flows | zeolitic andesite member (Tz) | Vicks Peak rhyolite Tuff | La Jencia Tuff |
| | lower Luna Park tuff | volcaniclastic member (Tvc2) | rhyolite tuff of Pinon Mountain | basaltic andesite |
| | lower volcanic group | upper andesite member (Tua) | latite of Dick Springs | |
| | Red Rock Ranch Formation | Priest Mine andesite member (Tpa) | rhyolite of The Gorge | |
| | Seferino Hill conglomerate | pyroxene andesite member (Tpa) | latite of East Red Canyon | |
| | Red Rock Arroyo andesite | Hells Mesa Tuff (Tha) | flow and dome member | |
| | Luna Peak andesite | andesite flow member (Ta) | tuff member | |
| | Uvas Canyon pyroxene andesite | Shipman Spring tuff (Tss) | Hells Mesa Tuff | |
| | Placitas Canyon lake beds | Hump Mountain member (Thm) | Spears Formation | |
| | Jose Maria andesite | Luna andesite member (Tla) | upper tuff member | |
| | Whiskey Hill hornblende andesite | Shipman Canyon andesite member (Tsca) | andesite member | |
| | Paleozoic rocks | Luna Park latite (Tlp) | lower tuff member | |
| | | lower andesite member (Tla) | andesite dike member | |
| | | lower Luna Park tuff (Tllpt) | Precambrian granite | |
| | | Red Rock Ranch Formation | | |
| | | Luna Peak andesite member (Tlp) | | |
| | | upper andesite member (Ta) | | |
| | | Garcia Falls andesite member (Tgf) | | |
| | | shale member (Ts) | | |
| | | volcaniclastic member (Tvcl) | | |

Table 1. Stratigraphic nomenclature used in the vicinity of the San Mateo Mountains.


Figure 3. Locality relief map of the San Mateo Mountains showing approximate outlines of two ash-flow cauldrons 1 = Mt. Withington cauldron; 2 = Nogal Canyon cauldron; A = Vicks Peak; B = San Mateo Peak; C = San Juan Peak; D = A-L Peak; E = Potato Canyon; F = Ranch Supply Canyon and Point of Rocks Canyon; G = Beartrap Canyon.

Source: Deal and Rhodes (1976).

The source vent for the ignimbrite is usually assumed to be within the collapsed region and may be obscured by structural effects related to caldera collapse or buried by later volcanic flows. Some data useful in locating a caldera and unraveling the geologic history of a resurgent caldera cycle are presented in Table 2.

Data used by Deal and Rhodes (1976) to define the boundary of the of the proposed Nogal Canyon caldera consist of: (1) The presence of several porphyritic igneous stocks exposed in an arcuate pattern around the southern San Mateo Mountains. (2) The presence of a relatively thick section of the Vicks Peak rhyolite (>500 meters) within the proposed caldera, while typical outflow thicknesses are nearer to 100 meters (Osburn and Chapin, 1983). And (3) The reported thick sections of Vicks Peak rhyolite and younger intermediate lavas in the northern and northwestern portions of Deal and Rhodes' (1976) proposed caldera (Furlow 1965).

The above data indicate the possible existence of a caldera in the area but do not prove its presence. Examination of the volcano-stratigraphic and structural features of the area was necessary to link the eruption of the Vicks Peak tuff with concurrent collapse of a caldera.

The main reasons for studying the area and goals for this study are as follows: (1) The volcanic rockstratigraphy is insufficiently described to allow a detailed

. GEOLOGIC EVENTS OF THE RESURGENT-CAULDRON CYCLE

| Stage | Structural Events | Volcanic Events | Sedimentary Events | Plutonic Events | Duration in the Valles Caldera |
|---|---|---|---|---|---|
| I | Regional tumescence and propagation of ring and radial fractures with possible apical graben subsidence | Eruptions due to leakage along radial or ring fractures | Erosion of the volcanic highland. | Compositional zonation in magma chambers. Increasing magma pressure. Minor intrusion. | < 4 × 10⁵ yrs |
| II | — | Major ash-flow eruption, 50-500 mi³. | — | Degassing and skimming of zoned top of chamber | < 10 yrs. (est) |
| III | Caldera collapse | Overlap with stage II in some calderas | Avalanches and slides from caldera walls. | Disequilibrium | < 10 yrs. (est) |
| IV | — | Minor pyroclastic eruptions and lavas on caldera floor in some calderas. | Caldera fill: talus, avalanches, slides, fans, lake deposits | Consolidation of magma caught in ring fractures (residual ring dikes). Progressive recovery of equilibrium. Beginning of minor ring intrusion | < 10⁵ yrs |
| V | Resurgent doming | Possible ring-fracture volcanism and/or eruption or intrusion in dome fractures | Caldera fill continues. (Lake overflows and caldera is breached | Rise of central pluton and perhaps a ring-intrusion stage | |
| VI | Possible regional tumescence and reopening of ring fractures | Ring-fracture volcanism. Possible stage II eruption of next cycle | Caldera fill continues: late lake sediment. Erosion of fill. Fill > erosion | Final emplacement and differentiation of ring intrusions. Possible stoping by central pluton | 8 × 10⁵ yrs ± 10⁵ yrs |
| VII | — | Terminal fumarolic and hot spring activity (hydrothermal alteration) | Erosion. Erosion > fill. | Crystallization of major plutons. Possibly a major ore-forming stage | > 10⁵ yrs |

Characteristics of Ash Flows
and related deposits relative to vent proximity

| | |
|---|---|
| Overall geometry of ash flow sheet | Thickness generally increases toward source area. |
| Pre-ignimbrite surge and air fall deposits | Usually localized or thicker near vent. |
| Co-ignimbrite lag fall deposits | Present only near vent. |
| Cauldron collapse breccias | Usually within or near cauldron margin. |
| Densely welded zone | Typically thickens toward source area. |
| Partially welded zone | Lower zone may thin near vent. |
| Zone of no welding | Basal zone may be missing near source for thick ash-flows deposited at high temp. |
| Zone of devitrification | Often thicker near vent. |

Table 2. Adapted from Smith (1960b), Smith and Bailey (1968), and Walker (1985)

interpretation of the volcanic and tectonic history or the area. (2) The area contains larger regions of hydrothermally altered rock and the mineral resource potential of the area needs further study. And (3) the presence of the Nogal Canyon caldera has been suggested (Deal and Rhodes 1976) but needs more study before a caldera can be adequately defined in this area.

# METHODS OF STUDY

Initial interpretation of geomorphological, topographical and physiographic features of the area was accomplished through inspection of Landsat false color MSS images, natural color, color infrared, and black and white aerial photography. Mapping was done at 1:24000 scale using U.S.G.S topographic 7.5 minute quadrangles as base maps. Extensive talus deposits were partially delineated using 1:15840 scale aerial photographs. Aerial photography was also useful in interpretation of structurally complex areas after geological mapping was partially complete.

Correlation of various rock stratigraphic units was done using standard geological mapping techniques as well as interpretation of earlier reconnaissance mapping and lithologic descriptions. Whenever possible nomenclature introduced or used by earlier workers was adapted and applied, particularly for extensively exposed units (regional ash-flow tuffs etc.).

Many of the currently mapped contacts coincide roughly with those delineated in earlier studies (specifically Farkas' detailed map of the Rock Spring area and some of Foruria's contacts). However, interpretation of various stratigraphic and genetic aspects of some units in the study area differs from those proposed in earlier investigations.

Units used by earlier workers were subdivided into thinner lithologic units. This was done to get a general view of the changes in thickness, sequence of deposition, order of emplacement of intrusives, and other geological aspects. Laterally continuous ash-flow tuffs (and possibly shale horizons) provide time lines and relative age relationships between the various volcanic rocks.

Thin sections were prepared to illustrate petrologic features of the distinctive units within the study area and to aid in correlations and genetic interpretations. Paleomagnetic data (courtesy of Bill McIntosh) aided in tentative correlations of various ash-flow tuffs with those exposed in surrounding areas of the Mogollon-Datil Volcanic Field.

Altered and mineralized areas were evaluated by assaying sediments from mineralized regions. Atomic absorption and plasma emission spectrometry were used to assay samples (courtesy John Husler of Albuquerque Geochemical, and Curtis Verpleogh of Academy Corporation).

## RED ROCK RANCH FORMATION

The Red Rock Ranch Formation was introduced by Farkas (1969) for the lowest Oligocene rock-stratigraphic units exposed within the Southern San Mateo Mountains. Farkas (1969) has defined the Red Rock Ranch Formation as the Tertiary volcanic and related rocks above Paleozoic rocks and beneath the Rock Spring Formation (or below the lower Luna Park tuff). Rocks lying stratigraphically below the lower Luna Park tuff were considered Red Rock Ranch Formation rocks in this study. This also roughly coincides with the upper and lower Spears Formation division of Foruria (1985). This division generally separates lower andesite lavas from an overlying section of silicic ash-flow tuffs and intermediate to mafic lavas. A diagrammatic representation of the stratigraphy of the Red Rock Ranch Formation is presented in Figure 4.

The Red Rock Ranch Formation consists of intercalated, layered, and interfingering lavas and volcaniclastic rocks. Porphyritic, megacrystic, aphanitic, vesicular and amygdaloidal lava flows and flow breccias range in composition from latitic to basaltic andesitic. Various sedimentary and volcaniclastic horizons are found in the lower exposures of the Formation within the study area.

Intrusive bodies are encountered throughout the Formation. These rocks range from porphyritic andesites

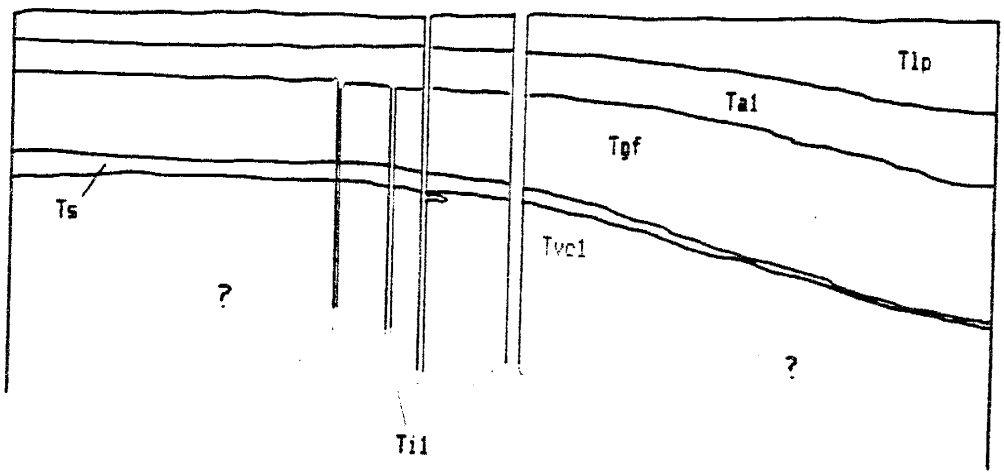


Figure 4. Diagrammatic stratigraphy of the Red Rock Ranch Formation. Only generalized vertical and lateral relationships are implied. Refer to Table 1 for symbols used.

and latite dike rocks to felsic (rhyolitic) dikes. Propylitization is widespread throughout the Red Rock Ranch Formation-rocks and is characterized by an assemblage of chlorite, epidote, and calcite. Minor zones of silicification and pyritization occur around some intrusive bodies.

Horizons of organic, pyritic, and calcareous shales and siltstones found near the lower stratigraphic levels seem to be characteristic of only the Red Rock Ranch Formation deposits. Within the study area, shaly units are interbedded with and overlie conglomerates, fine-grained volcaniclastic sediments, lithic-rich tuffs, and porphyritic andesite flows and flow-breccias.

The lowest stratigraphic portions of the Formation in this study area are exposed south of the intersection of the Rock Spring and Deep Canyon faults in the southwest part of the study area. The total thickness of the Red Rock Ranch Formation was not measured since only the uppermost rocks are exposed within the study area. Farkas estimates the thickness to be at least 1500 feet and possibly greater than 3000 feet in the southern part of the San Mateo Mountains.

Volcanic rocks (andesite-latite of Montoya Butte), which may correlate with the Red Rock Ranch Formation, overlying Cretaceous or Pennsylvanian sedimentary rocks have been described west of the study area in the Sierra Cuchillo (Maldonado 1974). Red Rock Ranch Formation rocks

overly Permian Abo Formation rocks or Pennsylvanian Magdalena Group limestones in the southern and southeastern part of the San Mateo Mountains about 4 miles south of the study area (Farkas 1969).

**Volcaniclastic Member.** The volcaniclastic member is exposed over a small area in the southwest part of the study area in the eastern part of sections 21 and 22, T9S, R6W, N.M.P.M. The member as defined underlies the shale member and consists of interbedded volcaniclastic rocks, tuffs, conglomerates, sandstones, and lithic rich, and altered ash-flow tuffs. Minor felsic to mafic lava flows and breccias are found locally in the member. Dark green aphanitic intrusive bodies similar to those described within the Garcia Falls member and lower portions of the Rock Spring Formation are found locally within the member.

Only the uppermost part of the volcaniclastic member is exposed within the study area. No exposures were examined outside of the study area so the total thickness of the member is unknown.

To the south and southeast of the study area, the Placitas Canyon laminated lake beds (which may be equivalent to the shale member) are interbedded with altered andesites (Farkas 1969). The existence of other shale units lower in the section is possible but evidence for them could not be found due to poor exposures of the

lower parts of the Red Rock Ranch Formation within the study area. Farkas also suggests complex vertical and horizontal relationships between the lower Tertiary sedimentary and volcanic rocks in the southern part of his map area.

Two thin sections were prepared from altered volcaniclastic rocks from the member, one from the eastern part of section 21 (Figure 5-A) the other from the eastern part of section 22 (Figure 5-B). Samples were taken near the contact with the overlying shales (stratigraphically high in the member).

**Shale Member.** The name shale member of the Red Rock Ranch Formation is used for a distinctive sequence of variegated, thinly bedded, fissile, pyritic and calcareous organic shales, and siltstones. These rocks lie beneath the Garcia Falls andesite and above the volcaniclastic member of the Red Rock Ranch Formation.

The member is exposed over a relatively small area in the southwest, and bordering areas of section 22 T9S, R6W, N.M.P.M.; it attains a maximum thickness of 150 ft in the western exposures of the member near Deep Canyon and thins gradually to the northwest to a thickness of about 10 ft in Cañon de Quirino. The member is overlain by the Garcia Falls andesite east of Cañon de Quirino within the study area. Laterally discontinuous lenses of the shale occur

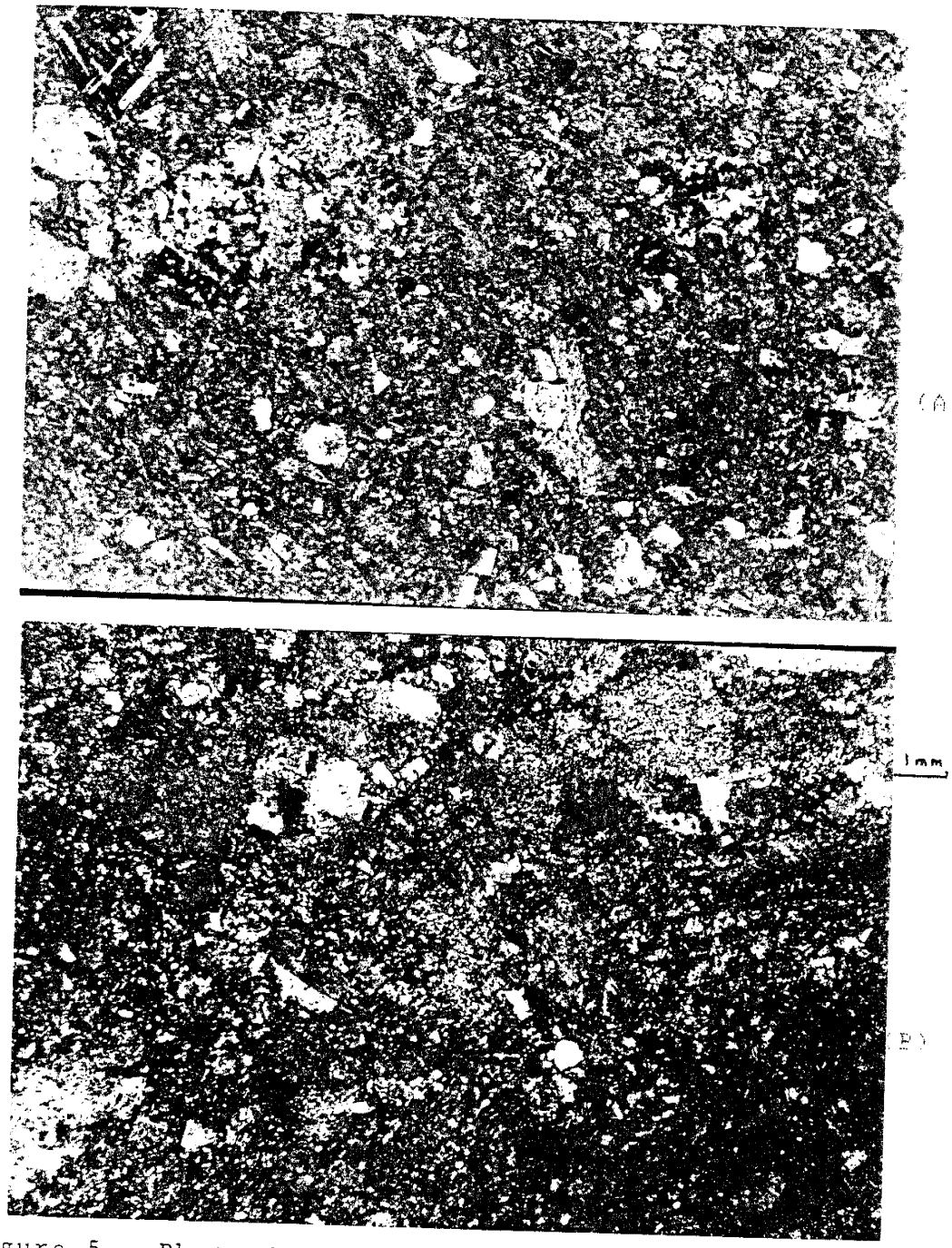


Figure 5. Photomicrographs of the volcaniclastic member of the Red Rock Ranch Formation (crossed polars). Altered feldspars and lithic fragments in an altered devitrified? matrix.

interbedded with some of the overlying flows of the Garcia Falls member in the southwestern part of the study area. Shale zenoliths of various sizes are also common in the Garcia Falls member.

Western exposures of the member generally exhibit laterally continuous planar bedding (Figure 6), but some exposures in Cañon de Quirino (about 1 mi to the east where the member is thinner) show contortion and folding of the layering within the shaly laminated horizons. Soft sediment deformation is evident in thin discontinuous shale beds between flow units of the overlying Garcia Falls - andesite and the underlying volcaniclastic rocks of the Red Rock Ranch Formation. The presence of overturned folds in the shale and contorted layering in zenoliths in the overlying andesites indicate that the sediments were plastic or poorly consolidated when the overlying lavas were deposited.

The geometry of the folds within the shaly units in the eastern part of the study area may be indicative of direction of tilting during tectonic activity or stress field orientation. The noses of the folds generally point in southeasterly direction, roughly down-dip. Alternately, the folds may be related to the stress transmitted to partially consolidated sediments while the lava flows of the Garcia Falls andesite flowed over and into a lake or its previously deposited sediments.

Figure 6. Planar, bedded, shale member outcrops, looking northwest in the SW/4 of the SW/4 of section 22, T9S, R6W, N.M.P.M.

The shale member (and possibly part of the underlying lower Red Rock Ranch deposits) may closely correlate in both space and time with the Placitas Canyon laminated lake beds described by Farkas (1969).

**Garcia Falls Andesite Member.** The informal name Garcia Falls andesite member of the Red Rock Ranch Formation is proposed for a series of porphyritic, vesicular, amygdaloidal andesite and latite lava flows, agglomerates, and flow-breccias exposed in the southern part of the study area. In the southwest part of the study area, the member overlies the shale member and is under the Luna Peak andesite. In the southeast, the member is under the upper andesite member of the Red Rock Ranch Formation.

The member is intruded by andesite dikes and sills some of similar textures and mineralogies to the various flows of the Garcia Falls member, and smaller fine-grained sparsely porphyritic dikes and sills of rhyolitic composition. Some dike rocks are indistinguishable from various flows. Some dikes pinch out downward in outcrops indicating lateral or downward movement through fissures or fractures during intrusion.

Exposures of the Garcia Falls andesite member are distinguished from other lavas of the Red Rock Ranch Formation by stratigraphic position as well as a variety of lithologic characteristics. Vesicular flows in the upper

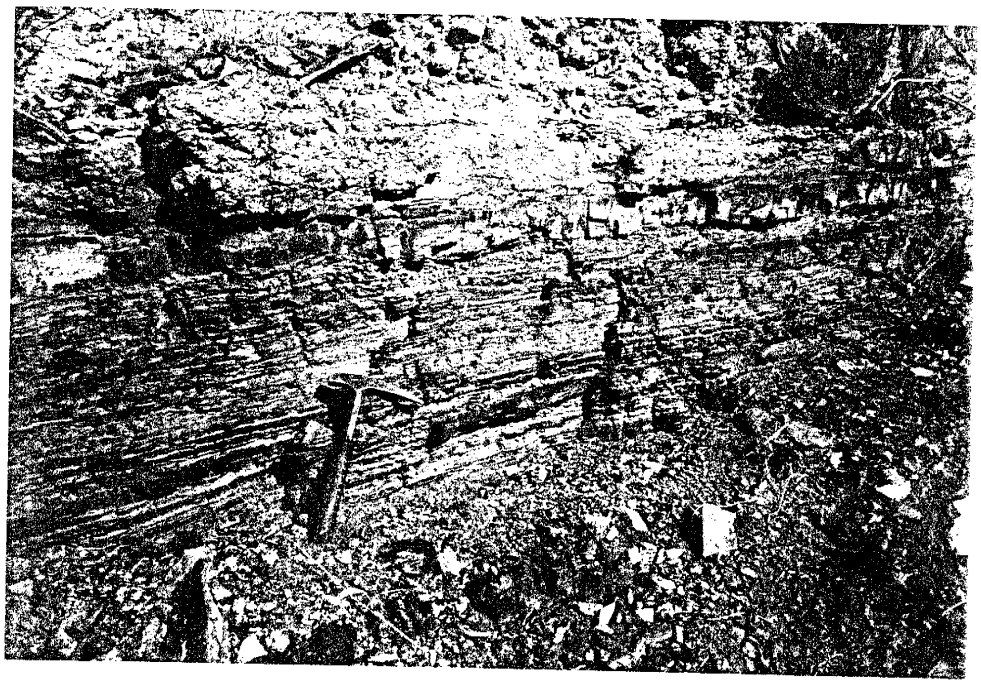

Figure 7. Palagonitized Garcia Falls andesite member flows above the shale member, looking east in the S/2 of the SE/4 of section 22, T9S, R6W, N.M.P.M.

parts of the member, flow-breccias in the middle and lower flows, and irregular dips of bedding and foliations are found within the member. Noticeable paleovalleys and undulatory and interfingering contacts between flows, the presence of cuspate shale fragments, rounded to subangular fragments of andesite, and massive gray limestone fragments in the lower parts of the member help distinguish the member from other members of the Red Rock Ranch Formation. Occasionally large lenticular lithic fragments of slightly deformed shale are encountered within lower parts of the member.

Along the trace of the Deep Canyon fault north of Garcia Falls pervasive propylitic alteration and weathering has obscured the primary textures of the member beyond recognition. Stratigraphic position above the shale member is evidence that the rocks are flows of the Garcia Falls member. Here a stockwork of calcite veins and intensely altered rock is encountered (Figure 8).

Some of the upper flows of the Garcia Falls andesite member may be indistinguishable from lower flows of the Luna Peak Andesite. The rocks are often similar in texture and mineralogy and stratigraphic relationships are not always apparent.

Hand specimens of flows are typically well indurated and are speckled gray, greenish, purple, or brown. Most flows are porphyritic rocks with phenocrysts of euhedral

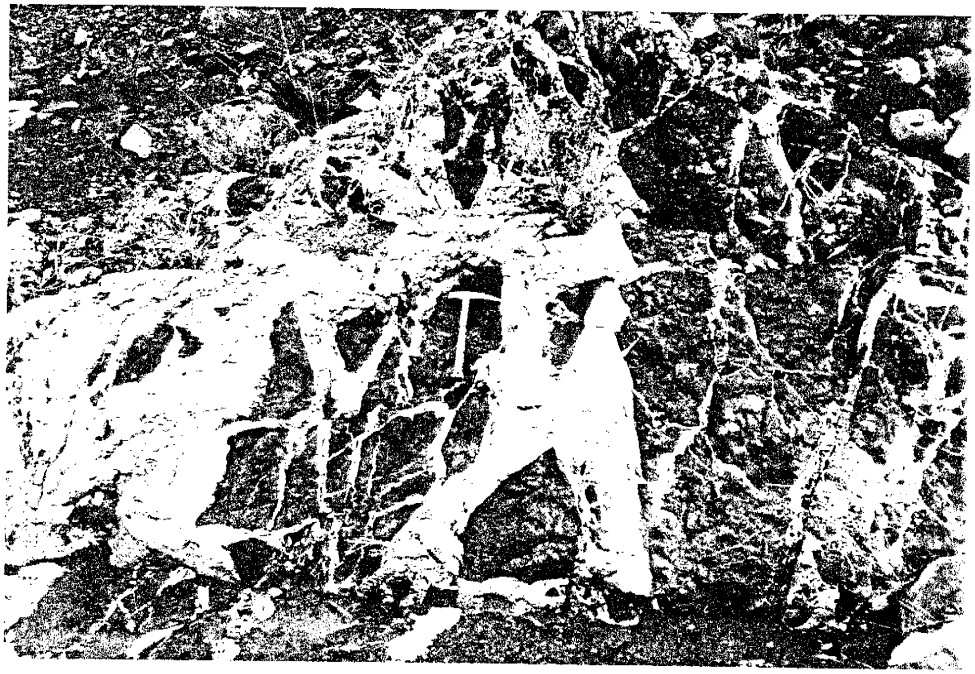

Figure 8. Altered outcrops of the Garcia Falls andesite member, cut by white calcite veins. Looking northwest in the NW/4 of section 28, T9S, R6W, N.M.P.M.

tabular plagioclase and subhedral pyroxene crystals in a dark fine-grained to aphanitic groundmass. Localized light brown and tan, fine-grained, vesicular flows are present in well exposed outcrops in Garcia Falls and Quirino Canyons.

A thin section from one of the less altered lavas is illustrated in Figure 9 showing the porphyritic (seriate) - nature of the rock. This sample is porphyritic with phenocrysts of plagioclase (oligoclase), and clinopyroxene in a felty groundmass of plagioclase, clinopyroxene, opaques, calcite, chlorite, serpentine, and interstitial cryptocrystalline and microspherulitic areas.

Plagioclase phenocrysts make up about 25% of the rock. The phenocrysts are partially epidotized euhedral to anhedral Carlsbad, albite and complexly twinned laths and blocks up to 5 mm long, dusted with opaque inclusions. Clinopyroxene (augite) phenocrysts make up about 15% of the rock as colorless to light yellow (non-pleochroic) euhedral to subhedral simple and lamellar twinned equant crystals up to 2.5 mm in size. Some exhibit cumulophyric relationships with plagioclase, opaques and other pyroxene crystals; many display oscillatory zoning or overgrowth textures, resorption textures and partial alteration to chlorite or serpentine.

Groundmass plagioclase makes up about 30% of the rock as fragmental subhedral and anhedral laths up to 1.5 mm long. They are usually similar to the phenocrysts.


Figure 9. Photomicrograph of a flow of the Garcia Falls andesite member (crossed polars).

Groundmass pyroxene makes up about 10% of the rock as lath-like crystals and broken crystals. They are also similar to the phenocrysts. Groundmass opaques make up about 10% of the rock as blocky euhedral and anhedral skeletal crystals up to 0.5 mm in diameter. The remainder of the groundmass consists of patches and interstitial regions of calcite, chlorite, and microspherulitic material.

**Upper Andesite Member.** The upper andesite member is exposed on the west flank of Luna Peak on the east side of Cañon de Quirino in the western portions of section 26, T9S, R6W. Outcrops of the member are generally slope forming and consist of alternating steps of angular and rounded layers of flaggy and massive flow-units (Figure 10). The member consists of light-gray to brownish-gray and black microcrystalline, aphanitic and porphyritic andesitic lavas. The flows are restricted apparently to the southern parts of the study area. Chlorite filled vesicles and epidote and calcite mineralization is evident along joint surfaces in many outcrops.

The thickness of the member is about 200 feet in the northern exposures and thickens to over 500 feet southward. Both rubbly and sharp lower contacts with the underlying Garcia Falls andesites are encountered.

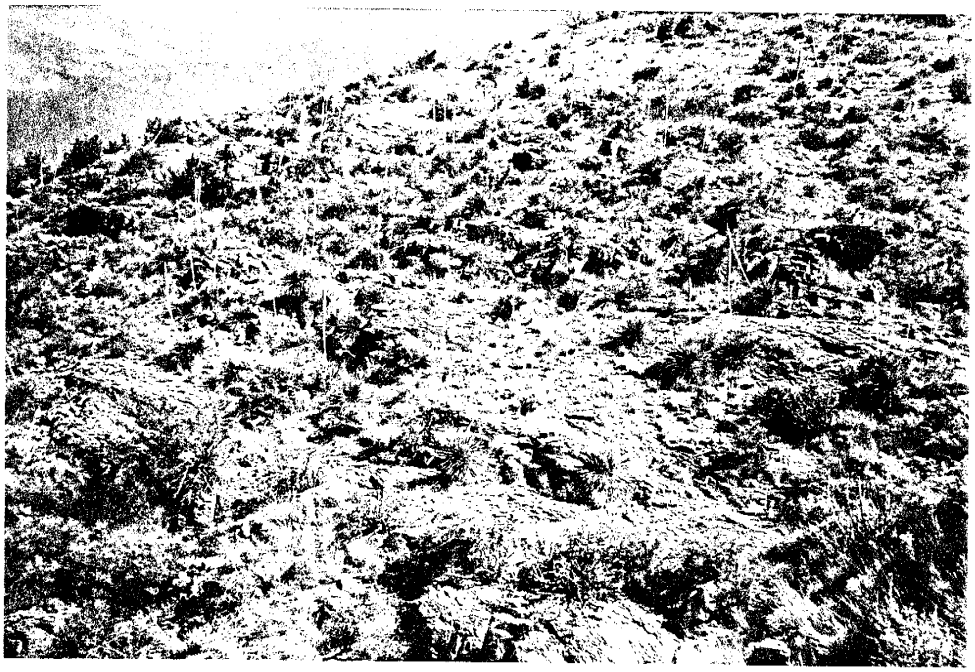

Figure 10. Outcrops of the upper andesite member. Looking northeast in the NW/4 of section 26, T9S, R6W, N.M.P.M.

**Luna Peak Andesite Member.** The Luna Peak andesite member of the Red Rock Ranch Formation consists of several coarsely porphyritic lava flows. The large euhedral phenocrysts of plagioclase in the uppermost layers (Figure 11) make this rock easily recognizable in the field. The Luna Peak andesite is exposed over an area of about 3/4 square mile west of Luna Park.

At Luna Peak the member reaches a thickness (top eroded?) of 300 feet (90 m) and overlies the upper andesite member of the Red Rock Ranch Formation. The Luna Peak andesite thins to about 120 feet (36 m) to the north where it is overlain by the lower Luna Park tuff.

The member is stratigraphically equivalent to the Luna Peak andesite described by Farkas (1969) and roughly correlates with the upper part of Foruria's (1985) lower member of the Spears Formation, and part of Maldonado's (1974) andesite-latite of Montoya Butte. The rock is also lithologically similar to the dike member of the Spears Formation described by Atwood (1981). Extensive exposures of similar rocks beyond the boundary of the study area to the south and southeast have been described by Farkas (1969).

Outcrops vary in appearance from red-brown, purple, or gray, spotted, spheroidally weathered, massive cliffs and hummocky dip slopes in the upper flows to dark grey and black angular intensely jointed exposures in lower layers.

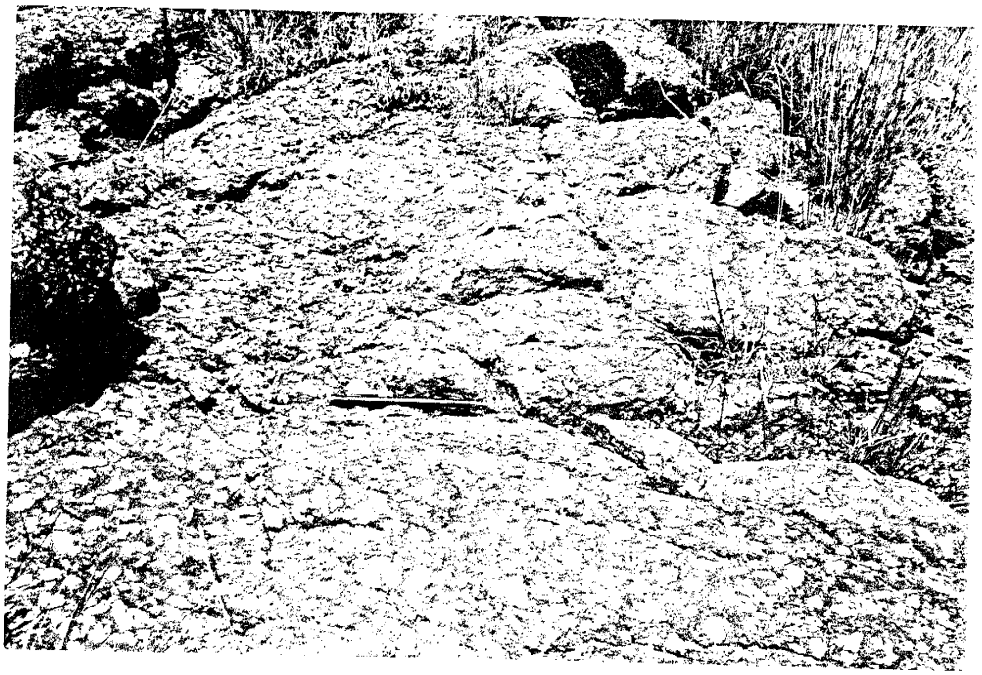

Figure 11. Outcrop of the Luna Peak andesite member. Looking east near Luna Peak in the central part of section 26, T9S, R6W, N.M.P.M.and northeast 1/4 of sec. 26, T9S, R6W.

A few angular lithic fragments of the underlying andesitic lavas up to 1 m in size are found locally near the base.

Varying degrees of propylitic alteration are encountered throughout the member. Intensity of alteration is usually greatest near faults and in laterally discontinuous vesicular horizons.

Upper flows are porphyritic with megacrysts of euhedral plagioclase, and sparse phenocrysts of magnetite in an aphanitic or glassy groundmass; lower flows are more holocrystalline with plagioclase and green pyroxene phenocrysts in a trachytoid groundmass of plagioclase and pyroxene.

Zones of preferentially oriented phenocrysts, layers of vesicles or amygdules, vertical changes in mineralogy and texture, and incorporation of clasts from previous flows indicate a multiple-flow origin for the member. The similarity of texture and mineralogy of the lower flows of the Luna Peak andesite to the upper flows of the Garcia Falls andesites suggest that these members may be a continuously evolving genetically related sequence. The presence of rubble zones and volcaniclastic sediments at the base, and aphanitic andesite lavas beneath the Luna Peak andesite indicate a period of time elapsed between the deposition of the two members. Farkas (1969) suggested possibly complex interfingering relationships between lavas of the Red Rock Ranch Formation outside of the study area.

No field evidence was found to locate the source(s) for these lavas within the study area.

In hand specimen, the upper parts of the member are dense, porphyritic, vesicular and amygdaloidal with abundant altered and zoned euhedral, tabular, rhombic, megacrysts of plagioclase up to 3 cm long; lesser amounts of smaller (0.5 to 10 mm long) subhedral and fragmental phenocrysts of altered feldspar (plagioclase), and sparse euhedral opaques (up to 0.5 mm). Phenocrysts occur in a dark brown to purple-brown aphanitic to glassy vesicular and amygdaloidal groundmass.

Plagioclase megacrysts make up as much as 40 percent of the rock and show a planar orientation parallel to flow. Irregular-elongate vesicles partially or completely filled with quartz, chalcedony, calcite, chrysocolla and chlorite are common locally.

In thin section upper flows (Figure 12) are porphyritic with abundant (40 %) tabular euhedral to subhedral megacrysts of plagioclase (An 20) up to 3 cm long, 3 percent altered blocky euhedral feldspar phenocrysts 0.25 to 0.5 cm in size, and one percent equant euhedral opaques up to 0.5 mm in size. Less than one percent milky anhedral quartz phenocrysts up to 0.5 mm long, and one percent green anhedral to subhedral glomerocrystic patches of clinopyroxene up to 1.5 mm in size are present. Phenocrysts occur in a purple-brown

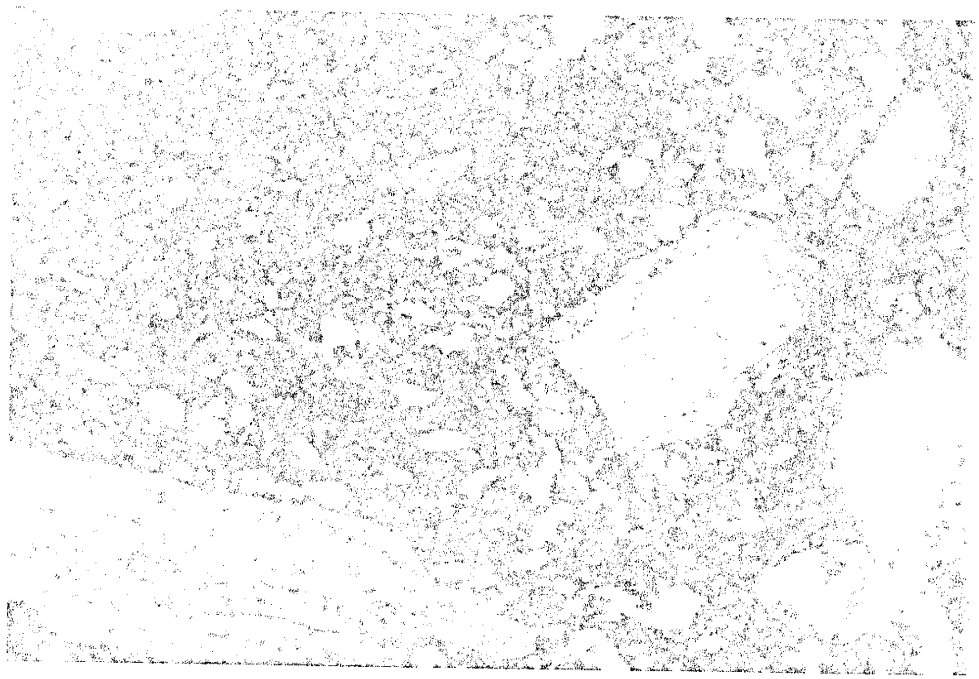


Figure 12. Photomicrograph of the Luna Peak andesite member (crossed polars).

microcrystalline to cryptocrystalline vesicular and amygdaloidal groundmass.

Plagioclase megacrysts exhibit Carlsbad and albite twinning, oscillatory zoning and partial replacement by calcite. Many of the megacrysts are rimmed by sausseritic alteration products and contain numerous tabular and dendritic opaque inclusions along cleavage planes.

The blocky feldspar phenocrysts are partially or completely altered to clays. If they were originally sanidine, the upper flows could have been latitic in composition.

Thin sections of middle flows show porphyritic texture with tabular Carlsbad and albite twinned phenocrysts and glomerocrysts of plagioclase up to 1 cm long, sparse euhedral magnetite up to 0.5 mm in size and sparse anhedral clinopyroxene phenocrysts.

The groundmass is pilotaxitic and hypohyaline, consisting of plagioclase microlites and dark glass. The groundmass is slightly amygdaloidal with vesicles filled with chlorite and unidentified clay minerals. Perlitic cracks in the groundmass are filled with serpentine or similar clay minerals.

# ROCK SPRING FORMATION

The name Rock Spring Formation was used by Farkas (1969) for a series of andesite and latite flows, flow-breccias and ash-flow tuffs exposed below the Vicks Peak Tuff and above the Red Rock Ranch Formation. In this study the rocks below the Vicks Peak Tuff and above the Luna Peak andesite member of the Red Rock Ranch Formation are considered Rock Spring Formation, roughly the same division used by Farkas. Some of Farkas' original names were retained. Figure 13 diagrammatically shows the stratigraphic relationships of the various Rock Spring Formation members used in this study.

The stratigraphically lowest exposures of the Formation are on the fault block between the Priest Mine fault and the Rock Spring fault in the south-central part of the study area. The best exposures of the Formation are southwest of Vicks Peak in the central part of the study area. In the rest of the map area the lower portions are concealed by fault contacts with older rocks or covered by alluvium, and the thickness of the Rock Spring Formation is unknown east or northeast of the Rock Spring fault.

The thickness of the upper part of the Formation northwest of the Rock Spring fault is estimated to be over 3000 feet (900 m). Only the upper few hundred feet of the Formation are exposed east of the Rock Spring fault within

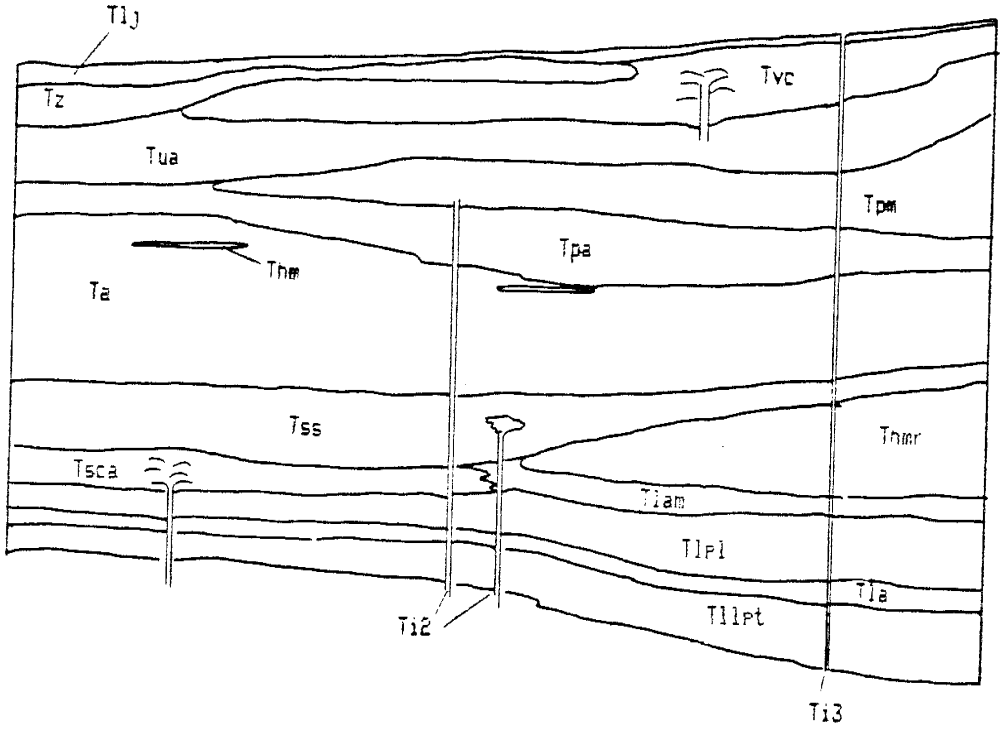


Figure 13. Diagrammatic section of the Rock Spring Formation. Only general vertical and lateral relationships are implied. Refer to Table 1 for symbols used.

the study area. Farkas (1969) reports the entire Rock Spring Formation to consist of only the upper and lower Luna Park tuffs near Peñasco Springs (eight miles southeast of Rock Spring).

The presence of dome structures, near-vent deposits and volcanic vents within the Rock Spring deposits indicate a close proximity to eruption sites for at least some of the deposits. Similarity of mineralogy of some of the intrusive bodies to some of the lavas is evidence for source areas of other members.

Intrusive bodies and vents for various members of the Rock Spring Formation occur along the Rock Spring fault. This combined with abrupt thickness changes for various strata across the fault is evidence for syn-volcanic related deformation along this structure. Proximity of Rock Spring Formation rocks to possible vent locations may explain the relatively steep dips of contacts and foliations encountered within flows exposed northwest of the Rock Spring fault.

Clasts of Red Rock Ranch Formation rocks within the basal Luna Park latite indicate possible uplift and/or erosion of regions southeast of the Rock Spring fault prior to the eruption of the Luna Park latite. Alternately, these clasts may be ejecta dragged up from the walls of a volcanic conduit.

**Lower Luna Park Tuff.** The lower Luna Park tuff is a moderately to densely welded, lithic- and crystal-rich, multiple-flow, single-cooling-unit, ash-flow tuff. The tuff is exposed over about 1/10 square mile within the study area in east-central part of section 22 and the northwest and southwest portions of section 23, T9S, R6W, N.M.P.M. The lower Luna Park tuff is possibly stratigraphically equivalent to the lower Luna Park tuff described by Farkas (1969), and correlates with the lower part of the upper Spears Formation of Foruria (1985). Extensive outcrops of this tuff and the upper Luna Park tuff (or possible equivalents) have been described south and southeast of the study area by Farkas (1969). The lower Luna Park tuff is the lowest rock-stratigraphic interval of the Rock Spring Formation; it lies above Luna Peak andesite of the Red Rock Ranch Formation, and is overlain by the lower andesite member of the Rock Spring Formation.

The tuff weathers to hummocky debris and colluvium covered slopes. Outcrops are typically light beige, blue-gray or light gray. Exposures are moderately to well-indurated, intensely jointed rounded knobs or slopes with resistant angular and subrounded dark lithic fragments protruding from the surface.

Within the study area the tuff is pervasively altered with areas of quartz-veinlet stockwork, bleaching, argill-

ization of feldspars and groundmass, epidotized joint surfaces, and disseminated pyrite. The relatively intense alteration of the upper portions of the tuff may be due to less intense welding and an originally high primary permeability compared to the lower part of the tuff. Propylitization of the abundant andesitic clasts within the tuff combined with bleaching of the matrix give the rock a green and white spotted appearance locally.

The basal contact of the lower Luna Park tuff with the underlying Luna Peak andesite is somewhat undulatory with up to 3 m of relief (Figure 14). The lower portions of the lower Luna Park tuff are locally extremely lithic-rich and contain angular rhyolite lithic fragments (up to 3 cm) and rounded to angular clasts of the underlying megacrystic Luna Peak andesite (up to 0.5 m in diameter) in a moderately indurated (welded?) crystal-rich matrix. A few discontinuous lenses of darker but texturally similar material are present locally near the base of the unit. Some of the lower flows may also be mud-flows or lahar deposits.

In thin section the rock is porphyritic and has phenocrysts of euhedral to subhedral laths of plagioclase (oligoclase) up to 3 mm long, anhedral and fragmental single crystals and complexly twinned potassium feldspar up to 1 mm in diameter, and euhedral to anhedral opaques up to 1 mm in diameter (replaced biotite?). Plagioclase and

Figure 14. Outcrop of the lower Luna Park tuff (upper right of photograph) overlying the Luna Peak andesite, showing undulatory contact. Looking northeast in the NE/4 of the SE/4 of section 22, T9S, R6W, N.M.P.M.

alkali feldspar phenocrysts make up 20% and 15% of the rock respectively.

Angular and subrounded epidotized lithic fragments up to 1 cm in diameter, devitrified flattened lenticular pumice fragments with relict tube structures 2.5 to 10 mm long, and lenticular gas cavities partially or completely filled with alkali feldspar (vapor-phase mineralization?) up to 1 cm long are scattered throughout the rock. The groundmass of the rock is partially to completely devitrified and consists of quartz-feldspar intergrowths, irregular patches of epidote and clays, and sparse areas of micro-spherulites and glass (Figure 15).

**Lower Andesite Member.** The lower andesite member consists of propylitized, amygdaloidal, aphanitic, fine-grained and porphyritic andesite flows. The flows separate the Luna Park latite and lower Luna Park tuff and are only exposed over a small area on the southwest flank of Hump Mountain. No thin sections were prepared from these rocks due to the intense alteration of most exposures and the relatively minor extent of the member.

**Luna Park Latite Member.** The Luna Park latite is a crystal-rich latite lava exposed in the northeast portion of section 21, the north-central part of section 22, the southwest portion of section 23, and the northeast portion

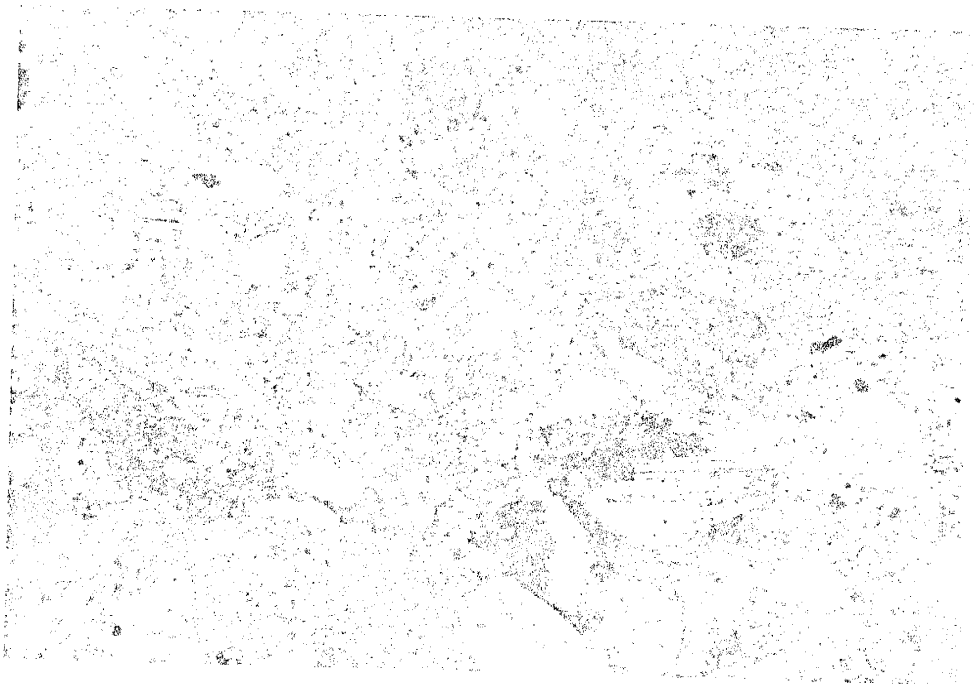

1 mm

Figure 15. Photomicrograph of the lower Luna Park tuff (crossed polars).

of section 26, T9S, R6W, N.M.P.M. Outcrops of the member within the study area are restricted to the area directly north of the Rock Spring fault and to the area between the Rock Spring fault and the Priest Mine fault. The member is typically 300 feet (100 m) thick, but thickens somewhat in the vicinity of the Rock Spring fault where it reaches a maximum thickness of 600 feet (190 m). Farkas (1969) has apparently included this lava in his upper Luna Park tuff of the Rock Spring Formation.

The Luna Park latite exhibits vertical zonation in phenocryst content, degree of induration and in styles and degrees of devitrification. The lower part of the member consists of thin-layered unwelded air-fall tuffs with bombs or cognate lithic fragments up to .5 m in diameter at the base (Figure 16). An overlying, indurated, spherulitic zone grades upward into a crudely layered flow-banded zone. Gas cavities increase in size upward and vapor phase mineralization becomes more evident. Devitrification and alteration obscure primary structures in outcrop and thin sections.

The basal portion of the member is slope forming, the middle portions form steep cliffs (crude columnar jointing) with numerous shallow caves (1 to 10m) giving outcrops a cavernous spheroidally weathered appearance. Weathered outcrops vary in color from white to brown and often have a granular flow-banded or layered appearance. Steeper

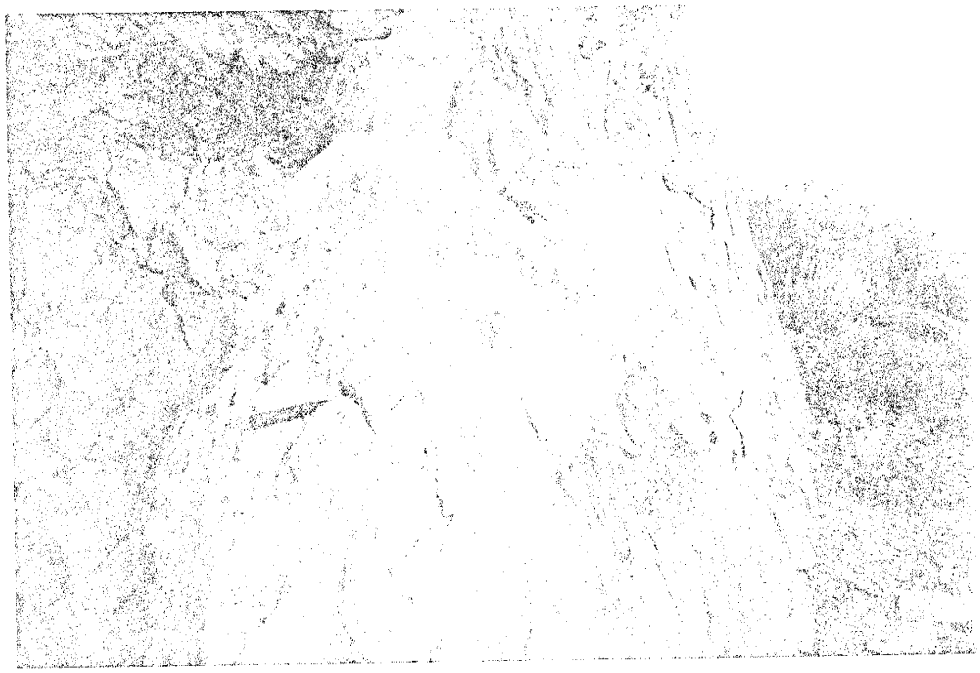

Figure 16. Basal part of the Luna Park latite. Looking east in the SW/4 of section 23, T9S, R6W, N.M.P.M.

foliations which resemble drag folding or prograding flows is evident near the fault boundary with older rocks near Luna Park (Figure 17).

Hand specimens are typically white to gray porphyritic rocks with phenocrysts of sanidine, plagioclase and biotite, and brown cognate lithic fragments (pumice?) in a light brown spherulitic (lower portions) to gray aphanitic (upper portions) groundmass. Upper zones are typically less indurated than the lower spherulitic zone, and contain numerous irregular gas cavities (1-3mm) filled with drusy quartz. Crystal content increases in the lower dense portions of the member.

Photomicrographs of thin sections from various levels are presented in Figures 18 A, B, and C, illustrating changes in phenocryst content, vapor phase mineralization and style of devitrification of the groundmass.

**Luna Andesite Member.** The Luna andesite member consists of vesicular and porphyritic lavas. The member lies above the Luna Park latite and below the Hump Mountain member of the Rock Spring Formation. Exposures of the andesite are confined to the southwestern part of section 23 and the extreme northeastern corner of section 26, T9S, R6W. The flows apparently pinch out westward in the vicinity of the Rock Spring fault.

Figure 17. Outcrops of the Luna Park latite, looking southeast from the west central part of section 23, T9S, R6W, N.M.P.M.

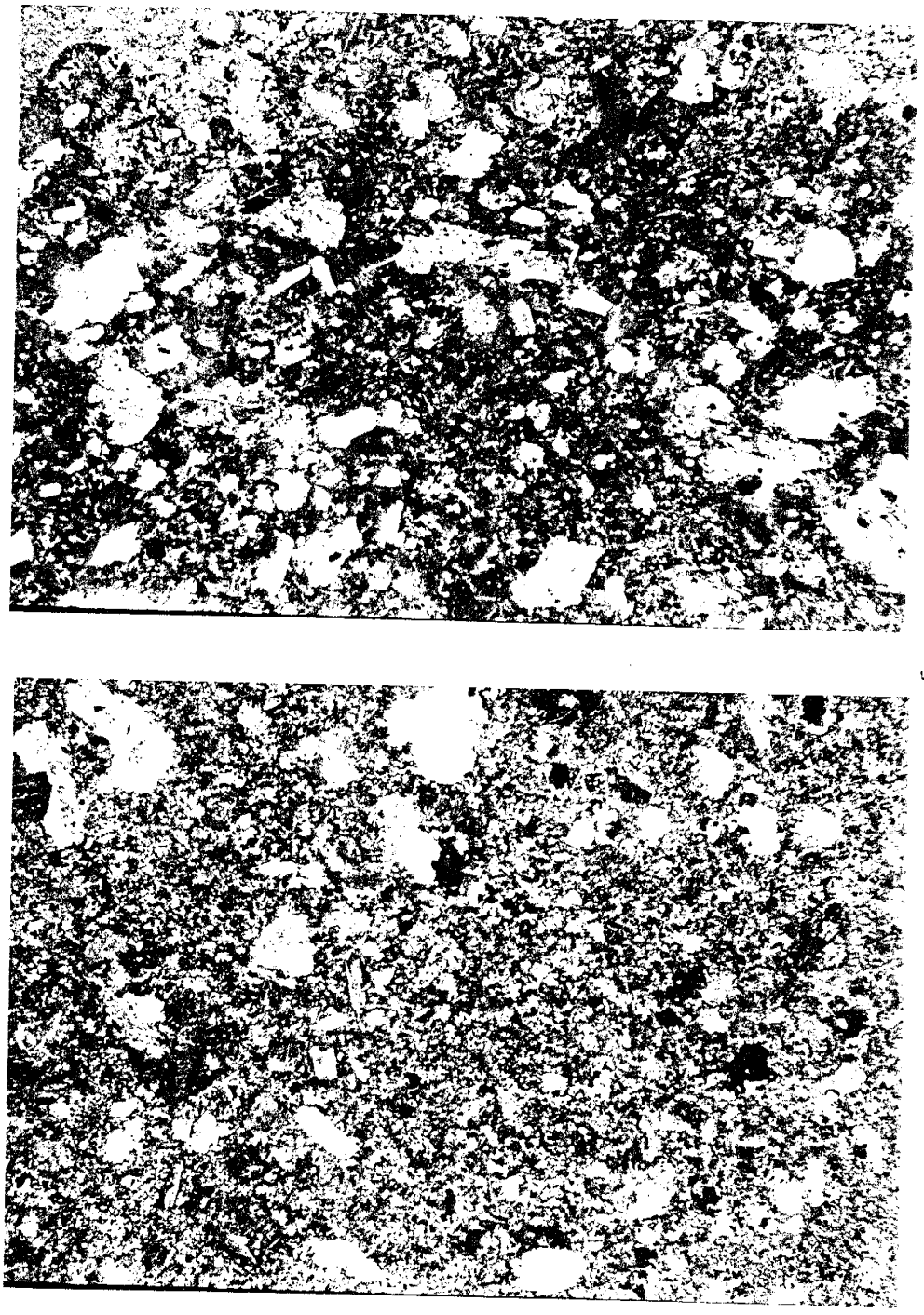


Figure 18. Photomicrographs (crossed polars) of levels in the Luna Park latite. A. basal part. B. middle part. C. Upper part

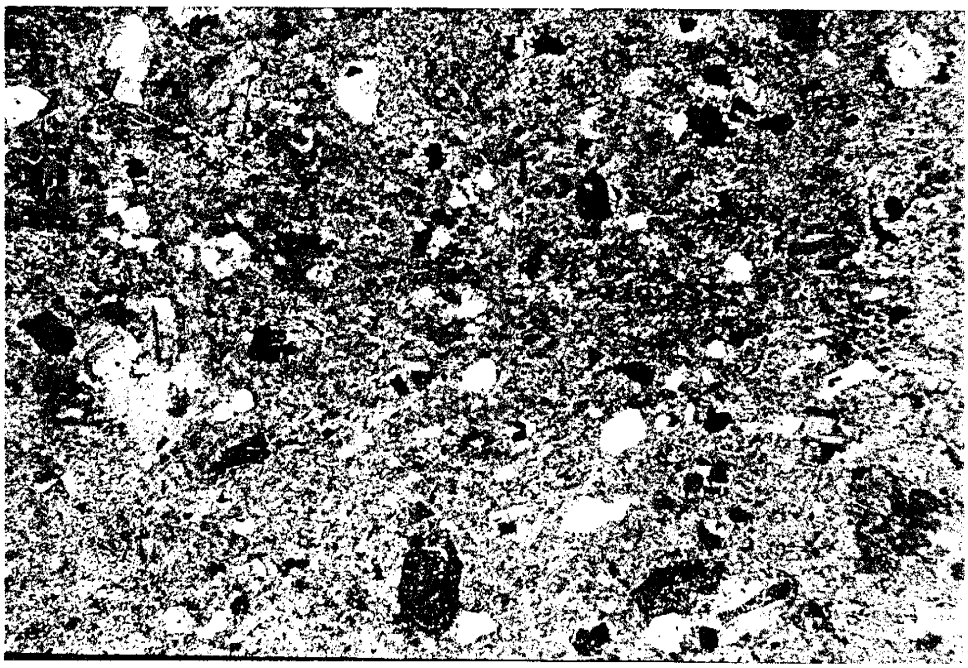

(C)

1 mm

Figure 18 continued.

The rocks consist of slope-forming brown to red-brown massive to flaggy lavas. Calcite and silica amygdules are common locally.

In thin section the rock is porphyritic and amygdaloidal with phenocrysts of plagioclase, altered pyroxene, and opaques in an amygdaloidal, trachytoid groundmass of plagioclase, pyroxene and opaques (Figure 19). In lower flows amygdules are filled with silica. Amygdules in upper flows are filled with calcite.

**Hump Mountain Member.** Exposures of Hump Mountain member of the Rock Spring Formation are restricted to an area of about 1/2 square mile northwest of Luna Park in the eastern portion of section 23 and the southeast corner of section 14, T9S, R6W, and west of the Rock Spring fault in the northeast corner of section 22 and northwest corner of section 23, T9S, R6W, N.M.P.M. No exposures were observed east of the Priest Mine fault or outside of the study area.

The Hump Mountain member is thickest directly east of the Rock Spring fault, reaching 600 feet (190 m), and thins to the west across the Rock Spring fault to less than 200 feet (60 m). It pinches out and interfingers with the Shipman Canyon andesite in the northeast 1/4 of section 22, T9S, R6W, N.M.P.M. Contacts with the overlying Shipman Spring tuff are generally relatively planar with little or no apparent relief.

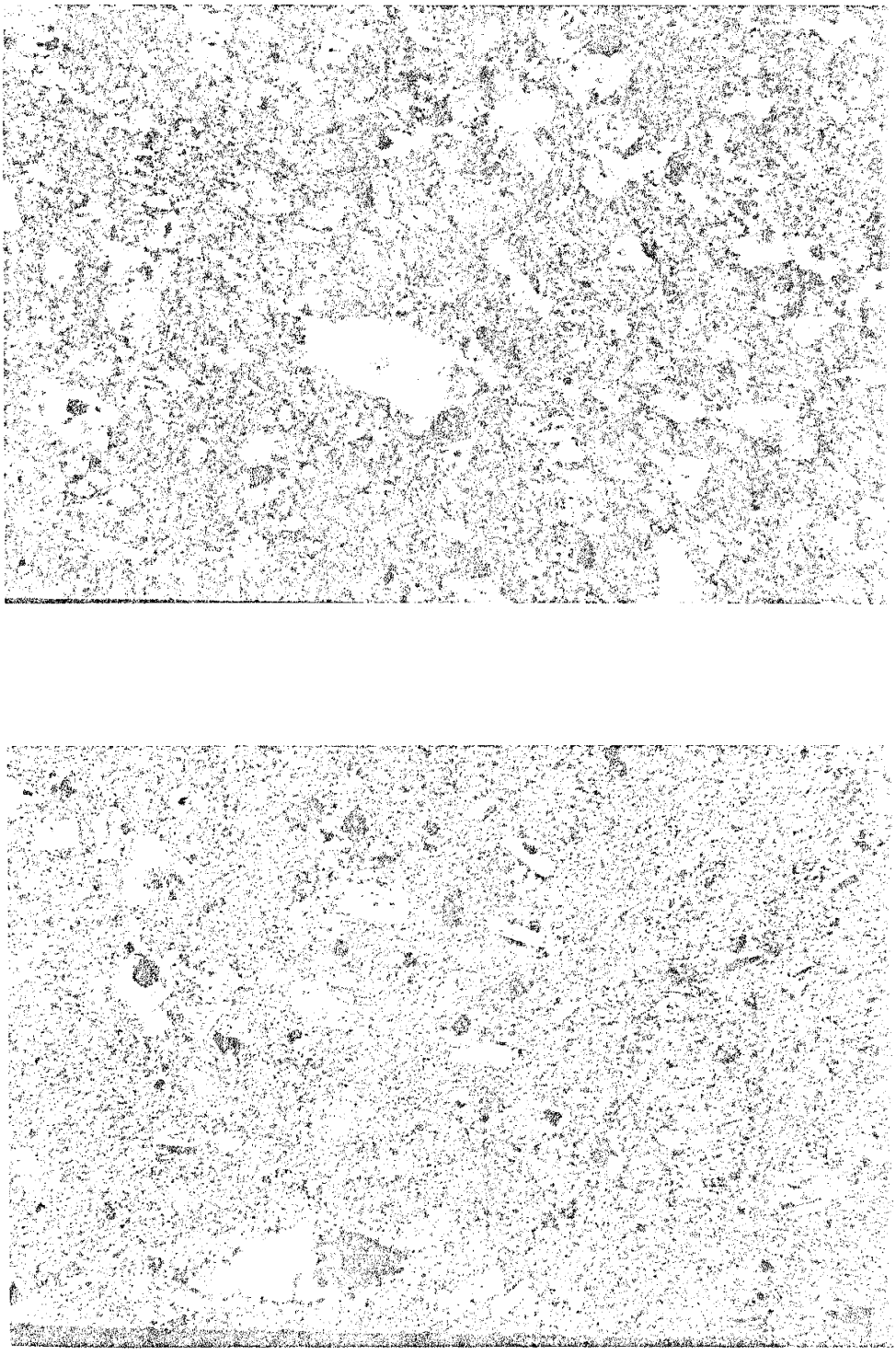

Figure 19. Photomicrographs (crossed polars) of the Luna andesite member; (A) upper flows, (B) lower flows.

The basal parts of the member are composed of thinly-bedded air-fall tuffs and pyroclastic deposits. These are overlain by a layered, flow-banded interval. These rocks consist of porphyritic flow-banded lavas, flow-breccias, welded lithic air-fall tuffs, welded bomb beds, and fine-grained welded ash layers. Matrix supported subangular to rounded cognate bombs range in diameter from 1 cm to 75 cm (some >1 m) in the upper portions and are apparently derived from petrographically similar rocks through dome collapse, or explosive eruptions (Figure 20). Bomb sag structures are apparent in the coarser lithic-rich layers. Minor unwelded slabby layers and sandstones can be found locally at the base and top of the member. Cross beds in the lower layers may indicate a possible surge origin for some of the lower parts of the member.

In outcrop the lower air fall tuffs are light brown or buff in color. They are poorly to moderately indurated with sparse blocks and bombs within alternating lithic-rich and fine-grained layers.

The flow-banded (layered) interval is slabby with light brown, dark red, purple or blue-gray layers, cliff forming, and exhibits crude columnar jointing (Figure 21). The lower portions are partially autobrecciated and grade upward into well indurated porphyritic flow-banded lavas or welded breccias with increasing lithic content upward. The average size of the lithic fragments also increases upward

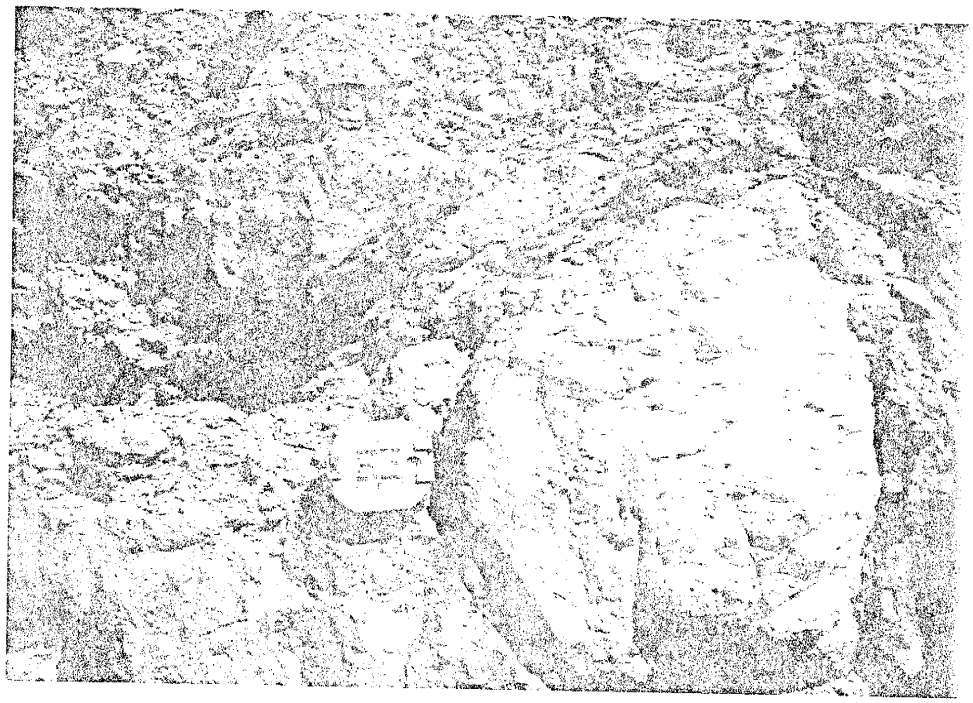

Figure 20. Bomb in the Hump Mountain member (looking east along road-cut in the SE/4 of section 14, T9S, R6W, N.M.P.M.

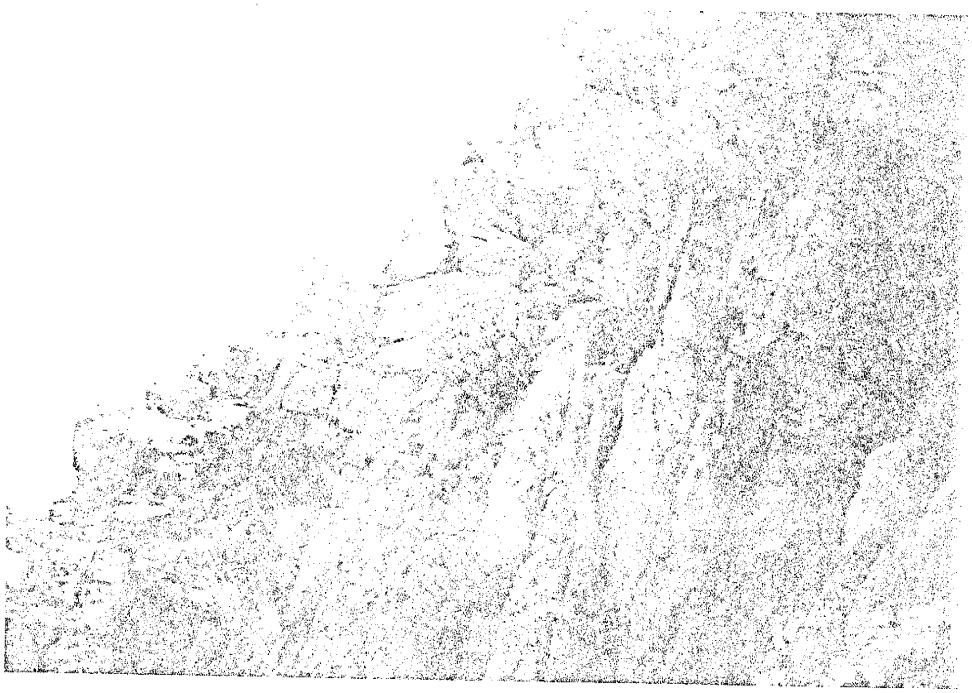

Figure 21. Outcrops of the middle part of the Hump Mountain member. Looking northeast in the SE/4 of the SE/4 of section 23, T9S, R6W, W.M.P.M.

from about 1 cm in the lower flows to about 10 cm in the upper layers. Locally the flows show contortion and folding of the layers with amplitudes of less than 1 cm to over 10 cm and wavelengths ranging from 1 cm to greater than 1 m. This may indicate post-depositional deformation. Flow grooves are common and are locally oriented. Lineation trends suggest a source region for these deposits to the north-northwest or to the southsouth-east of the center of section 23, T9S, R6W, N.M.P.M. No direct indications of the vent were observed within the study area, but the presence of bombs in the deposits indicate a relative proximity to a vent (<5 km). Several large bombs (>1 m in diameter) and local dome structures can be found near the Rock Spring fault, possibly indicating a source in the northwest part of section 23, T9S, R6W, N.M.P.M.

The flow-banded interval is overlain by a series of alternating red, purple, and gray layers of lithic-rich welded breccias, and volcaniclastic zones (Figure 22). Lithic fragments (lapilli and bombs) are angular to rounded and range in size from 0.5 inch (1.2 cm) to 3 feet (1 m) in diameter. Lithic fragments in the lower flows tend to be angular whereas those in higher flows are subangular and rounded. All lithic fragments observed within this interval and in the lithic-rich flow-banded interval are accessory in nature.

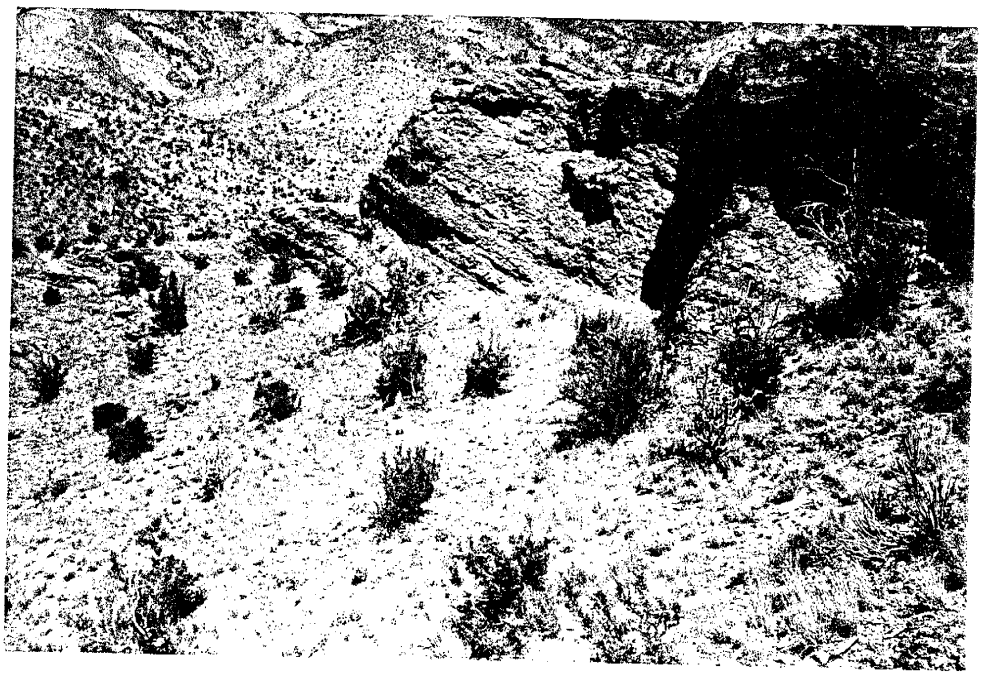

Figure 22. Outcrop of the upper part of the Hump Mountain member. Looking north in the southeast 1/4 of section 14, T9S, R6W, N.M.P.M.

The Hump Mountain member is part of the upper Spears Formation described by Foruria (1985). The upper portions of the Hump Mountain tuffs are stratigraphically equivalent to the variegated breccia of the Rock Spring Formation described by Farkas (1969).

The lower flow-banded interval in this map area was apparently mapped as the upper Luna Park tuff by Farkas (1969). Textures are similar to those found in flow-banded lavas or welded ash-flow tuffs. The lower parts of the Hump Mountain member closely resemble a densely welded lapilli ash-flow tuff, and are mineralogically similar to the Luna Park tuffs, but the brecciated base, flow grooves and contorted flow bands indicate that these rocks might be welded breccias similar to deposits found near the margins of lava domes or sheared zones in viscous lava flows (Ross and Smith 1960, p.11).

Hand specimens of the lower flow-banded interval are light chocolate-brown to purple-brown, well-indurated porphyritic rocks. Sparse blocky euhedral to subhedral phenocrysts of altered potassium feldspar up to 2 mm long, thin euhedral laths of plagioclase up to 2.5 mm long, randomly oriented, tabular, brown, euhedral, biotite phenocrysts up to 1.5 mm long, and a few equant, euhedral phenocrysts of magnetite up to 0.5 mm are scattered in a dark to light brown-purple fine-grained to aphanitic flow-banded groundmass.

Angular cognate lithic fragments from 2 to 20 mm make up to 30 percent of the samples examined in the lower flow-banded interval. Elongate irregular shaped vesicles up to 5 mm long are present in some of the layers. Local zones with spherulitic groundmass textures are also present in the lower flow-banded interval.

Microscopically the flow-banded interval is porphyritic containing phenocrysts of plagioclase, sanidine, biotite, quartz, and opaques. The groundmass consists of sinuous flow-banded hypocrystalline and micro-crystalline quartz-feldspar intergrowths, brown glass and dendritic hair-like opaque crystallites (Figure 23). Angular microcrystalline flow-banded lithic fragments up to 1 cm in diameter similar to the groundmass of the rock are present between some of the flow bands. Irregular lenticular vesicles up to 5 mm long, lined or filled with euhedral quartz microlites are also present. Phenocrysts are sparse and consist of plagioclase (1%), sanidine (1%), biotite (1%), quartz (0.5%) and opaques (0.5%). Sparse lithic fragments (10%), groundmass quartz-feldspar intergrowths (devitrified groundmass) (40%), groundmass glass (23%), and groundmass opaques (23%) dominate the composition.

Plagioclase phenocrysts are typically euhedral or fragmental laths up to 2 mm long and show partial alignment parallel to flow banding. Sanidine phenocrysts are

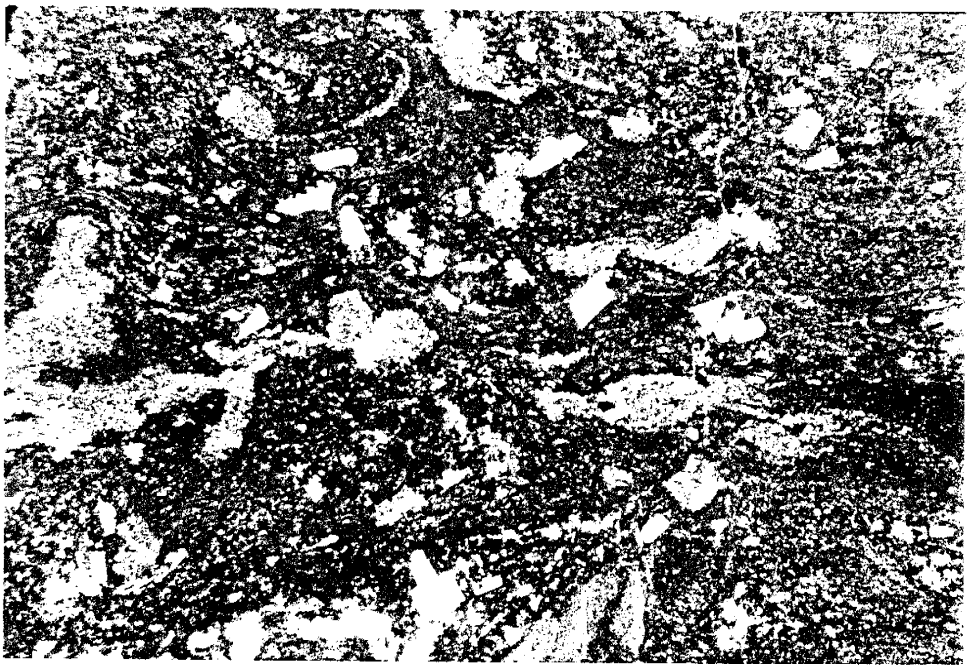


Figure 23. Photomicrograph of the Hump Mountain member (crossed polars).

typically milky white, euhedral to subhedral blocks and laths up to 2.5 mm long and occasionally contain equant glass inclusions up to 0.4mm in size.

Biotite occurs as randomly-oriented tabular euhedral to subhedral phenocrysts up to 1mm long and as radiating crystal groups up to 1 mm in diameter. Quartz occurs as equant, angular, anhedral phenocrysts up to 0.5 mm long and appears to be fragmental in nature. Opaques occur as equant, euhedral squares or blocks and irregular anhedral blebs up to 0.5 mm in diameter and usually are surrounded by a thin coating of blood-red hematite or limonite.

The groundmass of the rock is flow-banded (layered) and consists of microcrystalline quartz-feldspar intergrowths, gray-brown glassy areas, a few quartz and feldspar crystal fragments, and hair-like opaques. Flow bands are accentuated by alternating areas of high and low percentages of the hair-like opaque crystallites. These wrap around lithic fragments which are texturally and mineralogically similar to the groundmass.

**Shipman Canyon Andesite Member.** The informal name Shipman Canyon andesite member of the Rock Spring Formation is proposed for a series of porphyritic, vesicular, and amygdaloidal lava flows. The andesite is best exposed in Shipman Canyon in the NE part of Sec. 21 and the NW part of Sec. 22, T9S, R6W N.M.P.M. Here the member is overlain by

the Shipman Spring tuff. The member is underlain by the Luna Park latite in eastern exposures.

Outcrops of the member south of Shipman Canyon appear as dark purple-red to light purple or gray rounded to angular exposures (cliff forming lower and upper zones, slope forming in middle zones). Lower flows tend to have rounded outcrops, and minor dikes and sill-like intrusive bodies of a similar but coarser nature can be found. Upper flows tend to be flaggy, less phenocryst-rich and more angular in outcrop than the lower flows. Where upper parts are altered and bleached they are almost indistinguishable from the overlying crystal rich Shipman Spring tuff.

The andesites near Shipman Canyon are bleached and pyritized along joint planes in some flows, with varying degrees of alteration throughout. Alteration observed may be related to proximity to the Rock Spring and Deep Canyon faults or to intrusive bodies located east of Shipman Canyon.

In thin section, the rock is porphyritic with phenocrysts of plagioclase (complexly twinned and glomerocrystic), anhedral to euhedral biotite, potassium feldspar?, and opaques (after biotite). The groundmass is a felsic intergrowth of feldspar, quartz, clays and cryptocrystalline alteration products.

Some feldspar phenocrysts of are partially replaced by biotite and/or polycrystalline quartz intergrowths

(potassic alteration?), and others are totally replaced by epidote, sericite, clays, calcite, and opaques. Plagioclase phenocrysts are identified by relict albite twinning.

Biotite phenocrysts have apparently been intensely oxidized or altered to opaques and occur as euhedral laths or tabular crystals up to 1 mm long. Pleochroism is retained only in portions of some of the crystals (Figure 24).

**Shipman Spring Tuff.** The informal name Shipman Spring tuff is proposed for a laterally continuous, single cooling unit, moderately welded, moderately crystal-rich ash-flow tuff exposed in parts of sections 14, 15, 16, 21, 22, and 23 T9S R6W N.M.P.M. The Shipman Spring tuff is equivalent to the upper latite tuff of the Rock Spring Formation described by Farkas (1969). Paleomagnetic data indicate that the Shipman Spring Tuff is equivalent to the Blue Canyon Tuff (33.93 ma), which is exposed over large areas of the northeastern Mogollon-Datil volcanic field (Bill McIntosh pers. comm.).

In the western part of the study area, the tuff reaches an apparent maximum thickness of 400 ft (125 m) and occupies a stratigraphic position between the underlying Shipman Canyon andesite and the overlying andesite flow member of the Rock Spring Formation. The tuff thins to the

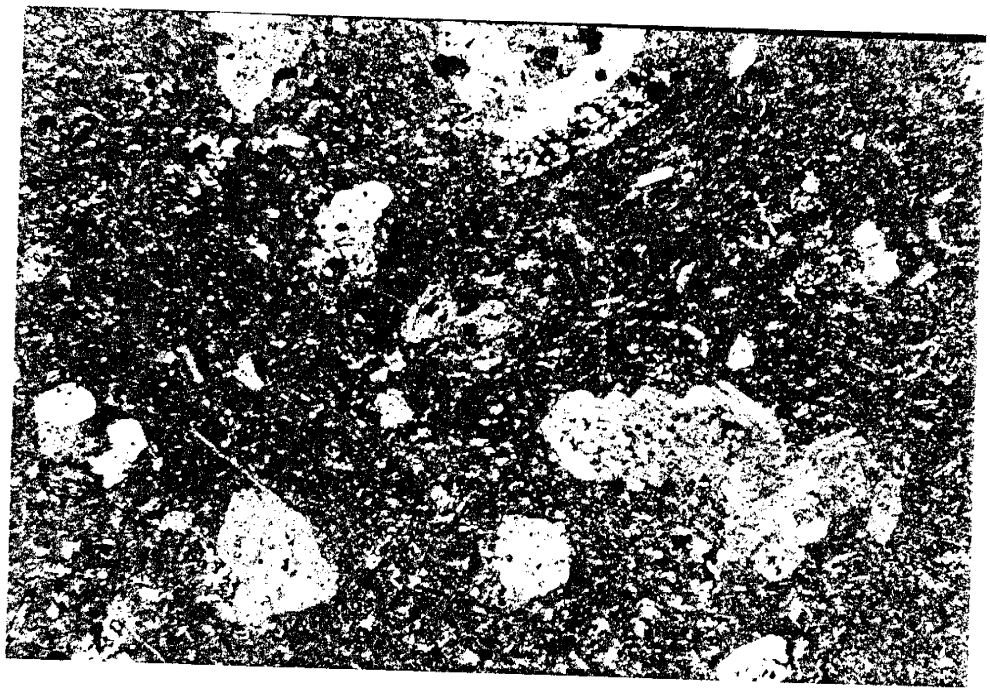


Figure 24. Photomicrograph of the Shipman Canyon Andesite member (crossed polars).

east to a thickness of 50 ft (15 m) across the Rock Spring fault and is not exposed east of the Priest Mine fault. In the eastern part of the study area, the tuff lies above the Hump Mountain member and below the andesite flow member of the Rock Spring Formation.

Outcrops of the tuff range in color from white to beige to light purple-gray in the western part of the study area and from brick-red to white in the eastern part of the study area. Joint surfaces are locally limonitic, particularly in areas near fault zones or intrusive bodies.

The tuff is usually moderately to well-indurated, cliff forming, and exhibits crude columnar jointing. Planar alignment of crystal-rich lenticular zones give the rock a granular flow-banded appearance (Figure 25) and zones of flattened propylitized pumice impart a eutaxitic texture locally. The vitroclastic nature of the tuff has been obscured or destroyed by devitrification or hydrothermal alteration except in a few outcrops near Villa Nerce Spring (where flattened pumice lapilli are preserved) and in road-cuts near Rock Spring fault in the vicinity of the Priest Mine (where the original glassy nature of the tuff is partially preserved).

A thin discontinuous basal layer of bedded altered air-fall tuff occurs in the western part of the field area. Near the intersection of the Rock Spring fault and the Priest Mine fault an underlying sequence of altered

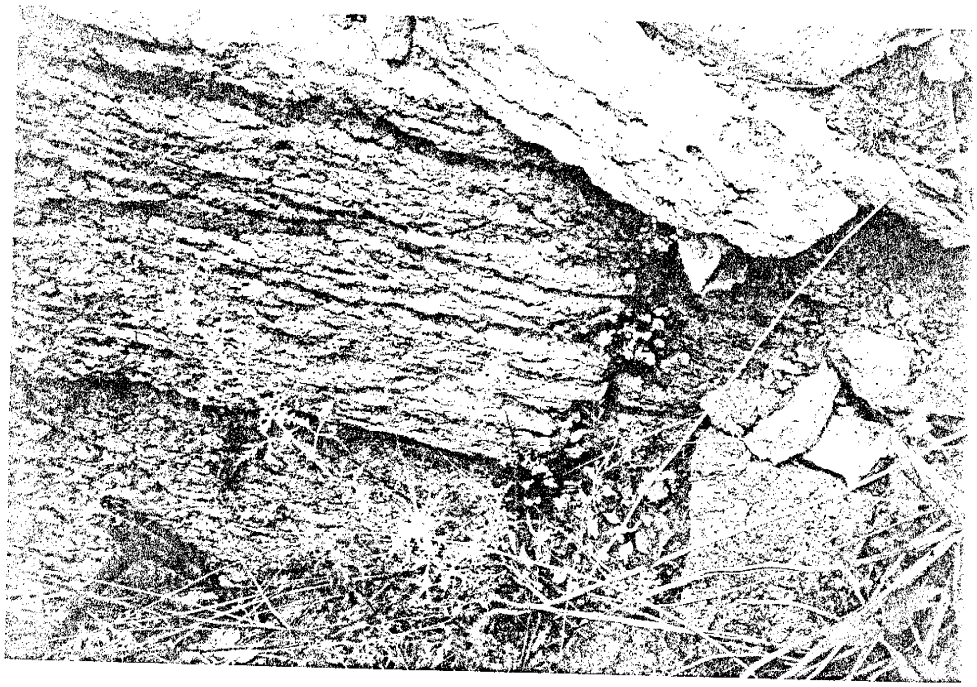

Figure 25. Outcrops of the Shipman Spring Tuff (NW/4 of the SE/4 of section 16, T9S, R6W, N.M.P.M.).

bedded conglomerates, sandstones, ash-flow, and air-fall tuffs exist. These deposits were mapped with the Shipman Spring tuff. Between Villa Nerce Spring and the Priest Mine a thin andesite flow separates an upper pumice-rich flow unit from the lower parts of the tuff. This flow was mapped as part of the andesite flow member of the Rock Spring Formation.

Outcrops of the tuff are usually easily identified due to the presence of abundant, copper-colored biotite phenocrysts. The tuff could be confused with the texturally and mineralogically similar Luna Park latite member of the Rock Spring Formation, or parts of the volcaniclastic member of the Red Rock Ranch Formation in isolated outcrops or in areas lacking stratigraphic control.

Hand specimens of the Shipman Spring Tuff are typically white to light-gray porphyritic rocks with euhedral to subhedral feldspar phenocrysts up to 3 mm long and euhedral biotite phenocrysts up to 1 mm long in a light gray to white devitrified ash matrix. Faint layers 5 to 10 cm thick are visible in some hand specimens and may represent relict eutaxitic texture. Zones containing sparse angular lithic fragments of fine-grained brown andesite up to 3 cm in diameter are found near the base of the tuff near Shipman Spring in section 16, T9S, R6W N.M.P.M.

Pumice content is obscured apparently by devitrification, except in the vicinity of Villa Nerce Spring (SE/4 sec 15, NE/4 sec 22 T9S, R6W), where alteration has accentuated the contrast between pumice fragments and the groundmass of the rock (Figure 26). The proportion of phenocrysts varies somewhat both vertically and laterally within the tuff and ranges from about 10% to 25% total phenocrysts.

Two thin sections of samples of the tuff, one from near Shipman Spring and another from the area near the Priest Mine are illustrated (Figures 27 A and B respectively). Figure 28 is an enlargement of an area in Figure 27 B showing relict vitroclastic texture preserved in the eastern parts of the study area. The rocks are generally porphyritic with phenocrysts of plagioclase, altered biotite, and altered blocky feldspar (sanidine?) in a devitrified groundmass of quartz-feldspar intergrowths and opaque crystallites. Altered latite and andesite lithic degrees of alteration to epidote, calcite and clay minerals, and exhibit relict albite and Carlsbad twinning.

**Andesite Flow Member.** The informal name andesite flow member is used to describe a series of aphanitic, sparsely vesicular, amydaloidal, fine-grained, and generally sparsely porphyritic lava flows (and multiple flows) of predominantly andesitic composition. Flows

Figure 26. Outcrops of the upper part of the Shipman Spring Tuff in the SE/4 of the SE/4 of section 15, T9S, R6W, N.M.P.M.

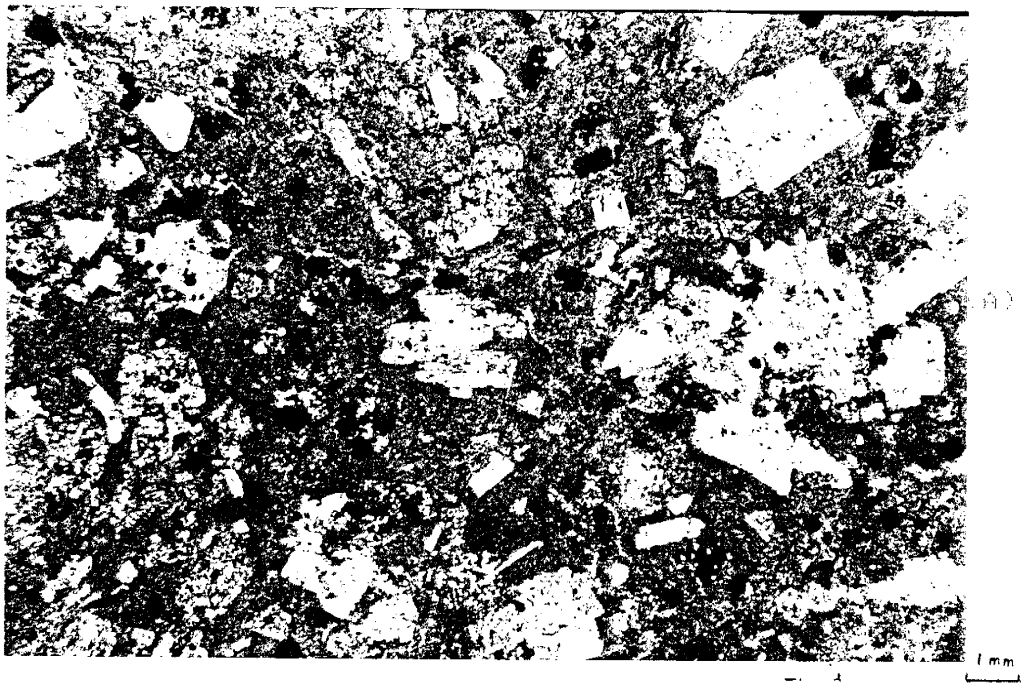


Figure 27. Photomicrographs (crossed polars) of the Shipman Spring Tuff. (A) Near Shipman Spring. (B) Near the Priest Mine.

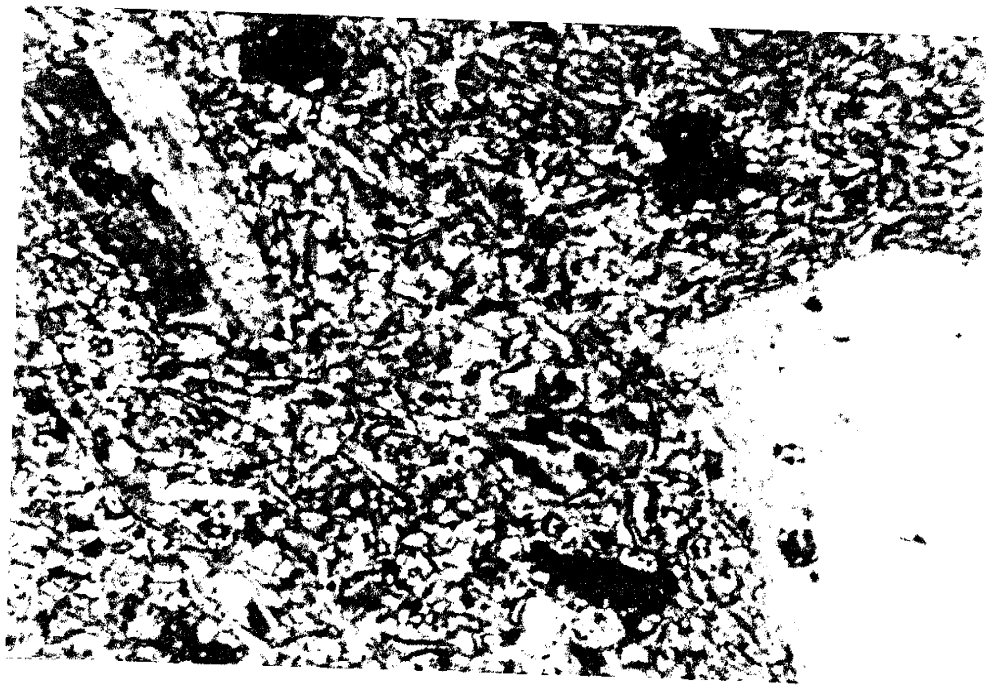


Figure 28. Enlargement of part of Figure 27 (B) illustrating the relict vitroclastic nature of the rock (crossed polars).

contain volcanic breccias, and rubble zones; minor volcaniclastic sediments occur between the flows.

The andesite flow member lies stratigraphically between the Shipman Spring tuff and the pyroxene andesite member. Up to nine individual lava flows can be observed where the overall thickness reaches its maximum in the west-central part of section 16, T9S, R6W, N.M.P.M.

The andesite flows correlate stratigraphically with the lower part of the upper andesite flows (trs4) of the Rock Spring Formation described by Farkas (1969), and part of Foruria's (1985) upper member of the Spears Formation. The member also possibly correlates with parts of the andesite-latite of Montoya Butte described by Maldonado (1974), and the andesite member of the Spears Formation of Atwood (1982).

The best exposures of the member are between Shipman Canyon and Rock Springs Canyon in sections 16, 15, and 14, T9S, R6W, N.M.P.M. In this area, the member attains its greatest thickness (1000 feet, 300 m), and lenticular exposures of the Hells Mesa Tuff are interbedded with the uppermost flows.

Only the lowermost flows are exposed between the Rock Spring fault and the Priest Mine fault due to erosion of the upper parts of the member. Pre-existing paleovalleys in altered early flows were later filled with a brown flow (Figure 29). Poorly to well-developed spiracles within

Figure 29. Lower flows of the andesite flow member of the Rock Spring Formation. Paleotopography is accentuated by a brown flow-unit filling in depressions in a lighter flow-unit. (Looking east in a road-cut in the western part of section 14, T9S, R6W, N.M.P.M.).

the brown flow indicate some of the flows were deposited over wet ground or into shallow water in this area (SE 1/4 of sec. 14, T9S, R4W, N.M.P.M.).

East of the Priest Mine fault the member is down--faulted and concealed. The thickness or extent of the exposures outside of the study area are unknown.

Outcrops of the various andesite to basaltic andesite flows range in color from black to dark gray to brown to red-brown. Exposures consist of well-indurated flow-banded to massive lava flows interbedded with variegated volcanic breccias and rubble zones. The matrix of rubble zones and volcanic breccias often exhibits pervasive propylitic alteration. The member usually forms rolling hills and slopes, except along the sides of major drainages or arroyos, where it forms steep cliffs. Nick points and dry waterfalls form where ephemeral streams cross contacts between resistant flows and less resistant rubble zones or less resistant lava flows within the member.

Joint styles vary from columnar to sheeted and many outcrops display irregular anastomosing joint patterns or semi-conchoidal fractures. Locally, joint surfaces are coated with drusy epidote or calcite. Vesicles and calcite amygdules are common in the lower flows and at the tops and bottoms of the individual flows. Vesicles are locally elongated in the direction of flow. Rarely some of the

more slabby flow-banded flows exhibit minor flow-grooves on flow planes.

A thin section made from one of the lowermost flows (Figure 30) shows sparse phenocrysts of plagioclase in a pilotaxitic groundmass of plagioclase (An 50), clino-pyroxene, and opaques, with secondary calcite, silica amygdules, and hematitic altered areas.

**Hells Mesa Tuff.** The Hells Mesa Tuff is a welded, crystal-rich, two feldspar, rhyolite ash-flow tuff exposed throughout the northeast Mogollon-Datil volcanic field. The source area for the Hells Mesa Tuff is considered to be the Socorro cauldron in Socorro County, New Mexico (Osburn and Chapin, 1983).

Within the study area the Hells Mesa Tuff occurs in discontinuous lens-shaped exposures up to 50 feet (15 m) thick. Outcrops occur in the upper part of the andesite flow member of the Rock Spring Formation in sections 15 and 16, T9S, R6W, N.M.P.M. The tuff occurs as two flow units separated by about 5 feet of andesitic breccia.

Paleomagnetic pole positions from upper portions of the tuff fit relatively well to those of the Hells Mesa Tuff from other locations in the Mogollon-Datil Volcanic Field (Bill McIntosh pers. comm.). No reliable paleomagnetic data was obtained from the lower flow unit.

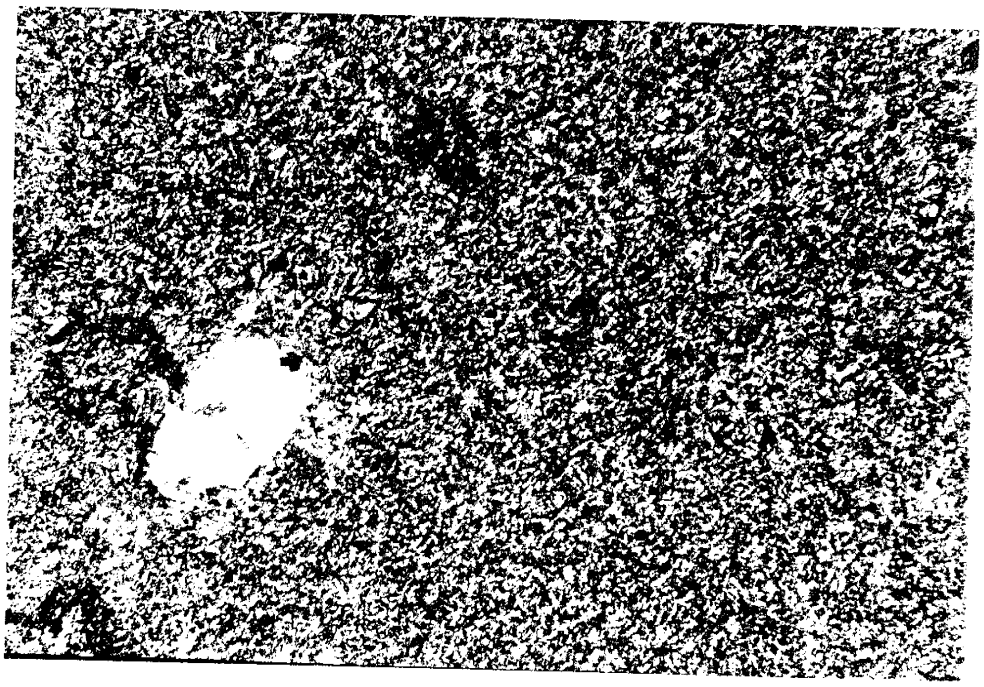


Figure 30. Photomicrograph of a lower flow of the andesite flow member of the Rock Spring Formation (crossed polars).

The tuffs were apparently deposited in paleovalleys or low lying areas on flow surfaces.

The best exposures occur in an arroyo east of Shipman Canyon in the northeast 1/4 of section 16, T9S, R6W, N.M.P.M., where a coarse andesitic breccia separates upper and lower flow units (Figure 31).

In outcrop the Hells Mesa Tuff is typically white, pink, or light gray in color. It is well-indurated and massive, and forms spheroidally-weathered cliffs and ledges. The middle breccia interval is usually poorly to moderately indurated and forms a break in slope between the upper and lower more resistant tuff units.

Hand specimens of the lower exposure are porphyritic with phenocrysts of altered feldspar, quartz and biotite, and brown and green (propylitized) lithic fragments in a light-gray ash matrix. Alignment of biotite and slight preferred orientation of lithic fragments impart a crude foliation to some hand specimens.

Feldspar and quartz phenocrysts make up 15% and 10% of the rock respectively. Feldspar phenocrysts occur as milky-white subhedral to euhedral laths and blocks up to 1 mm long. Quartz occurs as colorless transparent equant anhedral to subhedral crystals up to 1 mm in diameter. Biotite occurs as bronze and black euhedral hexagonal books up to 1 mm long and makes up about 3% of the rock.

Figure 31. Outcrops of the Hells Mesa Tuff looking northeast in the middle of the SE/4 of section 16, T9S, R6W, N.M.P.M.

Lithic fragments make up about 5% of the rock. Lithic fragments consist of brown and dark-brown angular to subrounded fine-grained andesite up to 3 cm in diameter. Smaller subrounded and rounded green propylitized andesite particles up to 5 mm in diameter are also present.

Microscopically the lower flow unit is porphyritic with phenocrysts of sanidine, anorthoclase (xenocrysts?), quartz, plagioclase, opaques, biotite, and orthopyroxene; lithic fragments of fine-grained andesite, propylitized andesite, polycrystalline quartz, and devitrified pumice are found in a partially to completely devitrified vitroclastic matrix (Figures 32 A and B).

Sanidine makes up about 15% of the rock as equant subhedral to anhedral single crystals and simple twins up to 1 mm in diameter. Some of the sanidine crystals exhibit exsolution lamellae. Anorthoclase makes up 10% of the rock and occurs as subhedral to euhedral blocks up to 0.6 mm and exhibits tartan twinning. Quartz makes up 10% of the rock as irregular or rounded anhedral to subhedral crystals up to 1 mm long and often appears embayed or corroded. Many of the quartz crystals contain inclusions of feldspar, and some exhibit undulatory extinction. Plagioclase makes up 6% of the rock as euhedral to subhedral Carlsbad and albite twinned laths and blocks up to 1 mm long with clay alteration products along cleavage and twin planes.

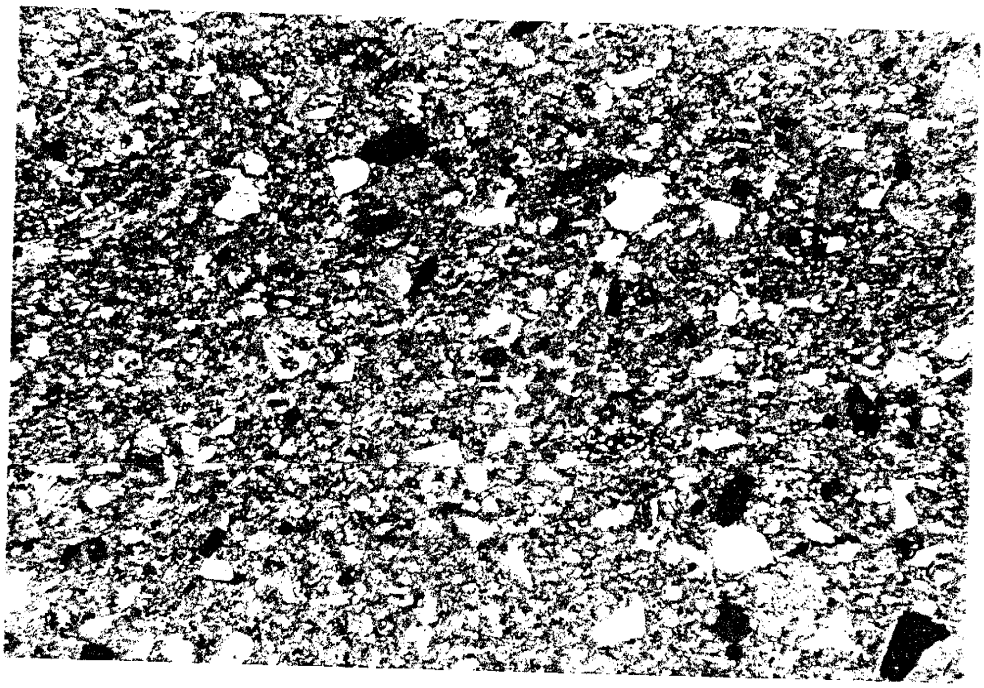


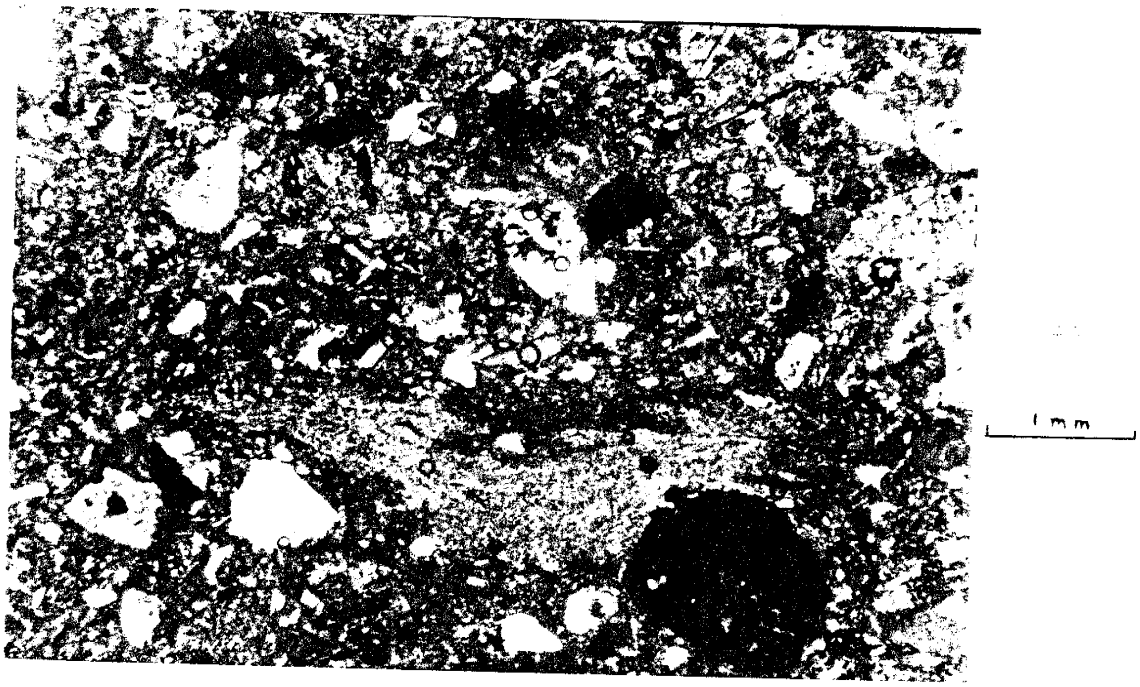


Figure 32. A. Photomicrographs (crossed polars) of the Hells Mesa Tuff. B. Enlargement of part of A showing relict pumice and vitroclastic nature of the rock.

Biotite makes up as much as 3% of the rock as wavy crinkled laths and blocks up to 1 mm long and often shows effects of oxidation or partial replacement by muscovite and opaque minerals. Opaque phenocrysts make up 2% of the rock as subhedral to euhedral irregular blebs and blocks up to 0.5 mm in diameter. Pink-brown pleochroic orthopyroxene phenocrysts make up about 2% of the rock. These occur as euhedral to subhedral laths up to 0.5 mm long and often have a glomerocrystic relation to opaque phenocrysts. The presence of pyroxene may indicate that the lower tuff is not part of the Hells Mesa Tuff.

The middle breccia interval contains a large proportion (up to 75%) of angular and rounded lithic fragments. They range from 3 to 60 cm in diameter and occur in a brown crystal and ash matrix of similar composition to the lower flow unit.

The upper flow unit is very similar to the lower flow unit in composition and texture, but contains less quartz phenocrysts and no pyroxene. The upper flow unit is overlain by andesitic, volcanic breccias similar to those found between the various flows of the andesite flow member of the Rock Spring Formation.

**Pyroxene Andesite Member.** The informal name pyroxene andesite member is used for a distinctive andesite flow (or flows) exposed in the central part of the study

area. Extreme western exposures are between the andesite flow member and the upper andesite member of the Rock Spring Formation. To the east, flows are overlain by the Priest Mine andesite. Blocky pseudomorphs of serpentine after pyroxene weather out giving the rock a pitted appearance.

In outcrop, flows are typically blue-gray to brown, somewhat flaggy, sheeted or flow-banded and exhibit semi-conchoidal fracture. Flows are typically slope forming or consist of alternating slopes and angular ledges. The lower few feet are usually brecciated or rubbly and the lower contact with the andesite flow member is relatively planar with little or no relief. The member is thickest in the southeast corner of section 15 in the vicinity of an altered intrusive of similar texture and composition.

In thin section, the rock is porphyritic with phenocrysts of clinopyroxene and plagioclase in a trachytoid groundmass of plagioclase, opaques, clinopyroxene, and secondary calcite. Ellipsoidal amygdules up to 1 mm long are found locally and are elongated in the direction of flow (Figure 33).

Clinopyroxene (augite) phenocrysts make up about 3 percent of the rock and occur as euhedral and subhedral simple, lamellar, and complexly twinned crystals up to 0.5 mm in diameter. The pyroxene phenocrysts are usually colorless and some show hourglass and sector zoning.

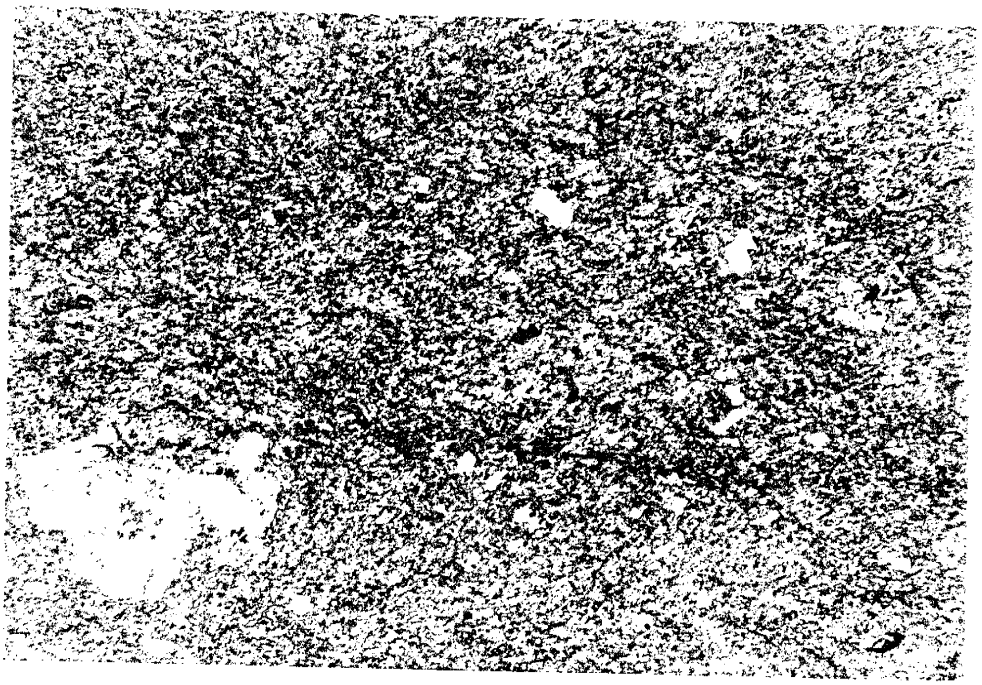


Figure 33. Photomicrograph of the pyroxene andesite member of the Rock Spring Formation (crossed polars).

Serpentine pseudomorphs after pyroxene or olivine? occur as blocky (glomerocrysts?) masses up to 2.5 mm.

Plagioclase phenocrysts make up about 1 percent of the rock and occur as albite and Carlsbad twinned laths up to 1 mm long and are often preferentially aligned parallel to flow. Groundmass plagioclase makes up about 61 percent of the rock as altered laths up to 0.5 mm long arranged in a trachytoid fashion.

Opaques make up about 20 percent of the rock and occur as anhedral to subhedral crystals up to .25 mm in diameter. Groundmass pyroxene makes up about 10 percent of the rock as anhedral and subhedral intergranular patches. Irregular masses of polycrystalline calcite occur as partial replacements of phenocrysts and groundmass crystals.

**Priest Mine Andesite Member.** The Priest Mine andesite member is exposed east of the Priest Mine fault in the southwest corner of sec. 13, T9S, R6W, and west of the Rock Spring fault in sections 14, 15 and 16, T9S, R6W. East of the Priest Mine fault the member is 200 feet (65 m) thick and dips to the east. West of the Rock Spring fault the thickness is somewhat variable with a maximum thickness of 350 feet (110 m). The member thins to the west and pinches out in the NE corner of sec. 16, T9S, R6W. West of the Rock Spring fault the member dips N-NE from 25 to 30 degrees.

The member lies conformably above the pyroxene andesite member and is overlain by the upper andesite member of the Rock Spring Formation. Upper and lower contacts rarely show more than 5 feet (1.5 m) of relief. West of the Rock Spring fault the member is underlain by thinly bedded volcaniclastic sandstone that probably occupies minor depressions in the underlying pyroxene andesite. Minor rubble zones are present locally at the top and bottom of the member. East of the Priest Mine fault the lower contact of the member is conformable to the underlying pyroxene andesite member.

The "turkey track" texture and phenocryst-rich, porphyritic nature of the member make it easily recognizable in the field. Weathered outcrops are typically speckled dark gray, red-brown or light gray-brown and exhibit spheroidal weathering. Lower exposures are locally flaggy and flow- banded whereas middle and upper portions tend to be massive and more phenocryst rich.

Variations in phenocryst proportion and the presence of discontinuous vesicular zones probably indicate the presence of several lava flows in the Priest Mine andesite. East of the Priest Mine fault, the flows contain pyroxene phenocrysts that weather out in a similar manner to those of the underlying pyroxene andesite.

In hand specimen, fresh surfaces are typically speckled dark brown, red-brown or black. Megascopically

flows are porphyritic with euhedral phenocrysts of plagioclase up to 2 mm long, and green subhedral pyroxene up to 0.5 mm in a dark gray to black aphanitic to microcrystalline groundmass. Plagioclase phenocrysts, which locally compose up to 40 percent of the rock, often exhibit a stellate glomerocrystic habit. Pyroxene phenocrysts make up about 10 percent of the rock and are often partially chloritized.

Microscopically the rock is glomerocrystic and cumulophyric with phenocrysts of plagioclase, orthopyroxene and clinopyroxene in a felty groundmass composed of plagioclase, altered pyroxene, opaques, clays, and cryptocrystalline alteration products. Euhedral stellate glomerocrysts of plagioclase (An 33) 0.5 to 2.5mm long make up about 30 percent of the rock as groups of oscillatory zoned Carlsbad and albite twinned crystals. Small inclusions of opaques are discernable in many of the plagioclase phenocrysts.

Euhedral to anhedral phenocrysts of pleochroic yellow-green orthopyroxene 0.5 to 1 mm make up 10 percent of the rock. Some of the orthopyroxenes have a cumuloporphyritic relation to the plagioclase glomerocrysts resulting in a subophitic texture over small regions of thin sections (Figure 34). Partial replacement by chlorite can be noticed along the margins and within some of the orthopyroxene phenocrysts. Rounded anhedral to subhedral


Figure 34. Photomicrograph of the Priest Mine andesite (crossed polars).

clinopyroxene (augite) phenocrysts up to 1 mm make up about 1 percent of the rock. Many show simple or complex twinning and resorption textures.

The groundmass is characterized by randomly oriented lath-shaped plagioclase microlites up to 0.07 mm long with interstitial pyroxene, euhedral to anhedral magnetite and cryptocrystalline clay alteration products. The groundmass is made up of 30% plagioclase, 15% pyroxene, 8% opaques and 6% clays and alteration products.

**Upper Andesite Member.** The upper andesite member of the Rock Spring Formation is a series of aphanitic, porphyritic, and amygdaloidal lava flows and interbedded agglomerates, breccias, and rubble zones. They are exposed in the south central parts of the study area (SE/4 sec. 9, SW/4 sec. 10, W/2 sec. 13, N/2 sec. 14, N/2 sec. 15, NW/4 sec. 16, T9S, R6W, N.M.P.M. Extensive alteration of flows makes classification difficult, based on texture flows probably range in composition from andesitic to basaltic andesitic. Minor latite lavas are exposed locally in the upper part of the member.

Eastern exposures of the member overlie the pyroxene andesite and underlie the zeolitic andesite of the Rock Spring Formation. Western exposures of the member overlie the Priest Mine andesite and underlie the volcaniclastic member of the Rock Spring Formation.

The upper andesite member correlates with the upper part of the upper andesite flows (Trs4) of the Rock Spring Formation described by Farkas (1969). The overall nature of the member is very similar to the andesite flow member of the Rock Spring Formation, and the intercalated andesites within the Vicks Peak Tuff. Certain identification of the member can only be made where stratigraphic relationships are evident.

A thin section from one of the more distinctive flows from the upper part of the member is shown in Figure 35. Clasts from this flow are abundant in the overlying volcaniclastic member of the Rock Spring Formation.

**Volcaniclastic Member.** The informal name volcaniclastic member of Rock Spring Formation is proposed for a series of lithic-rich, crudely-bedded, poorly-sorted, matrix supported, volcaniclastic breccias and felsic lava flows. Figure 36 shows a well-exposed outcrop of bedded material west of the Rock Spring fault.

The member occupies a stratigraphic position beneath the La Jencia or Vicks Peak Tuffs in the eastern part of the study area and between the zeolitic andesite and the upper flows of the upper andesite member of the Rock Spring Formation. In the western parts of the study area, the member overlies and interfingers with a hornblende bearing andesite of the upper andesite member. Discontinuous

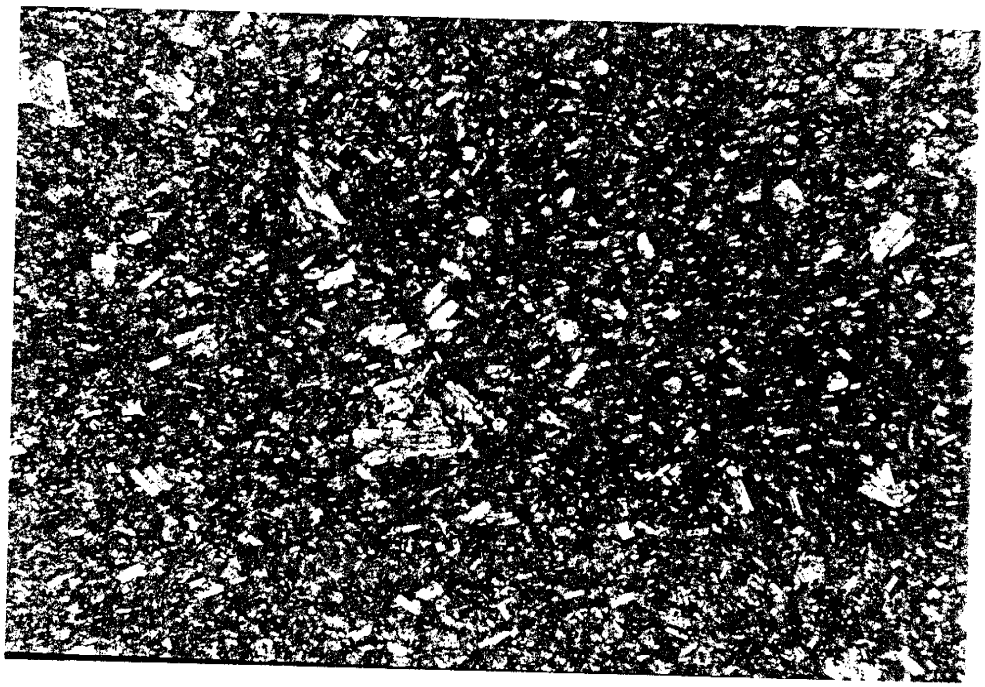

1mm

Figure 35. Photomicrograph of an upper flow of the upper andesite member of the Rock Spring Formation (crossed polars).

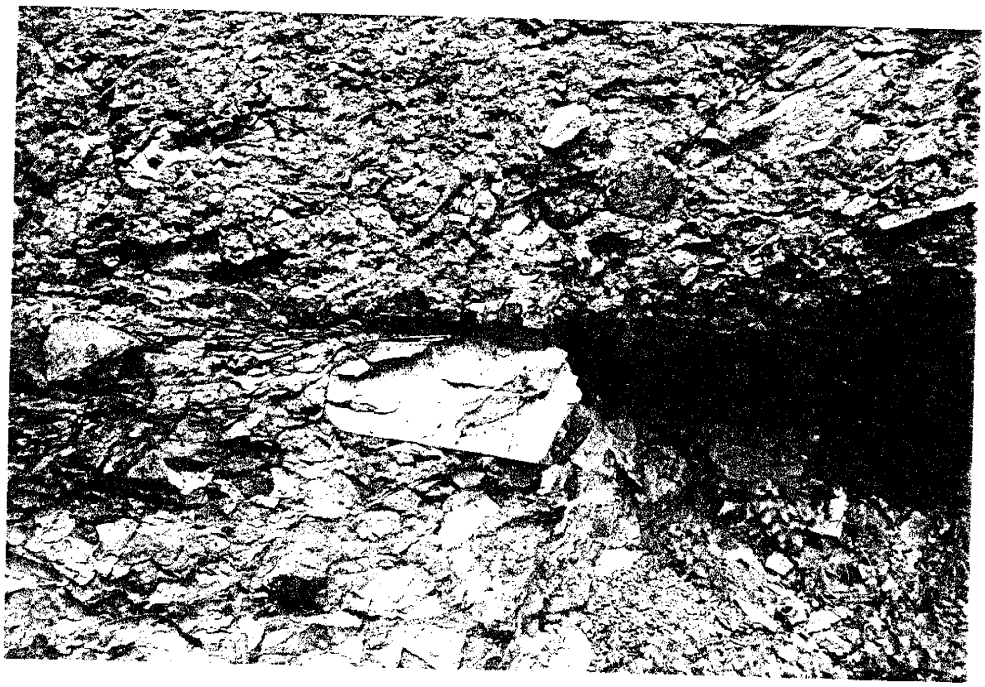

Figure 36. Outcrop of a relatively well-bedded part of the volcaniclastic member of the Rock Spring Formation. (Looking northeast in the NE/4 of the NE/4 of section 14, T9S, R6W, N.M.P.M.).

felsic lava flows and dikes are found in the member in western exposures. A possible vent for the member is exposed on the side of a steep canyon in the NW corner of section 14, T9S, R6W, N.M.P.M.

The member is thickest in the SW/4 of section 10, T9S, R6W, where it reaches a maximum thickness of 400 feet (125 m). It thins abruptly to the northwest, and has a variable thickness eastward toward the Rock Spring fault. The member is only about 50 feet (15 m) thick east of the Rock Spring fault and is of a distinctively different character, being composed of lava flows and/or finer grained lithic-rich flow-breccias with no apparent mud or clay material within the matrix. In the northwest part of the field area the member is missing or consists of thin discontinuous horizons of thinly bedded and cross-bedded volcaniclastic litharenite.

Figures 37 A and B illustrate the clastic nature of the matrix of the volcaniclastic member. The rock consists of angular to rounded, altered lithic fragments from 0.5 mm to 1.5 cm (up to 1 m in outcrop), in a clastic matrix. The matrix consists of grains and irregular patches of opaques, angular to subrounded quartz (0.1-0.75 mm), angular to subrounded alkali feldspar (0.1-0.25 mm), and rounded grains of plagioclase up to 0.3 mm long. The presence of clay (sericite and kaolinite?) pseudomorphs after feldspar up to 0.5 mm in size, anhedral polycrystalline blebs of

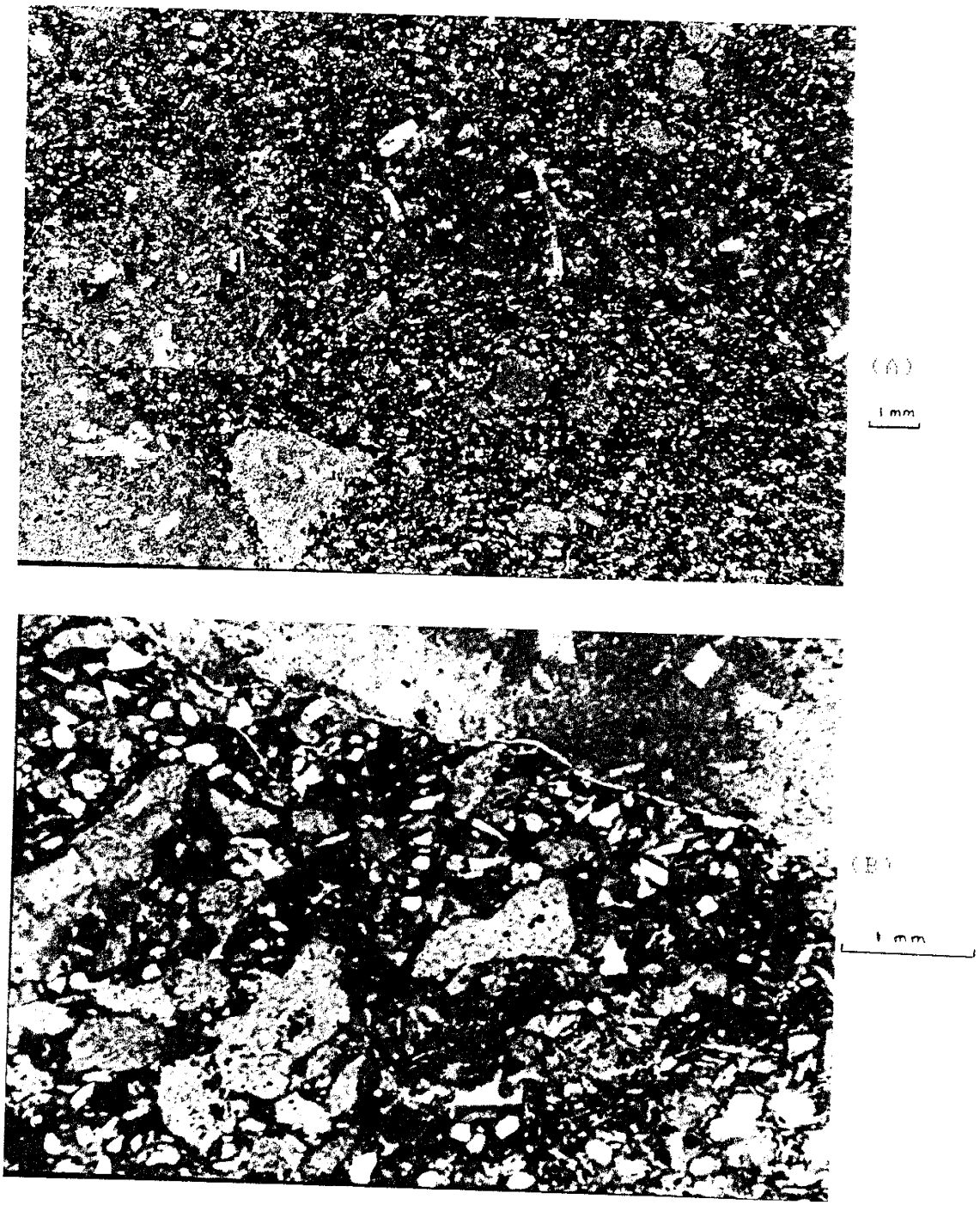


Figure 37. Photomicrographs of the volcaniclastic member of The Rock Spring Formation. A. Crossed polars. B. Plane polarized light.

calcite (pseudomatrix?) up to 1 mm across, and cryptocrystalline clay (smectites?) dusted with minute hematite crystallites in the groundmass indicates post-depositional alteration and/or diagenesis of the rock.

**Zeolitic Andesite Member.** The informal name zeolitic andesite member of the Rock Spring Formation is proposed for a series of gray and blue-gray altered fine-grained vesicular and amygdaloidal lava flows exposed over a relatively small area in Shipman Canyon in the central part of section 9 and in part of section 10, T9S, R6W, N.M.P.M. Exposures of the member east of Shipman Canyon are limited due to extensive talus cover.

Near Shipman Canyon the member unconformably overlies a hornblende-bearing andesite in the upper andesite member and is overlain by the La Jencia Tuff. To the east in the south central part of section 10, T9S, R6W the andesite is underlain by the volcaniclastic member of the Rock Spring Formation; the member pinches out under the La Jencia Tuff in this vicinity. Northwest of Shipman Canyon the member is concealed by alluvial fan sediments except in a small outcrop in the NW/4 of section 9, T9S, R5W, N.M.P.M. Here it is overlain by the Vicks Peak Tuff to the east and in fault contact with the Vicks Peak Tuff to the west.

In outcrop, the member is generally slope-forming, poorly to moderately well-indurated, massive to slabby and

ranges in color from purple-gray to blue-gray. Outcrops in Shipman Canyon are typically poorly indurated, and have a rough, bleached appearance. Outcrops of the member east of Shipman Canyon are generally less weathered and more indurated but show evidence of extensive zeolitization and/or propylitization. Preferentially oriented vesicles filled with radiating groups of acicular white zeolite crystals give the rock a spotted flow-banded appearance locally. Chloritization of the groundmass gives the rock a blue-green tint in some outcrops. Tabular, transparent, red zeolite crystals with a similar morphology to feldspar phenocrysts can be found locally. Hand specimens of the member are generally nondescript light blue to blue-gray, fine grained or aphanitic (and possibly originally sparsely porphyritic) amygdaloidal rocks composed of altered plagioclase, pyroxene and opaque oxides with interstitial alteration products.

In thin section, the rock is nearly holocrystalline with a felty texture. The rock is composed of euhedral to subhedral lath shaped, simple twinned, plagioclase up to 0.5 mm long, colorless to light green euhedral to subhedral octagon and lath shaped clinopyroxene crystals up to 0.5 mm long, euhedral microlites and intergranular anhedral dendritic and skeletal crystals of opaque oxides up to 0.4 mm long, and interstitial cryptocrystalline pyroxene or alteration products.

Irregular elongate vesicles up to 4 mm long are filled with zeolites exhibiting repeated lamellar twinning, which resemble twinning common to the plagioclase feldspars (Figure 38). (The uniaxial character of the zeolites tentatively identifies them as chabazite). Some vesicles are partially filled or lined with drusy calcite.

Plagioclase makes up about 60% of the rock and is partially altered to clays and contains minute opaque inclusions. Clinopyroxene (augite?) makes up about 15% of the rock as simple and complex twinned crystals exhibiting oscillatory and sector zoning and as anhedral interstitial crystals. Opaques make up about 15% of the rock as euhedral crystals and as partial replacements of pyroxene crystals.

**La Jencia Tuff.** Regionally the La Jencia Tuff is a multiple-flow, compound cooling unit, ash-flow tuff exposed extensively throughout the northeast Mogollon-Datil volcanic field. The La Jencia Tuff is thought to be from the simultaneous eruption of the Sawmill and Magdalena Cauldrons (Osburn and Chapin, 1983).

Within this area, the La Jencia Tuff occurs as thin discontinuous lenses below the Vicks Peak Tuff in the south-central part of the map area. The thickest exposures of the tuff occur on the south side of Shipman Canyon in the western part of section 9, T9S, R6W, N.M.P.M. In this


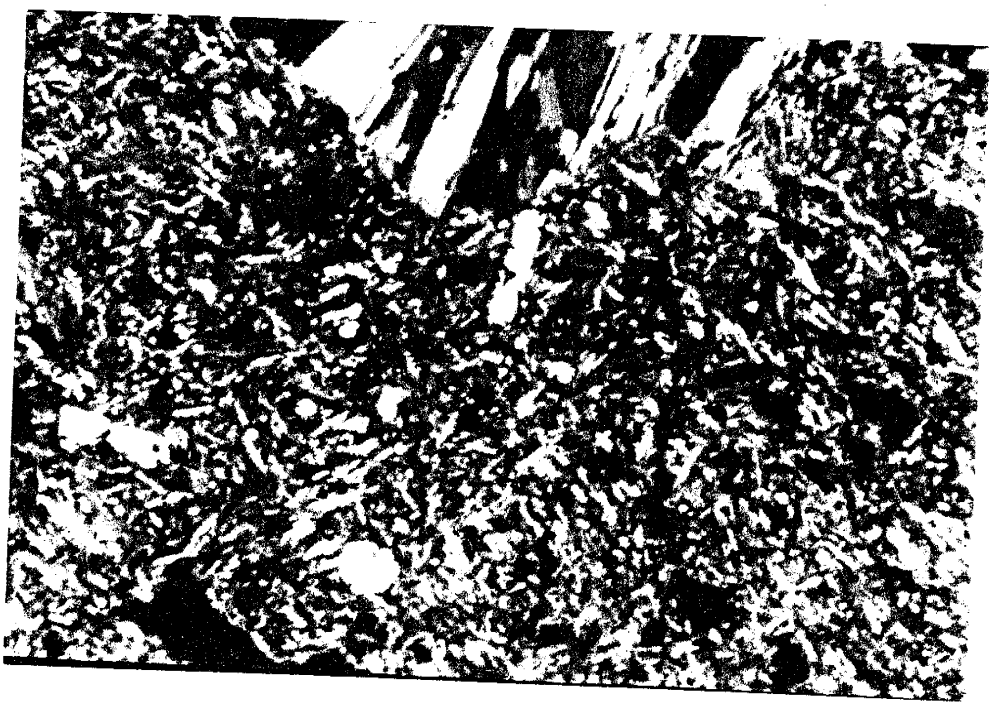


Figure 38. Photomicrographs of the zeolitic andesite member (crossed polars).

area, it reaches a thickness of about 60 feet (18 m). The tuff is composed of a lower moderately welded and an upper densely welded zone, and overlies a thin zone of interbedded volcaniclastic sediments (Figure 39). Eastern exposures of the tuff consist of discontinuous outcrops of welded, moderately crystal-rich tuff overlying the volcaniclastic member of the Rock Spring Formation.

Minor discontinuous lenses of crystal-poor gray tuff and Liesegang-banded material can be found above and below the tuff locally. These horizons may represent early and late flow units or air-fall tuffs related to the eruption of the La Jencia or Vicks Peak Tuffs.

Lower portions of the tuff vary in color from buff to light red-brown. Upper welded parts of tuff are usually chocolate-brown, purple-brown or dark brick-red. Crystal content is somewhat variable ranging from a few percent in lower portions to 15 percent in the upper welded zone. Highly flattened pumice in the upper welded zone give the rock a fluidal eutaxitic appearance locally.

Hand specimens of the welded zone are porphyritic with phenocrysts of sanidine up to 1.5 mm, sparse biotite up to 1 mm, and minor quartz in a red-brown fluidal groundmass. In thin section, the rock is porphyritic with phenocrysts of sanidine, plagioclase, quartz, biotite, pyroxene and opaques in a groundmass of axiolitic shards, lithic fragments, calcite, opaques and biotite (Figure 40).

Figure 39. Outcrops of the basal La Jencia Tuff, overlying volcaniclastic sediments in Shipman Canyon, looking northeast in the SW/4 of the NE/4 of section 9, T9S, R6W, N.M.P.M.

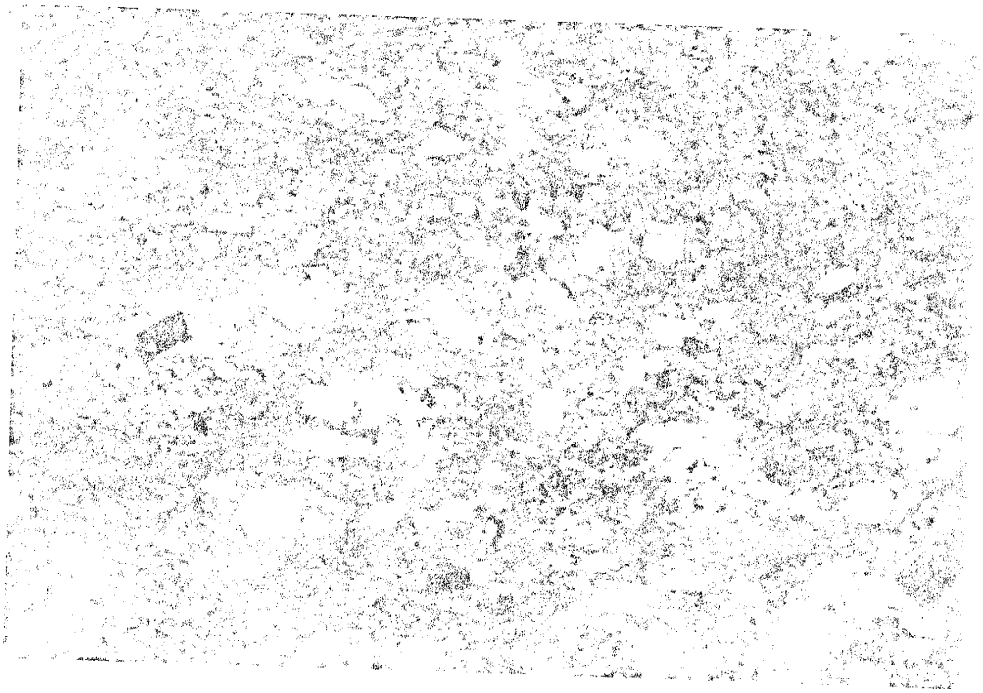

1 mm

Figure 40. Photomicrograph of the La Jencia Tuff (crossed polars).

Sanidine phenocrysts make up about 8 % of the rock as euhedral to subhedral simple twinned blocks and fragmental crystals up to 1 mm. Some exhibit a glomerocrystic habit and undulatory extinction. Plagioclase (An 10) makes up about 2 % of the rock as subhedral to anhedral simple twinned blocks and fragments up to 1 mm long. Some of the crystals have perthitic intergrowths and are partially replaced by calcite. Quartz phenocrysts make up about 1 % of the rock as anhedral, fragmental and polycrystalline grains up to 0.4 mm in diameter.

Biotite makes up less than 1 % of the rock as subhedral books up to 0.5 mm long. Pyroxene phenocrysts make up less than 1 % of the rock as anhedral crystals up to 0.5 mm in size rimmed by clays and calcite. Opaque phenocrysts make up less than 1 % of the rock as euhedral hexagons and blocks and as irregular anhedral patches up to 0.3 mm in size. Lenticular, devitrified pumice fragments up to 2 mm X 1 cm make up about 8 % of the rock, and altered fine-grained and porphyritic lithic fragments make up as much as 2 percent.

The groundmass of the rock consists of devitrified microcrystalline and cryptocrystalline axiolitic shards dusted with hematite and opaque crystallites along with irregular interstitial areas of calcite up to 1 mm across (secondary alteration). Shard structures often wrap around phenocrysts and lithic fragments and show a preferred

planar alignment giving the rock a micro-eutaxitic appearance in thin section.

## POST ROCK SPRING FORMATION DEPOSITS

A sequence of ash-flow tuffs, air-fall tuffs, rhyolite lavas, and volcaniclastic rocks lie above the Rock Spring Formation. The units overlie the La Jencia Tuff of the Rock Spring Formation where it is present and are overlain by the terrace gravels (Qtg) and Alluvium (Qal). Two ash-flow tuffs, the Vicks Peak Tuff and the tuff of Turkey Springs have been dated by high-precision $^{40}Ar/^{39}Ar$ methods. The Vicks Peak Tuff has been determined to be 28.46 Ma by Kedzie (1984). The tuff of Turkey Springs has been dated at 24.3 Ma (McIntosh 1986). A diagrammatic representation of the stratigraphy of the post-Rock Spring Formation deposits is presented in Figure 41.

**Vicks Peak Tuff.** The Vicks Peak Tuff is a densely-welded, multiple-flow, single cooling unit, crystal poor ash-flow tuff (ignimbrite) sheet exposed throughout the northeast Mogollon-Datil volcanic field. The thickest documented exposures of the Vicks Peak Tuff occur in the southern San Mateo Mountains. Deal and Rhodes (1976) have suggested that the source cauldron for the Vicks Peak Tuff (Nogal Canyon Caldera) is located near the southern end of the mountain range. An arcuate pattern of intrusive bodies (mapped by Farkas, 1969) is observable on Landsat images in this region.

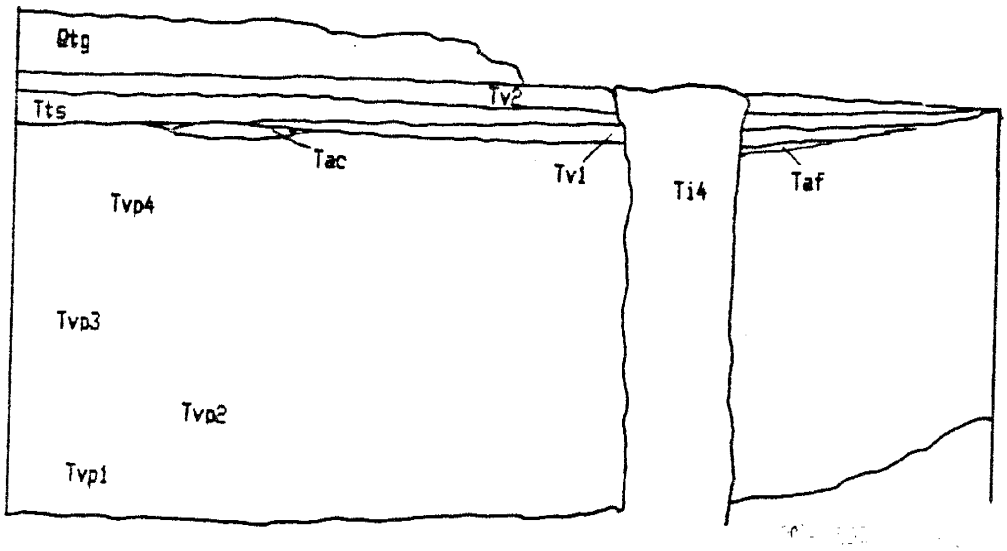


Figure 41. Diagrammatic stratigraphy of the post Rock Spring Formation deposits. Only relative lateral and vertical relationships are implied. Refer to Table 1 and Plate 1 for symbols used.

Reconnaissance indicates that a moderately thick section of Vicks Peak Tuff (>1500 ft.) is present in the southeastern parts of Deal and Rhodes' proposed Nogal Canyon Caldera, which has been generally accepted as the source of the Vicks Peak Tuff. The present study indicates that the thickness of the Vicks Peak Tuff increases dramatically northward in the vicinity of the northwestern boundary of Deal and Rhodes' Nogal Canyon Caldera. This indicates that a revision in the total areal extent and possibly a northwestward shift in the location of the caldera boundaries is necessary.

Exposures of outflow facies Vicks Peak Tuff have been described from the Joyita Hills, the northern Jornada del Muerto, and the Magdalena, Lemitar, Bear, Datil, and Gallinas Mountains (Osburn and Chapin 1983). Deposits of the Vicks Peak Tuff up to 300 feet (90 m) thick have been found as much as 60 miles (95 km) northeast of the proposed source area (Osburn et. al. 1986). Typical thicknesses of distal outflow Vicks Peak Tuff range from a few feet to 800 feet (300 m).

Proximal outflow and possible cauldron-fill deposits of Vicks Peak Tuff have been described by Furlow (1965), Farkas (1969), Atwood (1982), Foruria (1985), and Ferguson (1985) in the San Mateo Mountains and by Maldonado (1974) in the northern Sierra Cuchillo. Typical proximal deposits range in thickness from 100 feet (30 m) to 2000 feet (650

m). Deposits considered to be cauldron facies were thought to be more than 2000 feet (650 m) thick (Deal and Rhodes 1976).

The Vicks Peak Tuff is the most extensive and thickest volcanic rock-stratigraphic unit exposed within the study area; it covers a area of about 11 square miles, and reaches a maximum estimated thickness of 4000 feet (1370 m). Within the study area the Vicks Peak Tuff displays lateral variations in thickness. The thickest exposures (4000 feet) lie to the northwest of the Rock Spring fault; east of the Rock Spring fault the Vicks Peak Tuff reaches a maximum estimated thickness of 2000 feet (650 m). Diagrammatic stratigraphic columns of the Vicks Peak Tuff are presented in Figure 42.

Joint styles and erosion patterns in the Vicks Peak Tuff vary in vertical section. The lower part of the tuff is typically intensely and chaotically jointed, and forms slopes. This slope-forming zone is generally 200 feet (65 m) thick where the Vicks Peak Tuff is thickest.

The middle and upper parts of the Vicks Peak Tuff usually exhibit crude columnar jointing and form steep cliffs. A middle slope-forming zone is present west of the Rock Spring fault in the middle of the thick section of the Vicks Peak Tuff in an interval containing lithic-rich breccias and intercalated andesites.

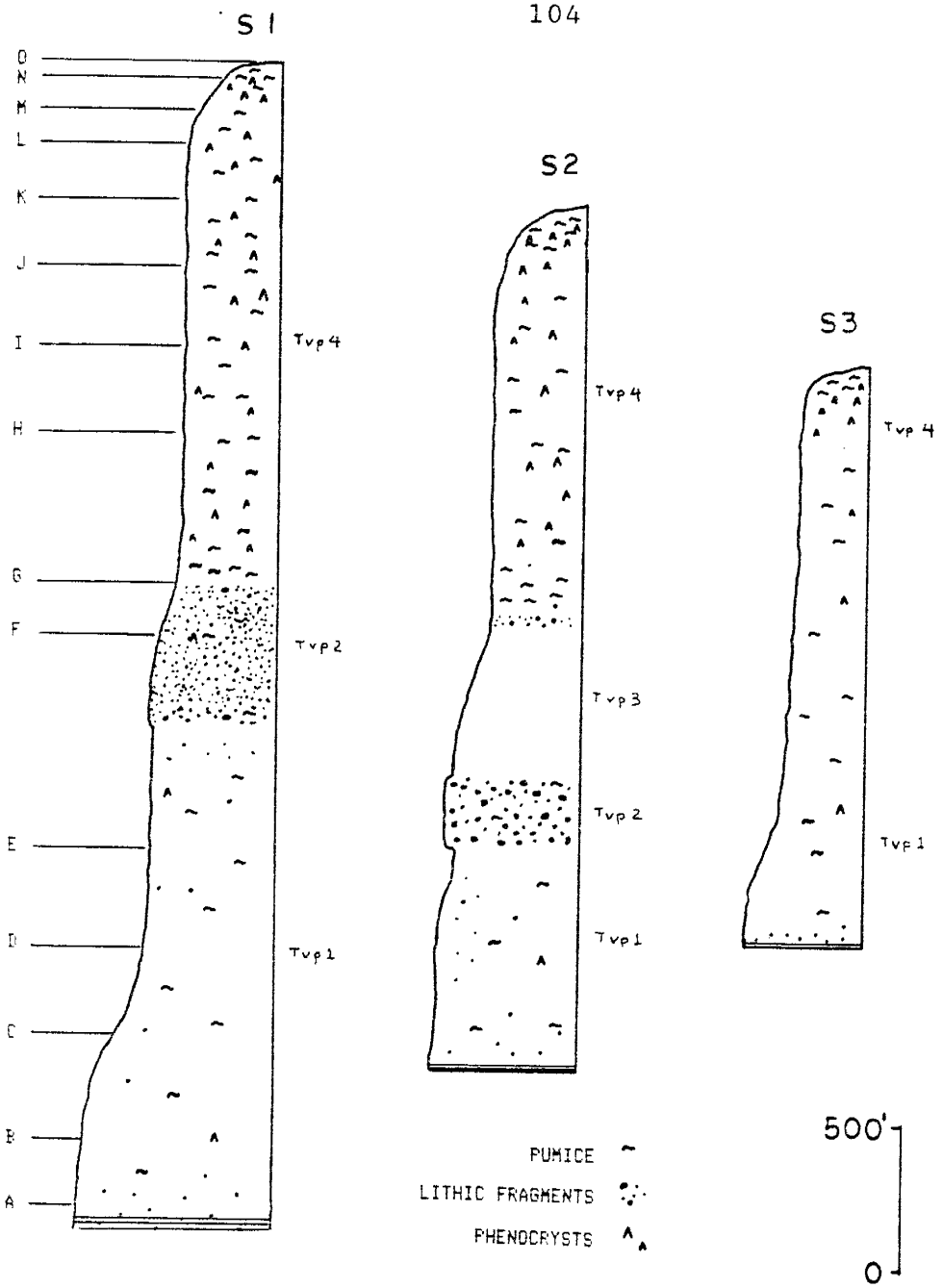


Figure 42. Diagrammatic sections of the Vicks Peak Tuff. S-1. North-central part of the study area. S-2. Between Vicks Peak and the Rock Spring fault. S-3. East of the Rock Spring fault. Letters in S-1 represent stratigraphic levels for samples illustrated in Figure 46.

Phenocryst content of the Vicks Peak Tuff also varies in vertical section. The lower part of the tuff typically contains less than one percent phenocrysts of sanidine. Phenocryst content increases upward in the tuff to 10 percent in the uppermost exposures. Traces of biotite are also found in the upper zones of the Vicks Peak Tuff.

Figures 43-45 illustrate outcrops of the Vicks Peak Tuff at different levels east of the Rock Spring fault. Illustrations of hand specimens of the Vicks Peak Tuff taken from various levels of the proposed cauldron fill deposits are shown in Figures 46 A-O.

Photomicrographs of thin sections from various levels in the proposed cauldron fill deposits of the Vicks Peak Tuff are presented in Figures 47 A-F. The devitrified nature of the tuff overall, along with the general increase in phenocryst content upward in the tuff are illustrated.

Dense welding extends to the base of the Vicks Peak Tuff. Exposures of poorly welded upper Vicks Peak Tuff within the study area are restricted to the area west of the Deep Canyon fault in the northwestern part of the mapped area.

Devitrification has apparently taken place in all but the uppermost portions of the tuff. Evidence of vapor phase mineralization is present, but more obvious in outcrop in the upper portions of the tuff where large gas cavities have remained relatively un-flattened.

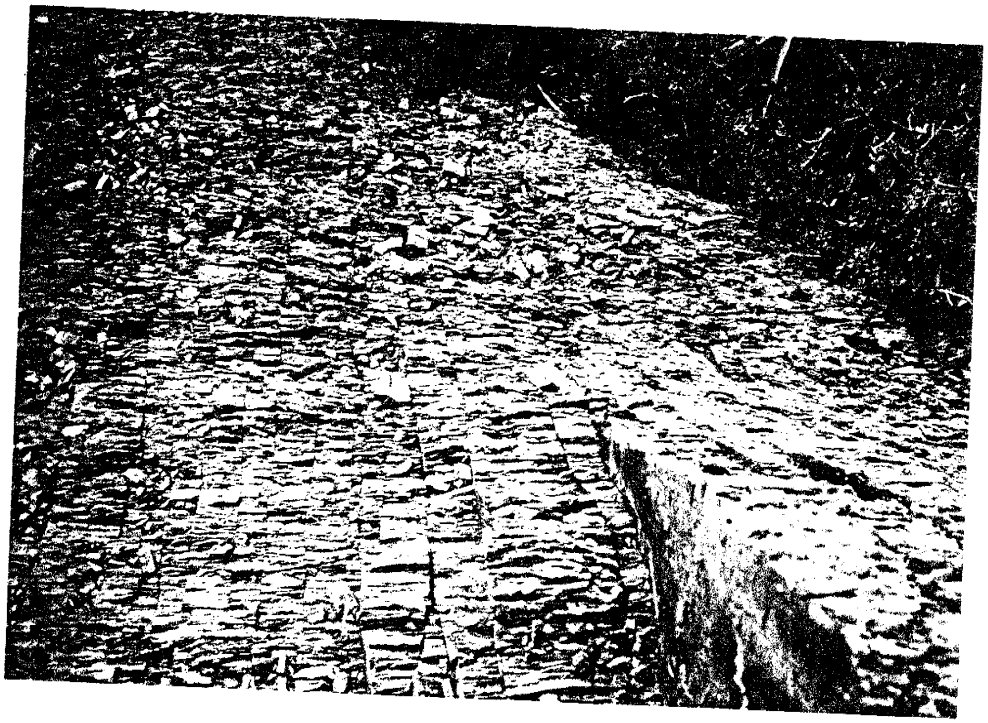

Figure 43. Intensely jointed outcrop of the lower Vicks Peak Tuff (Tvp1). Looking west in the SW/4 of section 11, T9S, R6W, N.M.P.M.

Figure 44. Outcrop of the lithic-rich zone of the Vicks Peak Tuff (Tvp2). Looking west in the SE/4 of the NW/4 of section 11, T9S, R6W, N.M.P.M.

Figure 45. Columnar-jointed outcrops of the upper Vicks Peak Tuff (Tvp3). Looking north from the east side of Shipman Canyon (SW/4 of section 3, T9S, R6W, N.M.P.M.

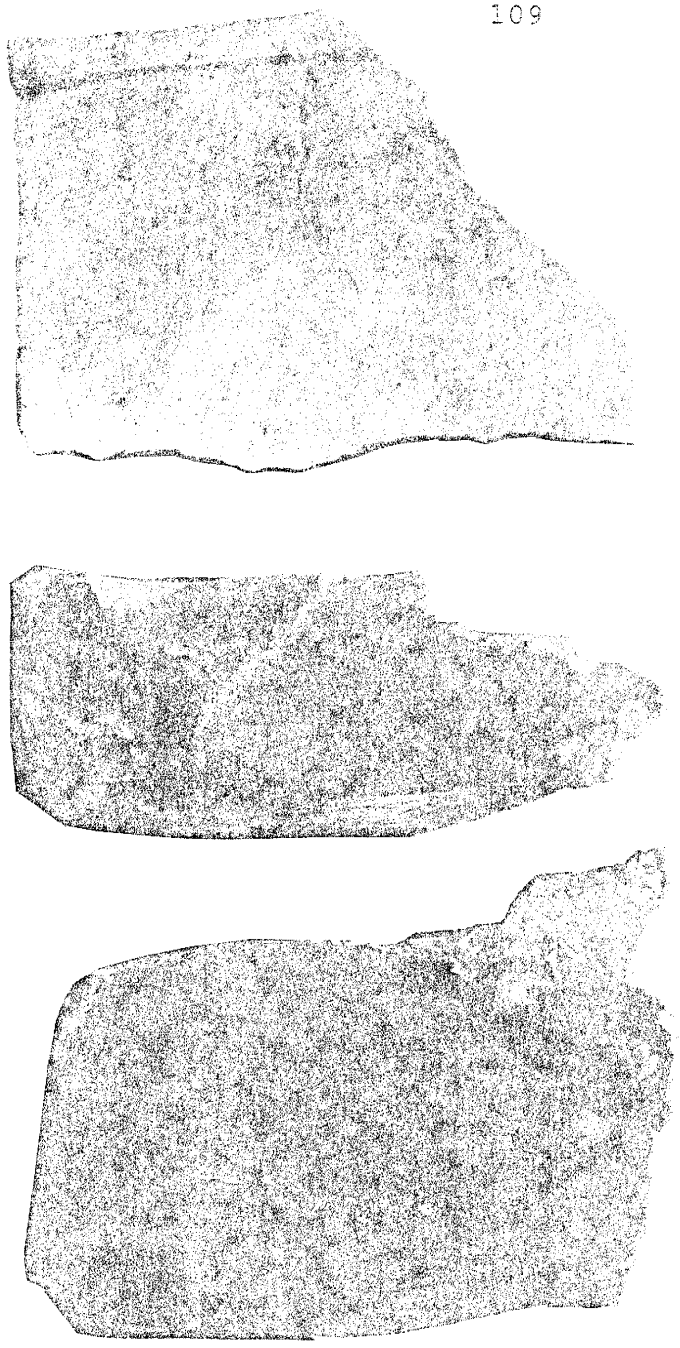


Figure 46. Hand specimens of the Vicks Peak Tuff taken at different levels above base. Shown at actual size.

Letters coincide with those shown in Figure 41 . (Samples taken along Shipman Canyon in sections 9, 10, 2, and 3. T9S, R6W, N.M.P.M.

F.

E.

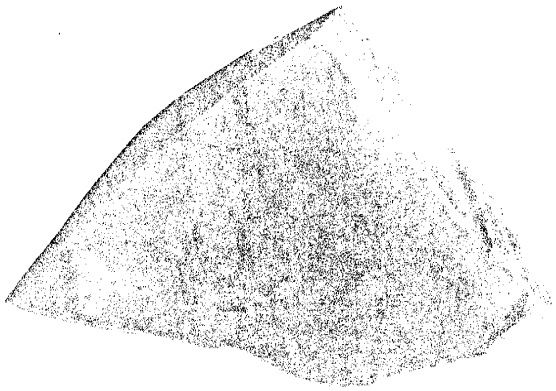

D.

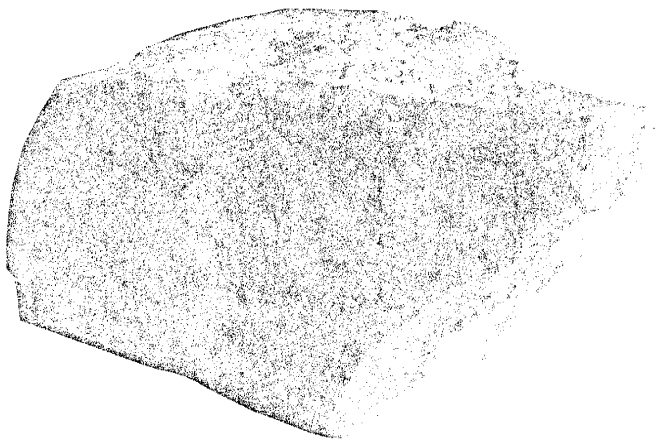

Figure 46 continued.

I.

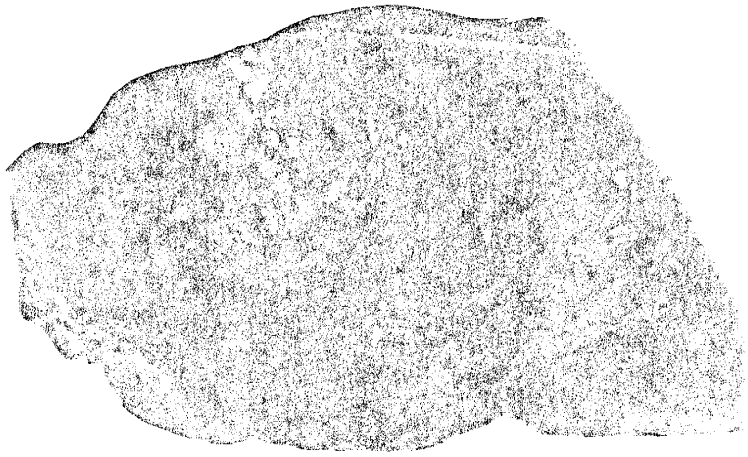

H.

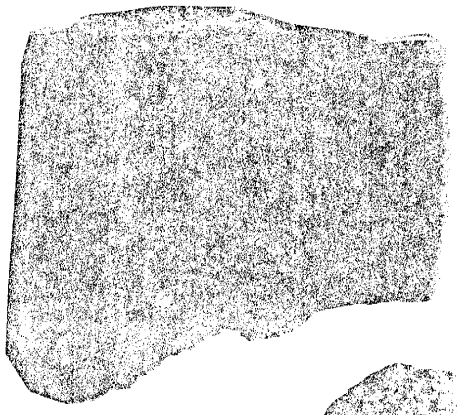

G.

Figure 46 continued.

L.

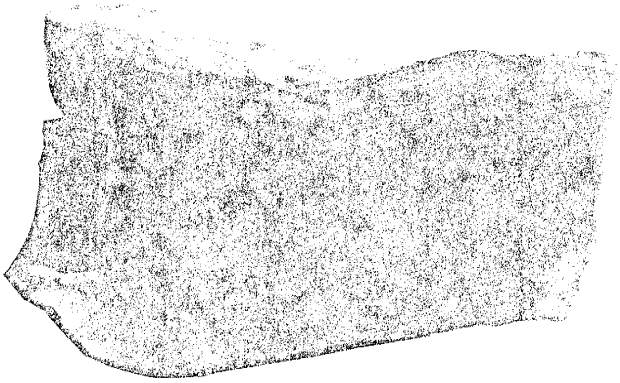

K.

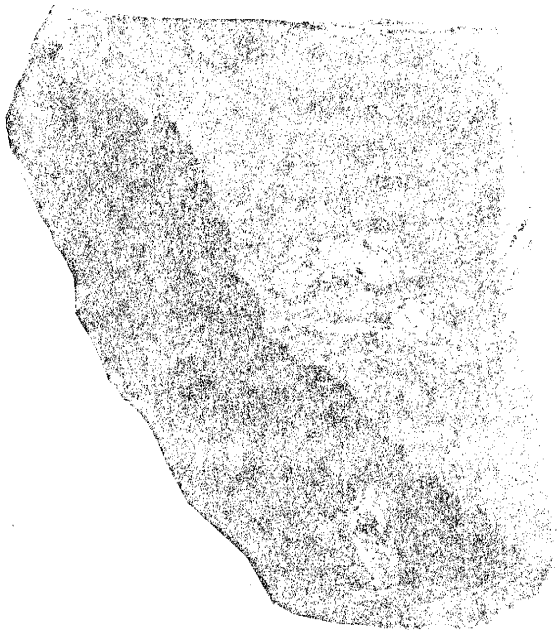

J.

Figure 46 continued.

O.

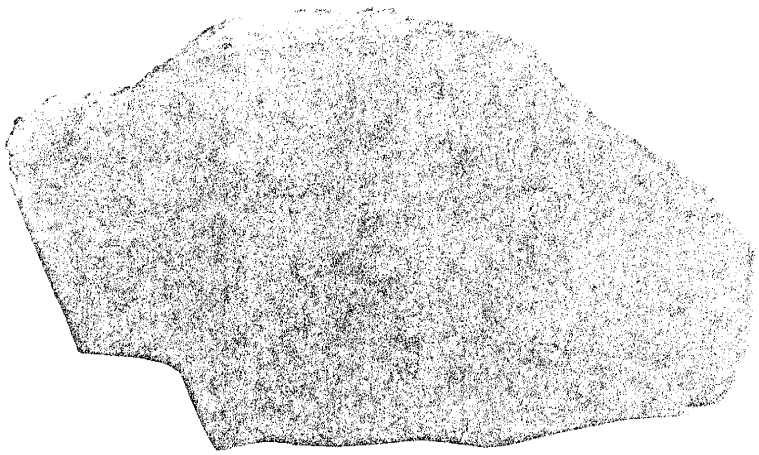

N.

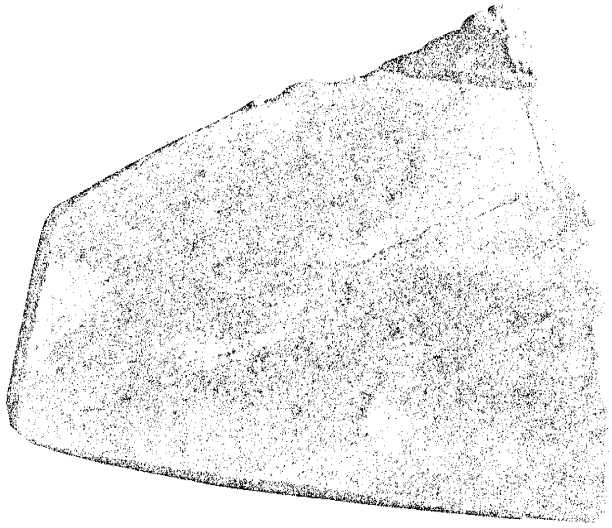

M.

Figure 46 continued.

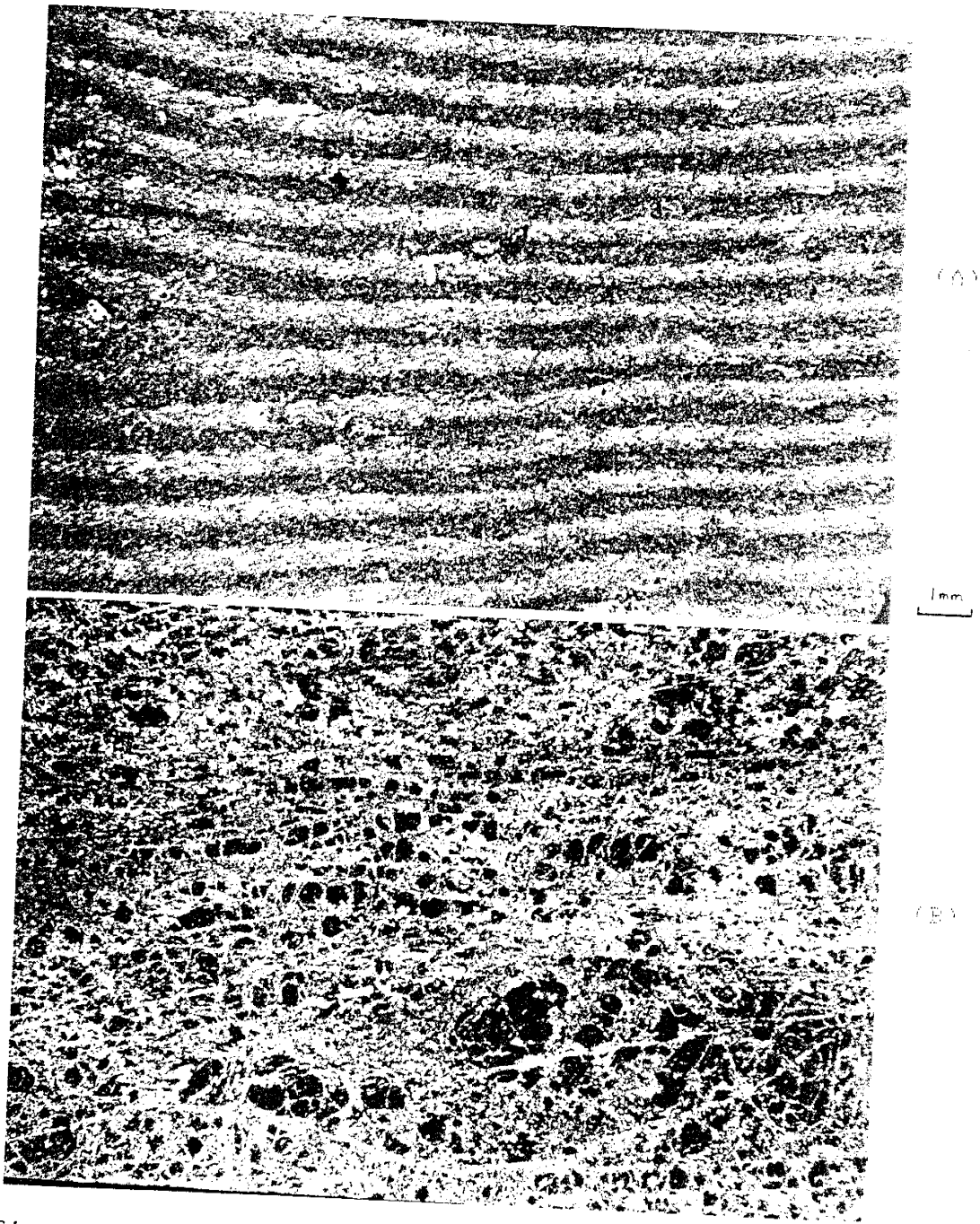


Figure 47. Photomicrographs of samples of the Vicks Peak Tuff taken at various levels. A. Basal liesegang banded zone (crossed polars). B. Perlitic zone (crossed polars).

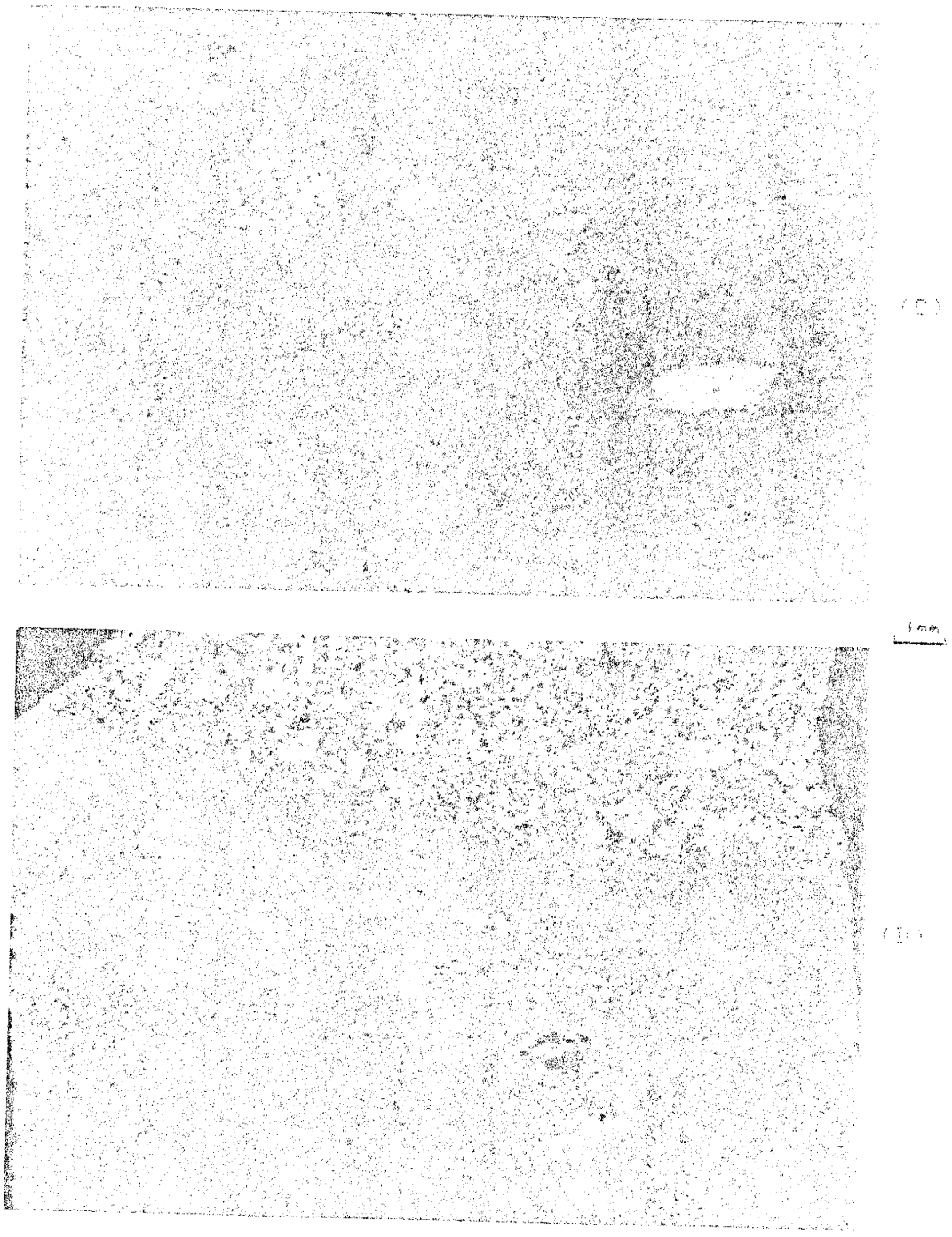


Figure 47 continued. C. Densely welded lower zone (crossed polars). D. Densely welded part below lithic rich zone (crossed polars).

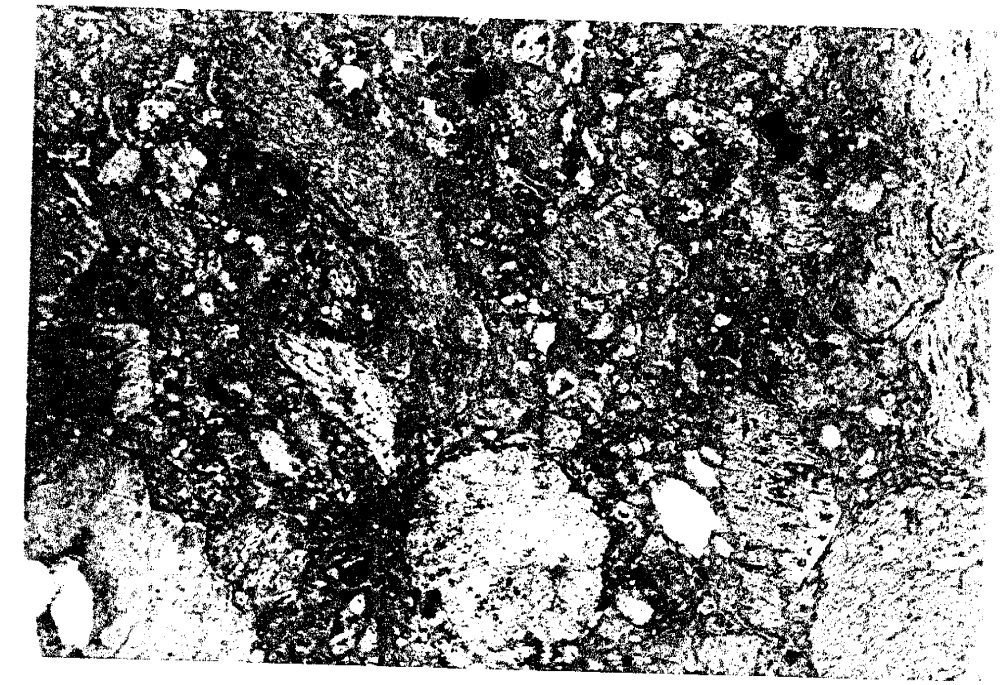

(E)

1mm

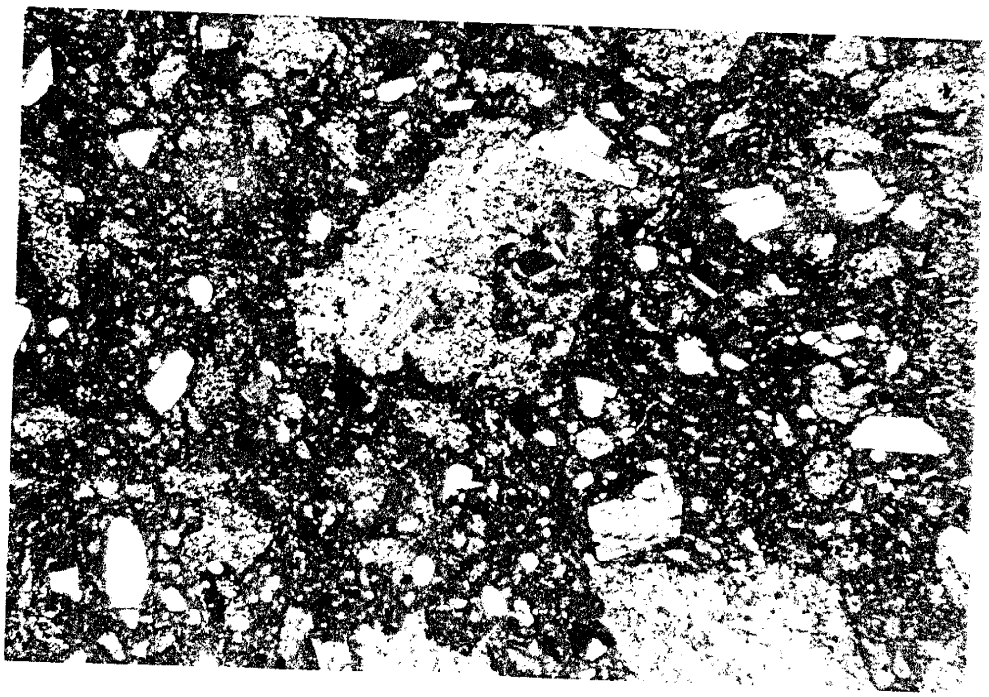

(F)

Figure 47 continued. E. Lithic rich zone (plane polarized light). F. Upper crystal rich zone (crossed polars).

The thickest and most complete section of the Vicks Peak Tuff exposed within the study area occurs on a gently eastward dipping fault block lying to the northwest of the Rock Spring fault and east of the Deep Canyon fault in sections 2, 3, 9, 10, and 11, T9S, R6W, N.M.P.M. In this area the Vicks Peak Tuff lies conformably above the La Jencia Tuff or unconformably above deposits of the upper Rock Spring Formation. The estimated thickness of the Vicks Peak Tuff on this fault block is 4000 feet (1200 m). The uppermost portions of the tuff may have been removed by erosion at Vicks Peak, and could possibly be represented in outcrops down-dip to the east of the study area and in outcrops west of the Deep Canyon fault. The upper Vicks Peak Tuff (bottom unexposed) is overlain by the tuff of Turkey Springs on a down-dropped fault block west of the Deep Canyon fault in sections 6 and 7, T9S, R6W, and sections 19, 20, 30, and 31, T8S, R6W, N.M.P.M.

The upper tens or hundreds of feet of the Vicks Peak Tuff present west of the Deep Canyon fault may be similar to portions of the Vicks Peak Tuff which have been eroded from the top of the well-exposed section near Vicks Peak. Adding this thickness could make the maximum pre-erosional thickness of the Vicks Peak Tuff as much as 4500 feet (1370 m).

The Vicks Peak Tuff thins abruptly to the southeast across the Rock Spring fault to a thickness of about 2000

feet (650 m). Various compositional and textural changes in the tuff accompany the thickness decrease across this zone. Although many of the lithologic changes in the Vicks Peak Tuff are gradational in nature, the presence of a laterally continuous lithic-rich horizon (northwest of the Rock Spring fault), along with a corresponding upward increase in phenocryst and pumice content, (in the tuff overall) allows the tuff to be subdivided into up to three units: 1. a lower crystal-poor zone, 2. a middle lithic-rich zone, and 3. an upper pumice and more crystal-rich interval. Near the Rock Spring fault another unit, the intercallated andesite sequence, is also present. Areas east of the Rock Spring fault and in the northern part of the map area can be divided into two units, a lower crystal-poor unit and an upper crystal-rich unit.

Sparse lithic fragments can be found in the lower portions of the Vicks Peak Tuff on both sides of the Rock Spring fault, but are generally more abundant to the northwest. A laterally continuous lithic-rich zone up to 200 feet thick is present northwest of the Rock Spring fault. Lithic fragments become coarser and increase in abundance as one nears the Rock Spring fault. Angular fragments as large as 1 m in diameter are not uncommon in the vicinity of the Rock Spring fault (between Rock Spring and Turkey Spring) but only 2 miles to the northwest in Shipman Canyon lithic fragments larger than 1 inch in what

is interpreted as being the same stratigraphic horizon are rare.

West of the Rock Spring fault a series of altered andesitic flows rest above this lithic-rich interval. These andesites reach a thickness of 500 feet near the Victorio mines in section 11 T9S, R6W, N.M.P.M., and apparently pinch out toward Shipman Canyon to the west. A lens of andesitic material up to 10 feet thick is also present below the well developed lithic rich zone. Megascopically the andesites are very similar to rocks encountered in the upper andesite member of the Rock Spring Formation or the andesite flow member of the Rock Spring Formation. West of the Rock Spring fault a thin discontinuous lithic-rich interval, and glassy perlitic horizon is present above the andesite lavas. This zone could possibly represent a cooling break and be evidence for a two-stage eruption of the Vicks Peak Tuff. However, evidence for a corresponding cooling break east of the Rock Spring fault could not be found.

Flattened pumice with well-preserved tube structures rarely shows stretching or preferred orientations over large areas within lower parts of the Vicks Peak Tuff northwest of the Rock Spring fault. Many of the primary features are obscured, apparently by welding and devitrification of the Vicks Peak Tuff. Flow grooves,

stretched gas cavities and elongated pumice are more common within the upper parts of the Vicks Peak Tuff.

The thick lithic-rich zone, the series of andesites, and part of the sequence of crystal-rich, columnar-jointed and layered Vicks Peak Tuff are apparently missing from the section southeast of the Rock Spring fault. This suggests that deposits produced mostly from the early and late stages of the eruption are represented east of the Rock Spring fault. This may also indicate that a large propotion of late stage erupted material may be confined within a deeper subsided part of the Nogal Canyon Caldera.

The lithology of the clasts in the lithic-rich breccias exposed northwest of the Rock Spring fault are progressively older up section. The lithic fragments in the lower portions of the interval consist primarily of angular fragments of crystal-poor, densely welded Vicks Peak Tuff very similar to the matrix. Apparently many of them are derived from the altered tuff deposits found at the base of the Vicks Peak Tuff. Many of the fragments of the altered tuff in the lithic-rich zones show a concentric banding. The middle portions of the interval contain a high proportion (up to 50% locally) of angular fragments. The upper portions of the lithic-rich zone contain angular fragments similar to various andesitic members of the Rock Spring Formation. This indicates a possible cauldron collapse origin for the deposits. These breccias were

mapped as a separate flow-unit and mark a change from a crystal-poor and pumice-poor lithology to a more crystal-rich and pumice-rich lithology in the Vicks Peak Tuff.

Limited exposure and extensive alluvial cover over deposits of the upper Vicks Peak Tuff do not allow direct measurement of the thickness west of the Deep Canyon fault. A relatively thick section is assumed due to the proximity of thick Vicks Peak Tuff deposits east of the fault in the northern part of the study area. Down-dropping of strata west of the Deep Canyon fault in the northwestern parts of the study area has apparently preserved the upper and post Vicks Peak Tuff deposits.

**Alamosa Creek Rhyolite.** The name given by Maldonado (1974) is used here for flow-banded rhyolitic lavas exposed in the southwestern part of the study area (NW/4 of Sec. 7, T9S, R6W un-surveyed). Extensive exposures of this or a similar rhyolite lava was mapped by Maldonado (1974) in the southern reaches San Mateo Canyon and along Alamosa Creek. Within the study area the upper contact is erosional.

The rhyolite lavas occur as blue-gray to light gray manganese oxide-stained cliffs and ledges on the southwest side of San Mateo Canyon. Flow banding is evident in many exposures and slit-like vesicles lined with euhedral quartz (locally amethystine) are common.

Hand specimens are typically light blue-gray to whitish and porphyritic. Phenocrysts include euhedral, blocky and tabular, pearly chatoyant sanidine up to 1 cm long (20%), equant, rounded, anhedral to subhedral clear and smokey quartz up to 2 mm in diameter (10%), and sparse biotite and pyroxene (1%). The groundmass of the rock is light gray with patchy spherulitic, fine-grained and aphanitic areas containing euhedral opaque crystals, and minute dendritic patches of manganese oxides.

The member superficially resembles the upper parts of the Vicks Peak Tuff due to similarities in vapor phase and devitrification mineralization, but undulatory flow-bands, the presence of rounded quartz phenocrysts, flow grooves, tension cracks, and localized contorted and overturned folds (Figure 48) help identify this as a rhyolite lava.

In thin section, the rock is porphyritic with phenocrysts of sanidine (20%), quartz (10%), biotite (1%) and pyroxene (1%). The groundmass is microspherulitic, aphanitic, microcrystalline (devitrified) and sparsely vesicular and contains radiating quartz-feldspar intergrowths, traces of orthopyroxene, clinopyroxene, opaques, altered biotite and clay alteration products (sericite?) (Figure 49). Irregular, elongate, slit like vesicles are partially filled with coarse quartz-feldspar intergrowths or euhedral quartz crystals.

Figure 48. Outcrop of the Alamosa Creek Rhyolite, looking northwest in San Mateo Canyon (NW/4 of the NW/4 of section 7, T9S, R6W, N.M.P.M.).


Figure 49. Photomicrograph of the Alamosa Creek Rhyolite (crossed polars).

Sanidine phenocrysts up to 5 mm long occur as single, simple and complexly twinned, or glomerocrystic blocky to rounded crystals. Many of the sanidines exhibit corroded, embayed and rimmed margins, as well as replacement perthitic textures.

Quartz crystals up to 2 mm in diameter occur as rounded and embayed anhedral single and polycrystalline phenocrysts. Biotite phenocrysts occur as irregular subhedral and anhedral patches up to 5 mm in size.

**Air-Fall Tuff.** The air-fall tuff is exposed over a small area in the northwest part of the study area in section 20 T8S, R6W, N.M.P.M., un-surveyed. The tuff reaches a thickness of 50 feet (15 m) (bottom unexposed) on the southeast side of San Mateo Canyon near Cookes Cabin, apparently overlies the upper Vicks Peak Tuff, and is overlain by the lower volcaniclastic unit.

The air-fall tuff is cliff-forming and consists of white, light gray and light brown, poorly indurated, thinly bedded air fall tuff. The air-fall tuff is composed of ash-sized glass shards, subhedral and anhedral crystal fragments, ash-sized angular to subrounded dark aphanitic lithic fragments, pumice fragments, and volcanic dust.

In thin section, the unwelded vitroclastic nature of the rock is well preserved (Figure 50). The rock is composed of small pumice fragments, glassy spheres,

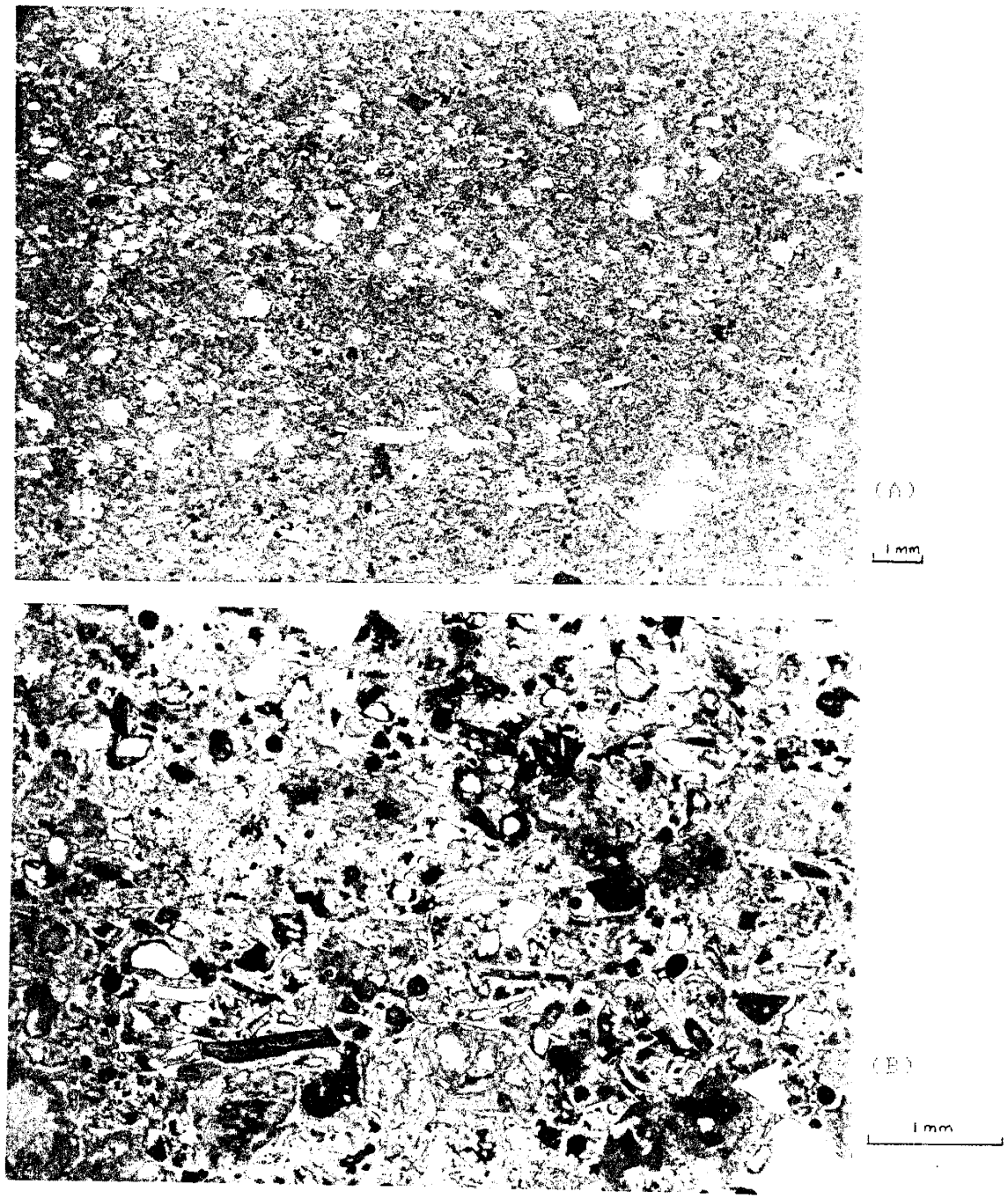


Figure 50. Photomicrographs of the air fall tuff. A. Crossed polars. B. Plane polarized light.

shards, sanidine crystals, opaques, lithic (andesite and latite) fragments, and quartz. Constituents of the rock range from ash to dust-size particles. Glassy particles, shards, and pumice fragments make up about 70% of the rock. Sanidine, opaques, and quartz make up 20% of the rock and rock fragments make up as much as 10% of the rock.

**Lower Volcaniclastic Unit.** The lower volcaniclastic unit is exposed on the east side of San Mateo Canyon just south of Milo Canyon. The unit lies above the air-fall tuff and below the tuff of Turkey Springs in section 20, T8S, R6W, N.M.P.M., un-surveyed.

The lower volcaniclastic unit consists of interbedded clast- and matrix-supported conglomerates, with minor altered air-fall tuffs, volcaniclastic breccias, and mudstones (Figure 51). The lower volcaniclastic unit is typically poorly sorted and poorly indurated. Abundant subangular and rounded fragments of dense purple rhyolite up to 1 foot in diameter in the lower parts of the unit help distinguish this sequence from the upper volcaniclastic unit.

The unit is interpreted to be locally derived alluvial fan material (fanglomerates). Reconnaissance indicates more extensive and thicker exposures north of the study area.

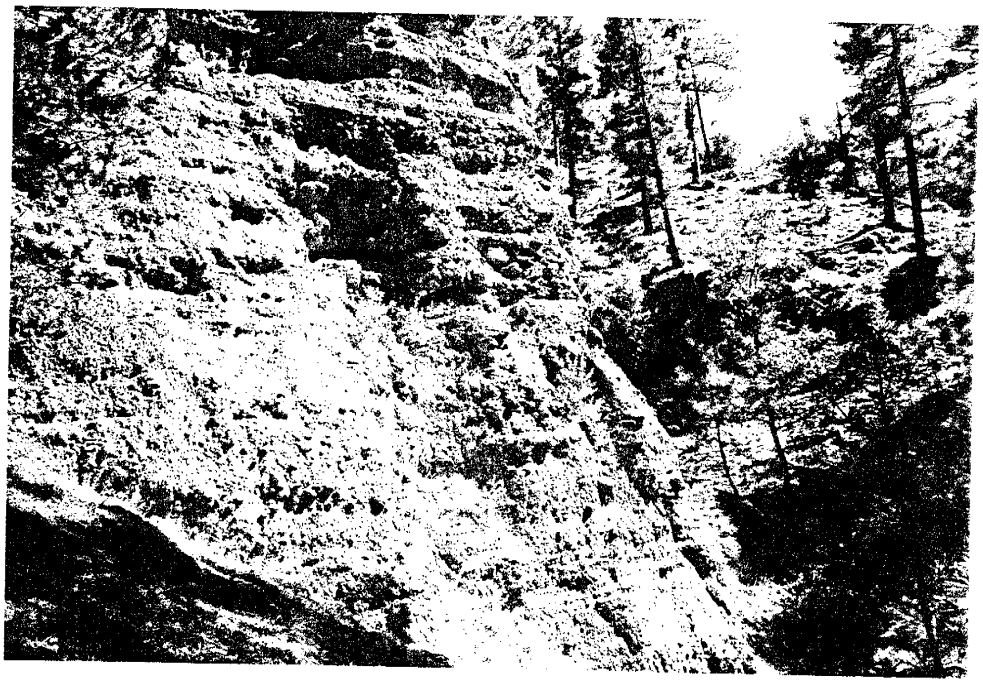

Figure 51. Outcrop of the lower volcaniclastic unit, looking east in San Mateo Canyon (central part of section 20, T8S, R6W, N.M.P.M.).

**Tuff of Turkey Springs.** The tuff of Turkey Springs is a multiple-flow, single cooling unit, ash-flow tuff exposed in the northwest part of the study area in sections 17, 18, 19, and 20 T8S, R6W, un-surveyed. Paleomagnetic pole positions indicate that the tuff is the tuff of Turkey Springs described by Ferguson (1986) who mapped and described the unit in the central San Mateo Mountains.

The tuff displays lateral and vertical zonation in color, mineralogy, thickness, and degree of welding. East of San Mateo Canyon the tuff lies between upper and lower volcaniclastic units and consists of an upper welded and a lower less welded zone. West of San Mateo Canyon the tuff overlies the upper Vicks Peak Tuff, consists of a lower unwelded, and an upper welded zone and is overlain by the upper volcaniclastic unit. In the study area, upper welded zones are generally more quartz rich and biotite-rich than lower parts of the tuff. Lower unwelded parts of the tuff are generally more lithic rich with angular clasts of brown andesite or dark rhyolite fragments (Figure 52).

Pumice content and size is variable in outcrop. Pumice content ranges from a few percent to several percent, and size ranges from a centimeter to 10 cm in length. Pumice fragments are usually flattened with length to width ratios of up to 5 to 1 (Figure 53). Abundant clasts of the tuff of Turkey Springs occur within the upper volcaniclastic unit.

Figure 52. Outcrop of the lower unwelded part of the tuff of Turkey Springs on the west side of San Mateo Canyon in the central part of section 20, T8S, R6W, N.M.P.M.

Figure 53. Outcrop of the middle part of the Turkey Springs Tuff on the east side of San Mateo Canyon in the central part of section 20, T8S, R6W, N.M.P.M.

The tuff of Turkey Springs is cliff or slope forming. The lower unwelded zone is poorly-indurated and white; the upper welded zones are well-indurated and pink. Welded portions usually exhibit crudely to well-defined columnar jointing. Welded rock specimens display sub-conchoidal fracture and shards are visible on fresh surfaces.

In thin section, the lower partially welded zone is porphyritic with phenocrysts of sanidine, plagioclase, quartz, and biotite. Lithic fragments welded ash-flow tuff and pumice are surrounded by a light brown hypohyaline groundmass with glassy and axiolitic shards, crystal fragments of sanidine and biotite, and anhedral opaque minerals. Upper more welded portions of the tuff are generally more crystal rich and have proportionately more sanidine and biotite crystal fragments.

Microscopically the welded zone is porphyritic with phenocrysts of sanidine, quartz, biotite and plagioclase, and lenticular axiolitic welded pumice in a partially devitrified groundmass of partially welded and flattened glass shards, sanidine, quartz and biotite crystal fragments (Figure 54).

Sanidine phenocrysts make up about 6% of the rock as simple twinned euhedral blocks and laths and subhedral and fragmental crystals 0.5 to 1 mm in size. Some of the sanidine crystals appear embayed or corroded and contain plagioclase inclusions up to 0.5 mm long.


Figure 54. Photomicrograph of the tuff of Turkey Springs (crossed polars).

Quartz phenocrysts make up about 3% of the rocks as irregular shaped anhedral single crystals and polycrystalline groups or fragments up to 1.5 mm in size. Biotite phenocrysts make up about 2% of the rock as euhedral to subhedral books up to 0.5 mm long. Plagioclase phenocrysts make up about 1% of the rock as euhedral blocks and laths and anhedral Carlsbad and albite twinned crystals up to 0.5 mm long. Pumice makes up about 10% of the rock as partially devitrified lenticular (partially flattened) fragments up to 4 mm long.

The groundmass of the rock consists of about 80% partially welded shards, 3% ash-sized sanidine crystals, 3% ash-sized quartz crystals and 1% ash-sized biotite crystals. Alignment of flattened shards and lenticular pumice and wrapping of shards around larger crystal fragments give the rock a fluidal banded appearance in thin section.

Upper Volcaniclastic unit. The upper volcaniclastic unit consists of poorly to moderately well-indurated, interbedded, conglomerates, siltstones, mudstones and minor bentonites. These are exposed over a small area in the northwest part of the study area in sections 20 and 29 T8S, R6W, (un-surveyed). The unit lies (conformably?) above the tuff of Turkey Springs, is intruded by the Wild Horse Canyon intrusives (Ti4) and is

overlain unconformably by the terrace gravels and alluvial deposits (Qtg) filling the "Alamosa graben" (east of the Deep Canyon fault).

Abundant angular to rounded clasts of Alamosa Creek flow-banded rhyolite up to .2 m in diameter are scattered throughout the unit. Horizontally continuous layers cemented with opal and chalcedony are present in upper parts of the unit in San Mateo Canyon. This helps to distinguish the upper volcaniclastic unit from the lower volcaniclastic unit and the texturally similar, but younger overlying terrace and alluvial fan sediments (Qtg).

In outcrop, the unit is typically poorly indurated and consists of poorly sorted interbedded conglomerates, sandstones, siltstones and mudstones. Rounded to subrounded clasts up to 1 m in diameter occur in the coarser layers. The upper volcaniclastic unit is interpreted to be locally derived fanglomerates and terrace gravels.

# INTRUSIVE ROCKS

Several types of intrusive rocks are encountered within the study area. Dikes, stocks and minor sill-like bodies cut rocks of all ages and range in composition from basaltic to rhyolitic. The intrusives range from coarse-grained holocrystalline, through porphyritic, aplitic, and aphanitic varieties. Size of individual intrusive bodies seems to be related to the degree of crystallization observed. In general, larger intrusive bodies are coarser and coarse-grained toward their interiors. Several small dikes show vertical flow banding near their margins, and some intrusive bodies have a sheeted or concentric joint pattern sub-parallel to their exterior boundaries. Perturbations of bedding and foliation attitudes in wall rocks surrounding many of the dikes and stocks indicate forceful intrusion.

Generally, the intrusive rocks can be divided into five types:

Diabase stocks and dikes. These rocks are generally dark speckled rocks and are medium-grained and holocrystalline in texture. The rocks consist of plagioclase, chlorite (after biotite?), and altered pyroxene.

Altered dark porphyritic rocks. An irregularly shaped stock of this rock type is exposed northwest of Villa Nerce Spring and is characterized by large blocky epidotized

phenocrysts (after pyroxene?) in a green aphanitic groundmass. This stock cuts the Shipman Spring Tuff, but no cross cutting relationship with other rocks was observed.

Porphyritic biotite-latite dikes. These rocks are light to intermediate colored rocks with phenocrysts of plagioclase (1-2mm), and biotite in a light brown or green groundmass. These rocks are usually found in the Garcia Falls andesite member as dikes up to 50 feet in width.

Fine-grained, aplitic, and sparsely porphyritic felsic (rhyolitic) dikes and small diameter stocks. These rocks are typically limonitic and/or pyritic with phenocrysts of plagioclase (albite after potassium feldspar?) and rounded quartz in a light-colored aphanitic or sugary groundmass. Dikes range from a few inches to 50 feet thick, and stock-like bodies reach up to 100 feet in diameter. These rocks intrude the Vicks Peak Tuff and mafic intrusive rocks and are unconstrained as to minimum age.

Coarse porphyritic and holocrystalline alkali rhyolite (or granitic) stocks. These bodies, up to 1/2 mile in diameter, are characterized by large perthitic phenocrysts in a light colored groundmass of sanidine and dark accessory minerals. Local zones of brecciation, silicification and limonitization are found in these intrusive bodies. The alkali-granite stocks intrude deposits of post-Vicks Peak Tuff age and are apparently the youngest intrusive rocks exposed within the study area.

For mapping purposes intrusive rocks were divided into four categories:

Ti1. Mafic intrusive rocks. Coarse-grained, porphyritic, fine grained, and aphanitic varieties. Dark porphyritic intrusives and diabase stocks and dikes were combined for mapping purposes due to similarities between fine-grained portions of the various lithologies.

Ti2. Porphyritic plagioclase-biotite (chlorite) dikes.

Ti3. Felsic fine grained and porphyritic (rhyolitic) dikes.

Ti4. Alkalai-granite intrusives.

The sequence (Ti1-Ti4) may roughly coincide with the order of intrusion. Order of intrusion is unclear for the intrusive bodies exposed only in the Rock Spring and Red Rock Ranch Formations members. Figures 55 through 59 illustrate some of the intrusive rocks encountered within the study area.

The presence of hydrothermal vent breccias, silicification, and disseminated pyritization of wall rocks in the vicinity of granitic stocks (Ti4) and rhyolitic dikes (Ti3) indicate a possible relation to intrusion and mineralization in the area. Pyritization, epidotization and silicification locally occur where rhyolitic dikes cut earlier mafic intrusives or flows. Epidotization and propylitic alteration of dikes and wall rocks is evident

Figure 55. Outcrop of intrusive stock (Ti-2) in Canon De Quirino (NE/4 of the NE/4 of section 22, T9S, R6W, N.M.P.M.).

Figure 56. Intrusive (Ti-2) against the upper part of the Shipman Spring Tuff, north of Villa Nerce Spring, looking north, in the SE/4 of section 15, T9S, R6W, N.M.P.M.

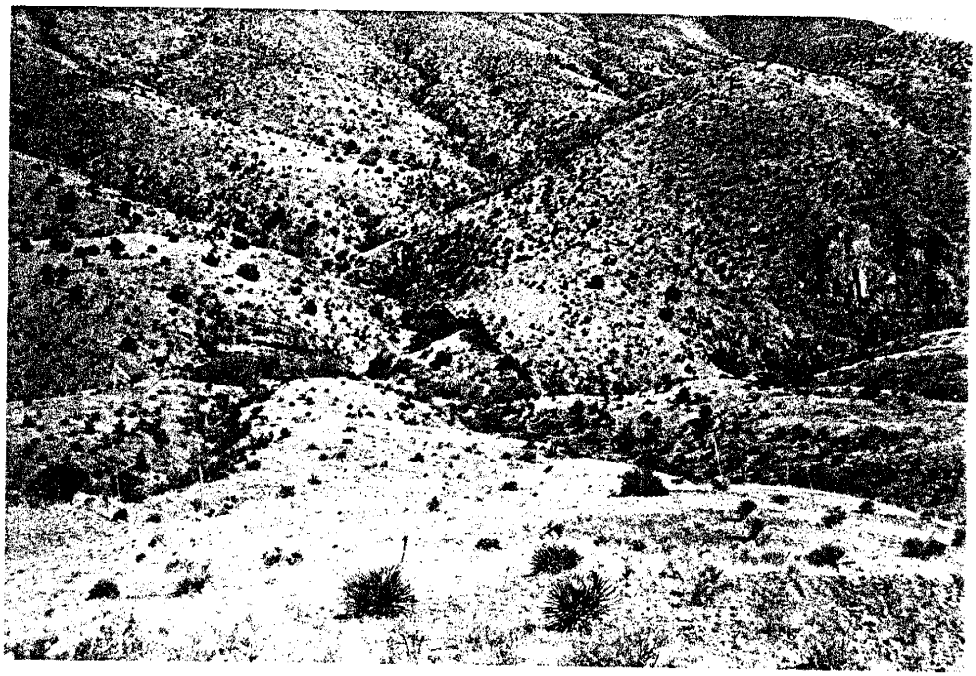

Figure 57. Dike (Ti-1) in Garcia Falls andesite member flows, looking east toward Canon De Quirino in the north part of section 27, T9S, R6W, N.M.P.M.

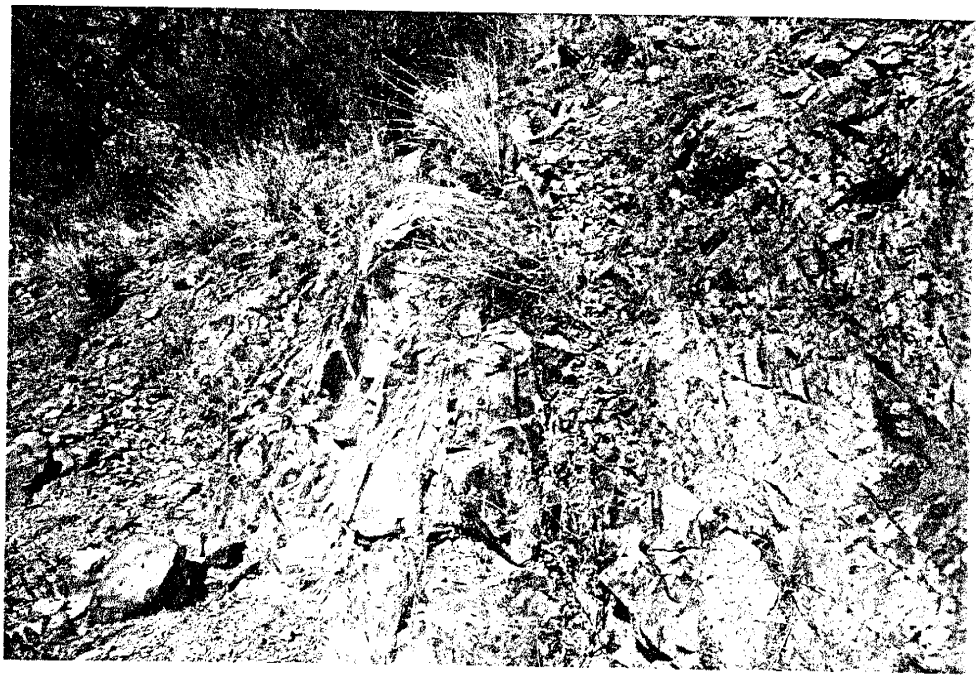

Figure 58. Limonitic rhyolite dike (Ti-3) cutting dark intrusive (Ti-2) in Canon De Quirino in the SW/4 of the NE/4 of section 22, T9S, R6W, N.M.P.M.

Figure 59. Outcrop of an alkali-granite intrusive (Ti-4), looking southeast, northwest of Vicks Peak in the NE/4 of section 3, T9S, R6W, N.M.P.M.

where intermediate and mafic intrusives cut lavas of the Red Rock Ranch Formation and Rock Spring Formation.

Propylitic alteration of andesite flows and ash-flow tuffs is widespread where an intrusive complex is localized

**Terrace Gravels and Fanglomerates.** The terrace gravels and fanglomerates consist of coalescing alluvial fan deposits and associated valley terrace deposits. The sediments are exposed extensively in the southwest part of the study area between the western front of the San Mateo Mountains and Alamosa Creek. Small isolated outcrops can also be found along some of the major canyons cut into the pedimented bedrock surfaces on the west slope of the mountain range. The total thickness of the sediments west of the Deep Canyon fault is unknown but over 500 feet of relief are expressed in Garcia Falls Canyon in the southern part of the study area. Outcrops of Vicks Peak Tuff are exposed in arroyos cut into the terrace gravels in the north part of the study area. This indicates a thinning of the terrace gravels to the northwest. The thickest deposits are probably west of the Deep Canyon fault in the southwest part of the study area.

The rocks consist of unconsolidated, interbedded, and poorly sorted, conglomerates, siltstones and mudstones. (Figures 60 and 61). Cobble and boulder sized clasts

Figure 60. Alluvial fan deposits (Qtg) looking southwest from the NW/4 of section 34, T9S, R6W, N.M.P.M.

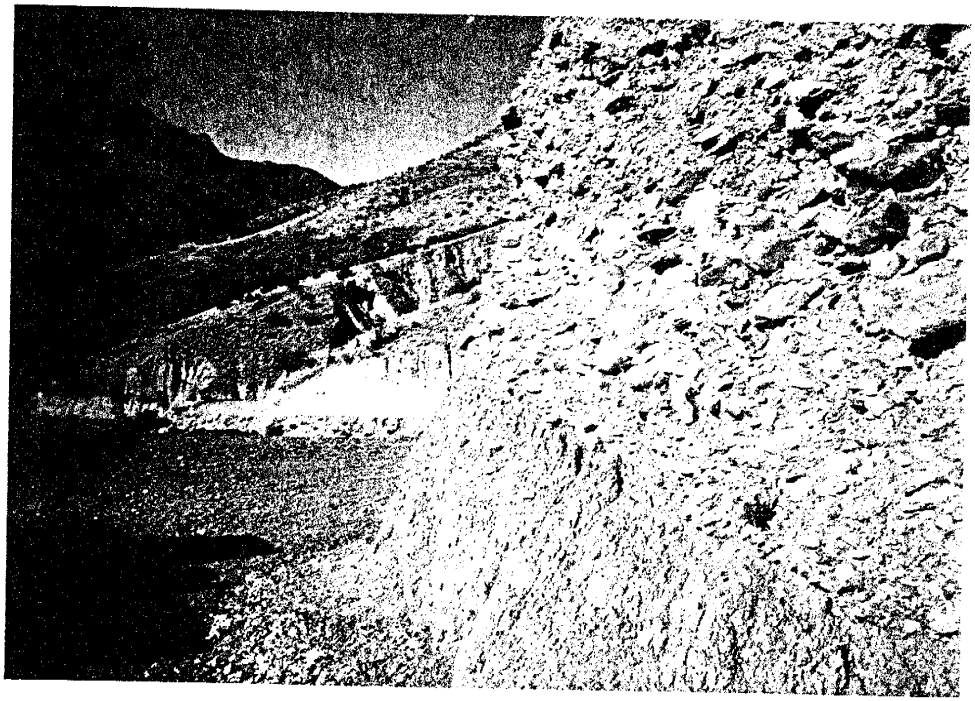

Figure 61. Outcrops of alluvial fan deposits (Qtg) in road cut along the Burma Road near the northwest corner of section 33, T9S, R6W, N.M.P.M.

within the upper parts of the unit are apparently derived from high relief areas east of the Deep Canyon fault.

The lithologies of the clasts observed coincide with the lithologies of the volcanic members east of the Deep Canyon fault. Clasts of Vicks Peak Tuff and post Vicks Peak Tuff rocks predominate in the northern exposures, whereas, clasts of older rocks (Red Rock Ranch Formation and Rock Spring Formation) predominate in the deposits south of Shipman Canyon. Proximal fan facies are more common in the northern parts of the study area. Intermediate or distal type fan deposits seem to be confined to deposits west of the Deep Canyon fault in the southern part of the study area. This may be in part due to depth of exposure in the southern area.

**Quaternary Alluvium.** The Quaternary Alluvium consists of locally derived, poorly sorted, channel lag, point bar and alluvial plain sediments. The deposits are exposed in canyon bottoms, streams and arroyos.

Degree of sorting is somewhat dependent on local rock types. Where deposits consist of reworked terrace gravels, degree of sorting generally increases. Boulders several meters in diameter are encountered where streams are cut into bedrock.

**Talus, Landslide and Debris Deposits.** Locally derived landslide and talus deposits occur near and below erosional scarps, along sides of steep canyons, and in high relief areas. The deposits consist primarily of angular and subrounded clasts ranging from several meters in size to centimeter sized material (Figure 62). Type, size and angularity of clasts are apparently dependent on proximity to source and joint density of source rocks.

Figure 62. Talus deposits (Qt) on the west side of Shipman Canyon in the western half of section 3, T9S, R6W, N.M.P.M.

## GEOPHYSICS, REMOTE SENSING AND AERIAL PHOTOGRAPHY

Characterization of lithologic units, and location of large scale structural trends, and areas of limonitic staining was attempted using U.S.F.S natural color aerial photographs (1:15840 scale), N.H.A.P. color infrared (1:58000 scale), black and white (1:80000 scale) photographs, and digitized Landsat MSS imagery using bands 4, 5, 6 and 7, from portions of scene #2276-17025 (Oct. 25,1975). MSS bands 4, 5, 6, and 7 image the 0.5-0.6 $\mu$m, 0.6-0.7 $\mu$m, 0.7-0.8 $\mu$m, and 0.8-1.1 $\mu$m wavelength regions of the electromagnetic spectrum. The linear resolution for the Landsat MSS data after digital enhancement and geometric corrections is approximately 65 meters.

Residual total intensity aeromagnetic maps (N.U.R.E 1983) and bouger anomaly gravity maps (Keller 1983) were compared with structural, geologic and remote sensing data to determine if any structural or geologic features observed during the field study may have corresponding geophysical or geo-optical signatures associated with them. Aeromagnetic and gravity maps at 1:100000 scale are presented in Figures 63 and 64 respectively for comparison with the generalized geologic maps and remote sensing data.

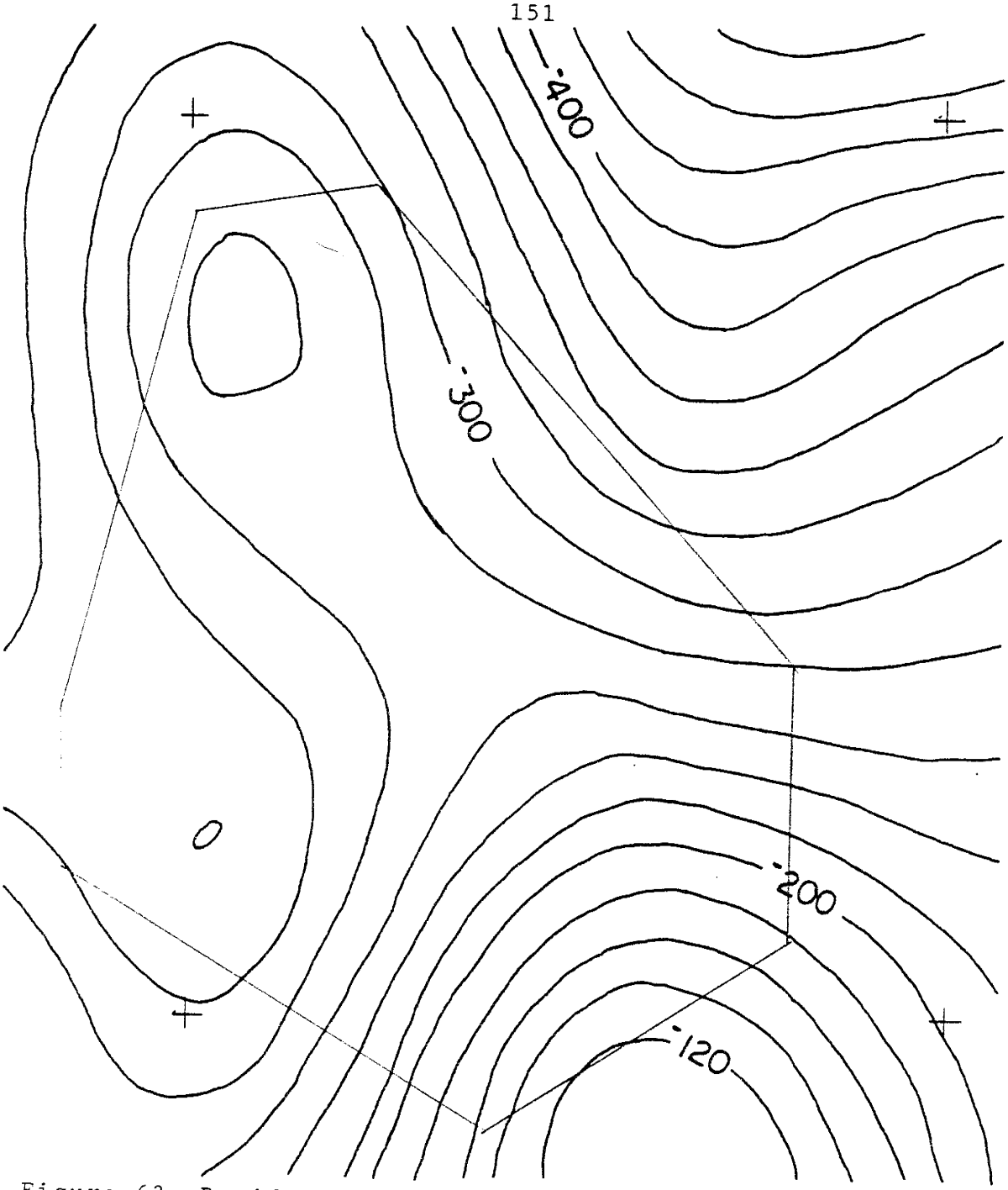


Figure 63. Residual total field aeromagnetic map of the study area. Scale = 1:100000, contour interval = 20 gammas (nT), flight line altitude = 400 feet. From Tularosa Quadrangle; Residual Intensity Magnetic Anomaly Map. (D.O.E Open FIle Map number GJM-403).

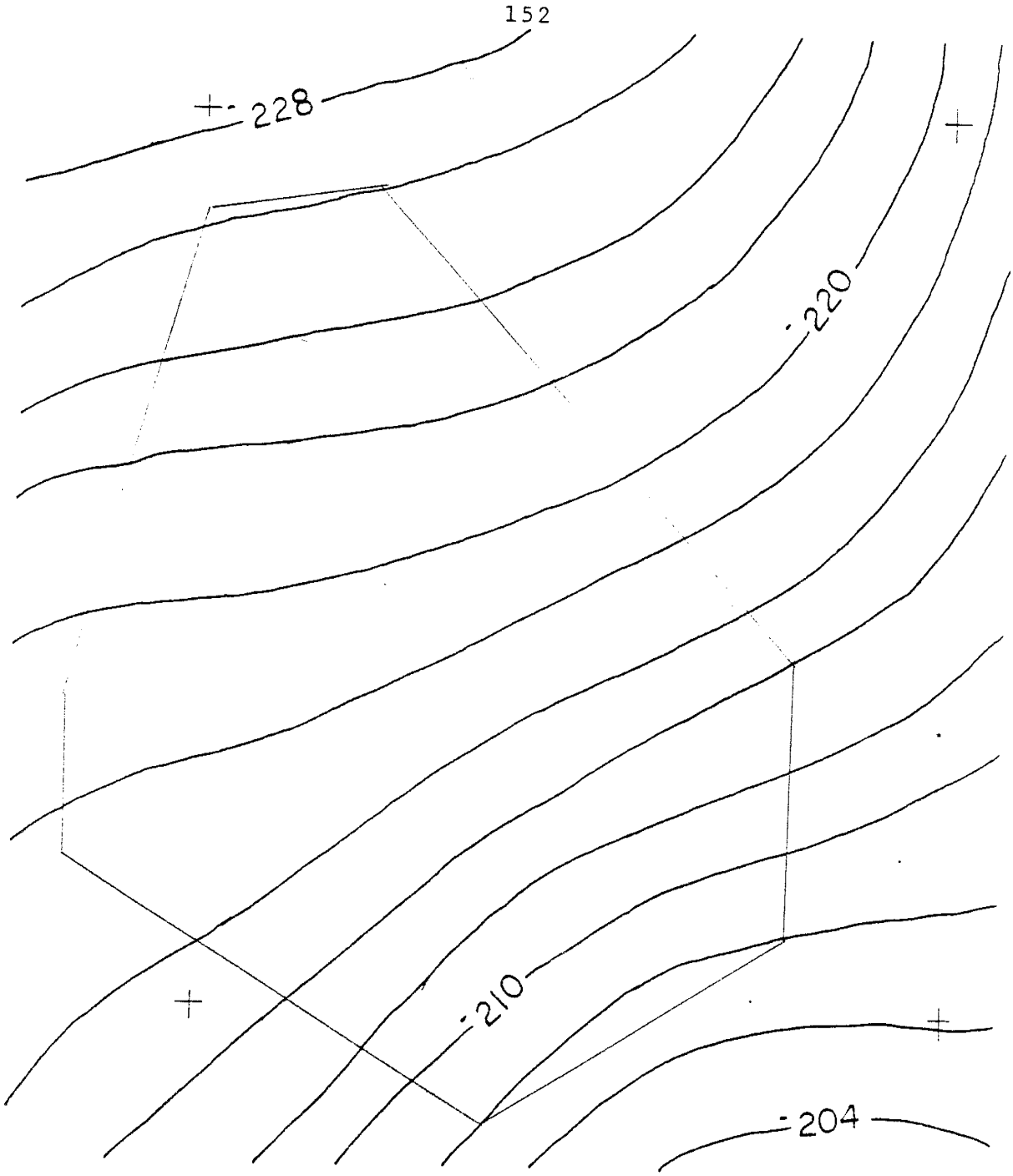


Figure 64. Bouger gravity anomaly map of the study area. Scale = 1:100000, contour interval = 2 milligals. From Keller, 1983).

False color Landsat MSS images and N.H.A.P color infrared photographs proved to be most useful in delineating major fault zones and in some cases defining contacts between different rock types. Characterization of rock types and the textural and color differences associated with them was best accomplished using natural color aerial photography.

Detection of limonitic areas using computerized enhancement techniques designed to highlight areas of iron oxide-hydroxide staining and to subdue effects of vegetative cover using digitized Landsat MSS data was attempted. The digital enhancement techniques used take advantage of the presence of absorption bands located near the 0.65 $\mu$m, and between the 0.85 $\mu$m and 0.95 $\mu$m regions in the ferric iron reflectance spectrum, and subdue the effects of high reflectance of vegetation in the 0.7 to 1.3 $\mu$m portion of the spectrum. The absorption bands for ferric iron fall in Landsat bands 5 and 6, while the high reflectance band for vegetation falls in MSS bands 6 and 7. The enhancement technique uses ratios of various Landsat MSS bands to separate limonitic rocks, non-limonitic rocks, and vegetation, enabling classification of a multispectral image into the respective categories. Using ratios of the intensity from the various bands instead of using absolute brightness levels in the enhancement technique also helps subdue the effects of

shadowing or irregular illumination of the area imaged by the multi-spectral scanner. A complete discussion of the data acquisition and ratioing technique is given by Segal (1983), and Conradson and Harpoth (1985).

Prior to enhancement, the Landsat image was geometrically corrected to facilitate accurate reproduction at various scales so that any limonitic zones could be compared with existing geophysical data and geologic data gathered in the field. Geometric corrections and processing of digitized data were done on a Vax??? and a R.I.P.S (Remote Image Processing System) using data and software provided by the Eros Data Center and the Technology Application Center, Albuquerque, New Mexico.

Figure 65 shows a false color reproduction of part of Landsat scene # 2276-1702S (10-25-75) using band 4 as blue, band 5 as green, and band 7 as red. The study area and the region of the Landsat scene used for digital enhancement are also shown in Figure 65.

Figure 66 is a false-color enlargement of part of the field area and the region used for digital enhancement and band ratioing. Figure 67 is a color ratio composite using the ratios band4/band5 as blue, band5/band7 as green, and band6/band7 as red.

The color ratio composite is included here because the general physiographic features of the area can be

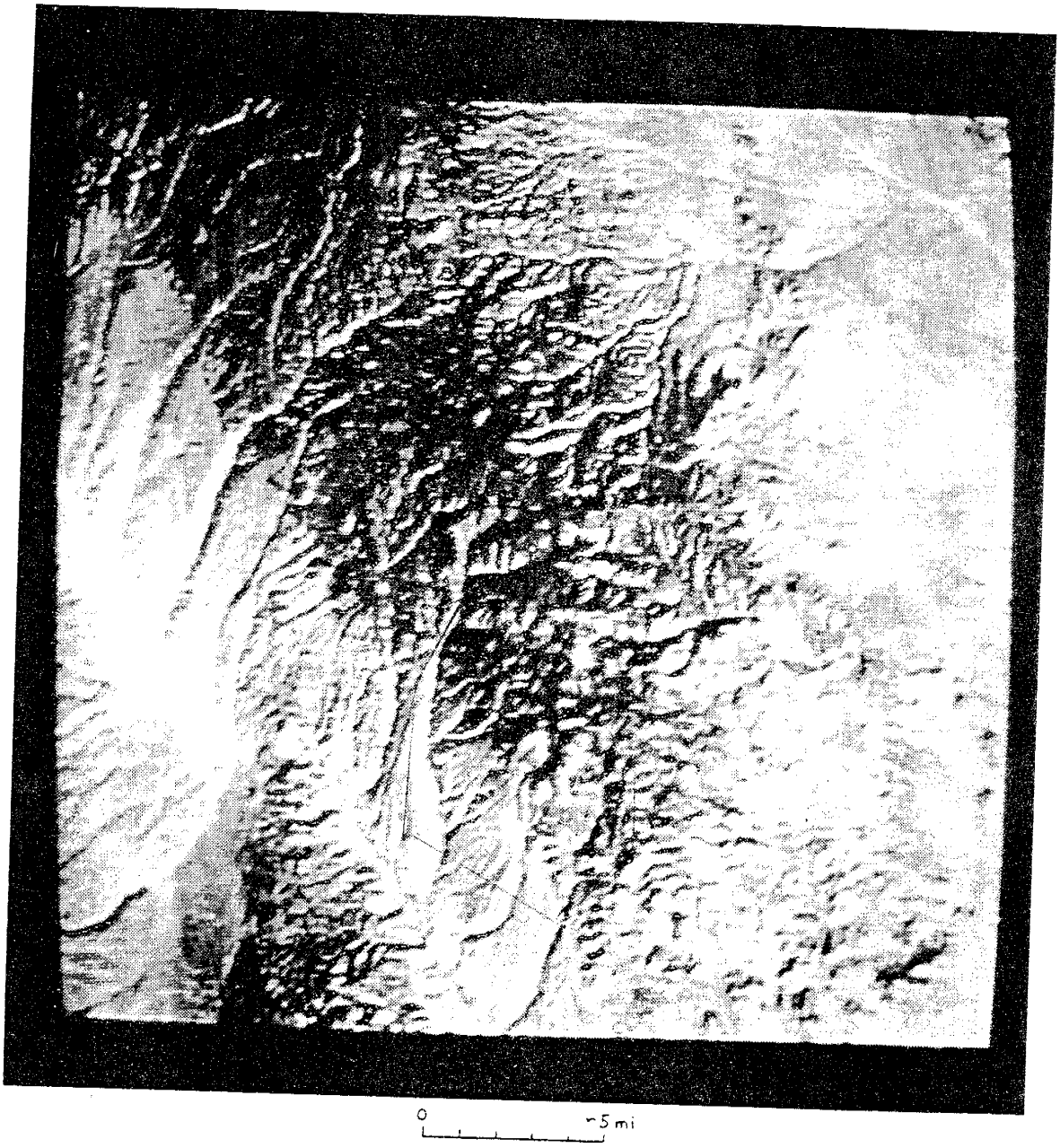


Figure 65. False color Landsat MSS image of the Southern San Mateo Mountains. Band 4 = blue, Band 5 = green, Band 7 = red.

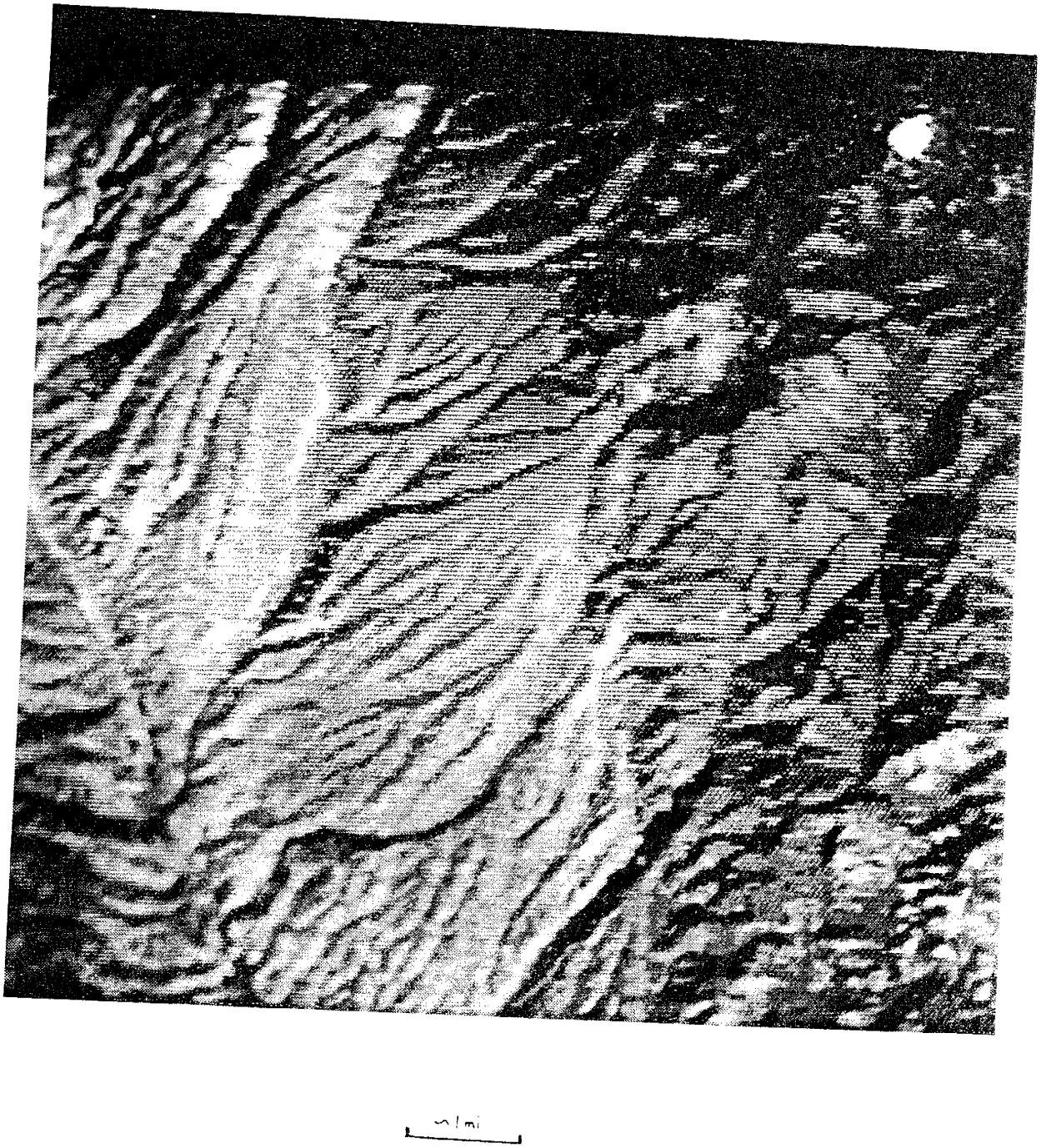


Figure 66. Enlargement of the area in Figure 65 used for image enhancement.

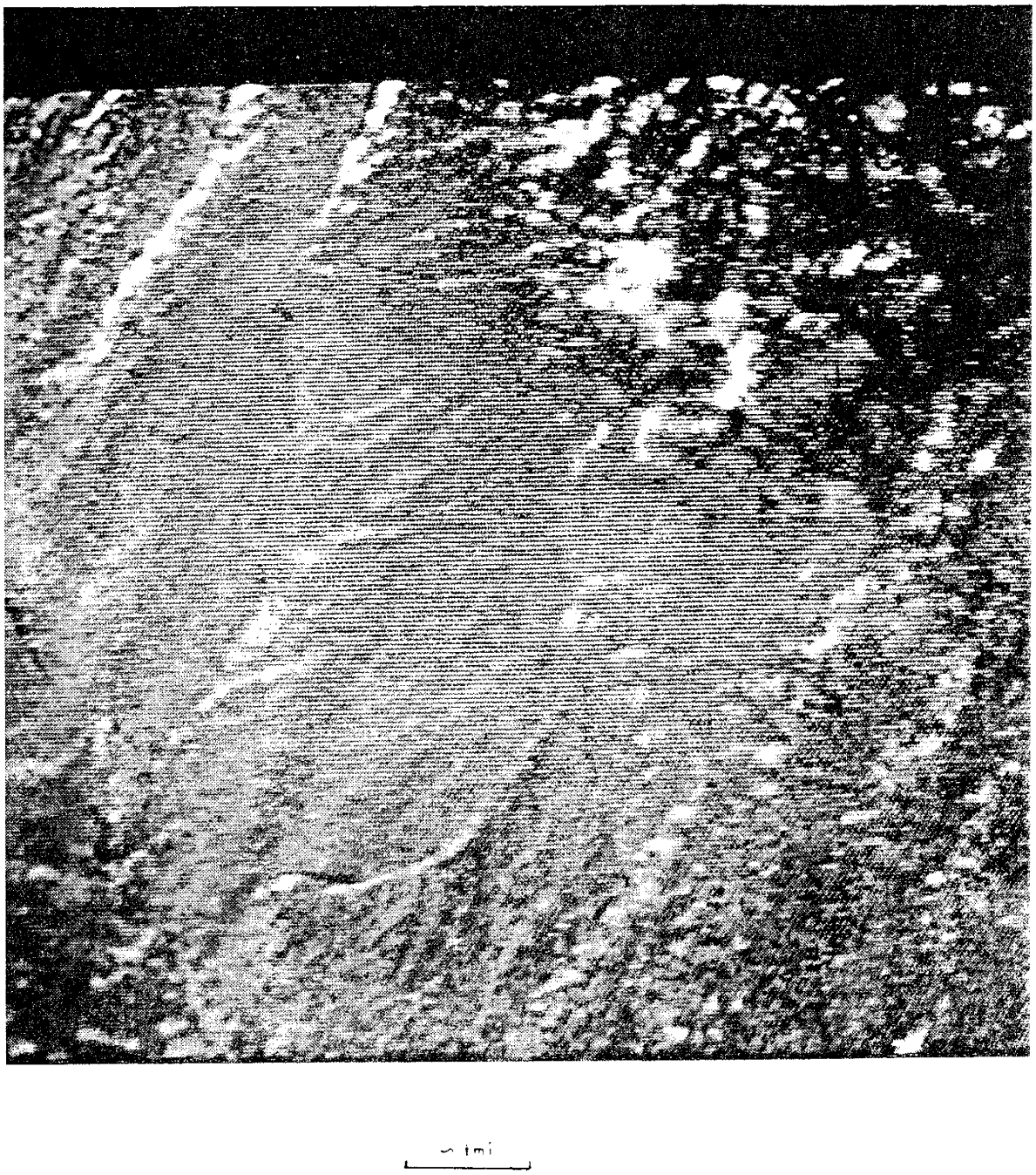


Figure 67. Color ratio composite of the area in Figure 66 (Band4/Band5 = blue, Band5/Band6 = green, Band6/Band7 = red).

recognized and the ratioing technique crudely shows areas of limonitic staining and areas of dense vegetation. Bright areas represent limonitic terrain, dark areas represent non-limonitic and heavily vegetated terrain.

The band4/band5 ratio highlights green copper minerals, the band5/band7 ratio subdues vegetation and highlights red iron oxides, and the band6/band7 ratio subdues vegetation and highlights yellow iron oxides/hydroxides. Blue and dark areas in the scene represent areas of dense vegetation, lighter areas and orange areas represent areas of limonitic staining.

Figure 68 is a 1:100000 scale generalized geologic map of the area covered in Figure 66. Figure 69 is a 1:100000 scale printout of the area in Figure 68 after digital enhancement to emphasize areas of limonitic staining. The lighter areas represent areas of most intense iron oxide-hydroxide staining as categorized by the Landsat band ratioing technique. Dark areas represent highly vegetated terrain and non limonitic areas.

The enhancement of Landsat images was done to see if previously undetected mineralized or altered zones could be located. Enhancement techniques used to detect limonitic rocks in digitized Landsat scenes (using bands 4,5,6, and 7), apparently could not distinguish some limonitic mineralized (Au/Ag) areas and non mineralized areas in iron oxide stained tuffs (apparently a common problem using

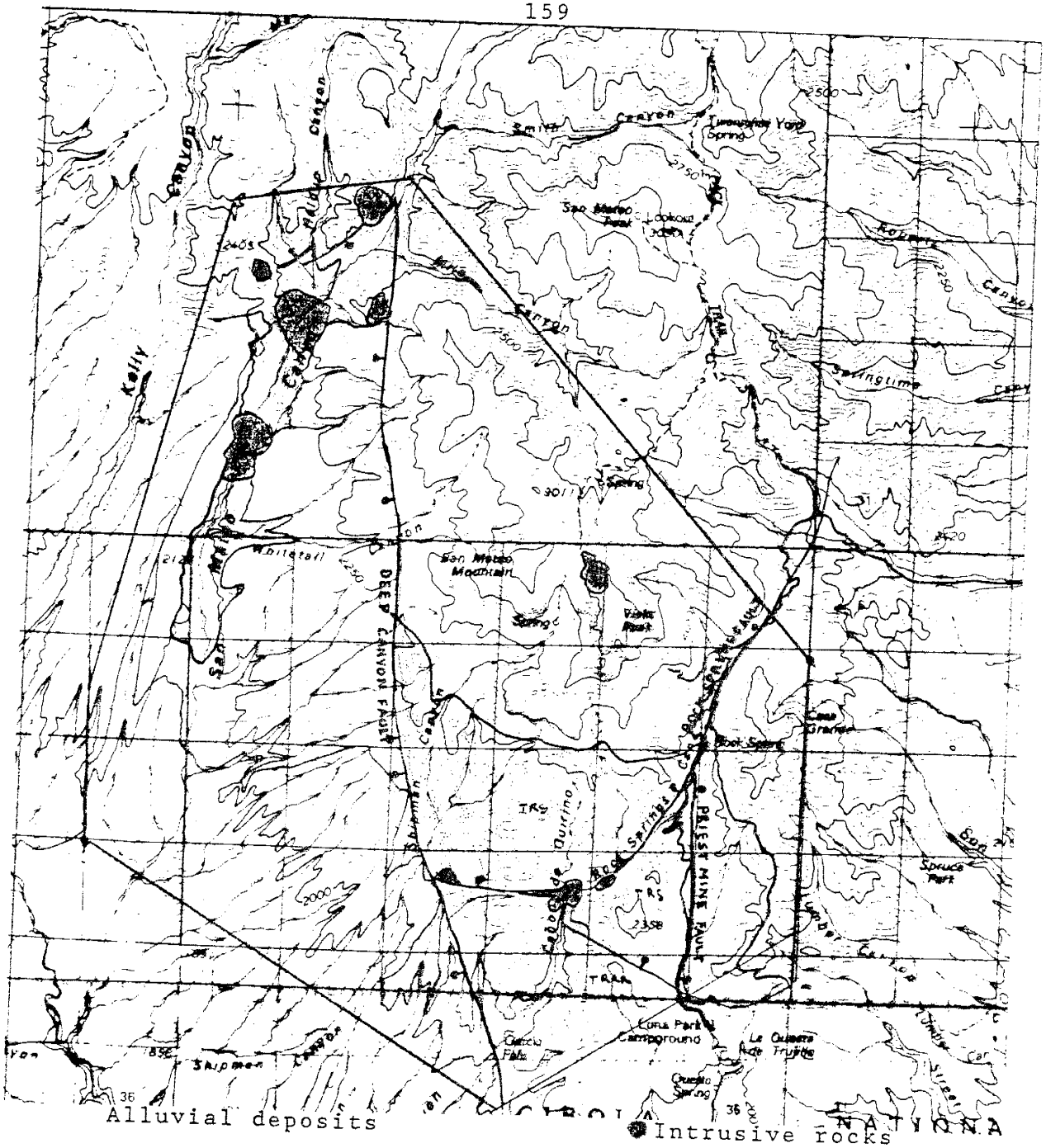


Figure 68. 1:100000 scale generalized geologic map of the study area and surrounding regions.

Figure 69. 1:100000 scale digitized limonite enhancement map of the area in Figure 61. Bright areas represent limonitic terrain, dark areas represent non-limonitic and heavily vegetated terrain.

Landsat MSS data due to its limited spectral resolution) (Abrams (1980). However, limonite signatures were more intense in some mineralized areas and the technique is useful if the stratigraphy of the area imaged is known. Known mineralized areas within more mafic rock units eluded detection in most cases or showed weak signatures over small areas using standard enhancement techniques on Landsat MSS data. This may be due partially to the widespread propylitization and pyritization observed in the field throughout the stratigraphically low members of the Rock Spring Formation and the Red Rock Ranch Formation.

# STRUCTURE AND REGIONAL GEOLOGY

The San Mateo Mountains lie in the northeast part of the Mogollon-Datil volcanic field near the boundary between the southeast part of the Colorado Plateau structural province and the Rio Grande Depression (Engle and San Marcial Basins) (Figure 70. Chapin et. al. 1978). The San Mateo Mountains are a northwest-southeast trending block-faulted uplift lying between the Mulligan Gulch Graben to the northeast and the Alamosa Graben to the southwest (Figure 70). The bedrock generally dips gently to the east or northeast within the mountain range and is almost entirely composed of Oligocene volcanic and volcaniclastic rocks. More recent fanglomerates and locally derived sedimentary rocks surround the high elevation areas and talus deposits form in areas of high relief.

Minor exposures of Precambrian rocks in the east-central part of the mountain range directly beneath Oligocene volcanic rocks (Atwood 1982) indicate that at least parts of the area were structurally and topographically high prior to or during the Oligocene. Cather (1983) suggests an extensive Eocene (Laramide) uplift (Sierra Uplift) in the area beneath the San Mateo Mountains and the southwest part of New Mexico. Chapin and Cather (1981) have suggested north-northeastward movement of the Colorado Plateau in the Eocene resulting in a series of en-echelon

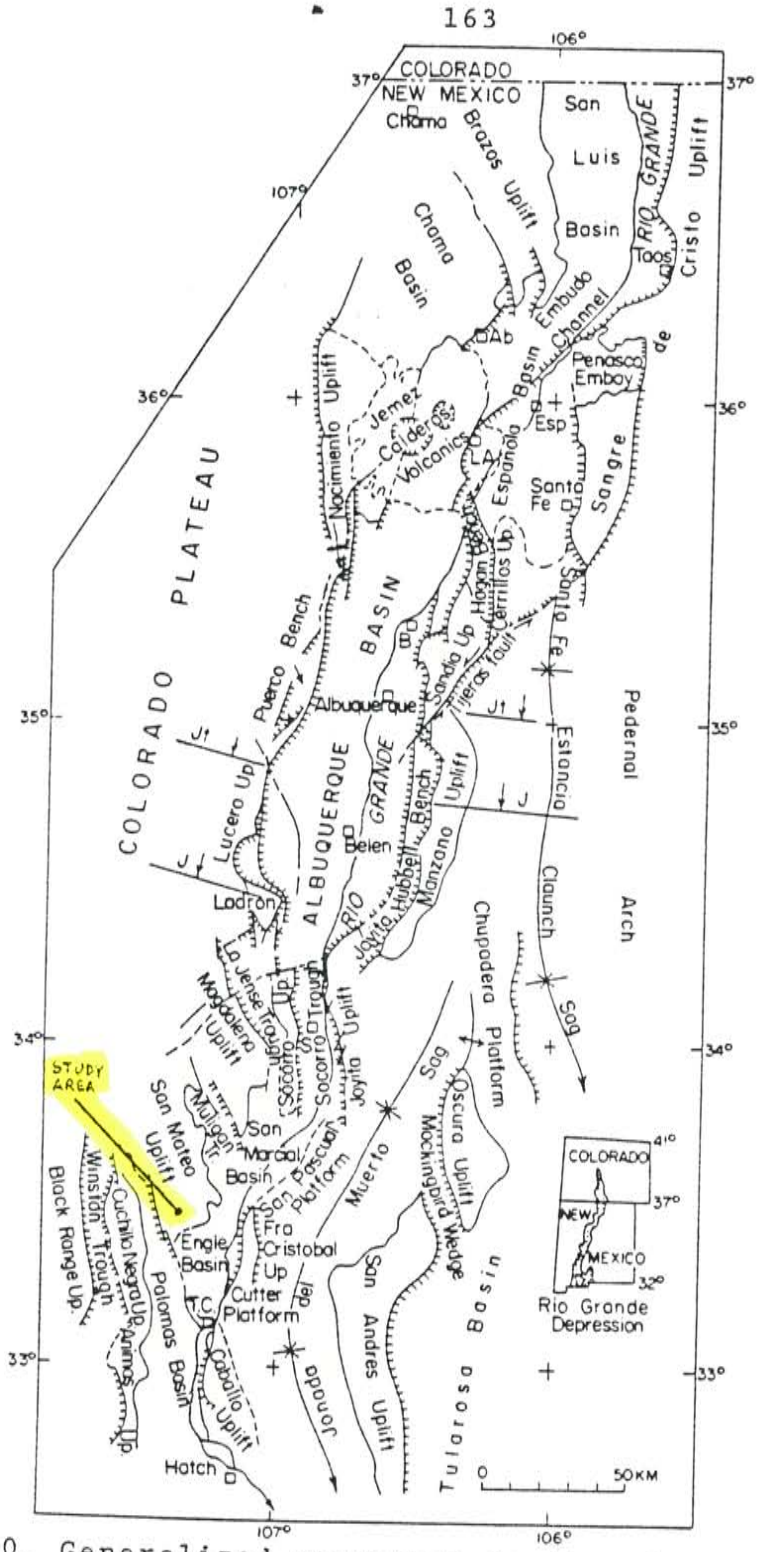


Figure 70. Generalized structure in the vicinity of the San Mateo Mountains. From Chapin et. al. (1978).

uplifts (including the Sierra Uplift) and basins (including the Engle Basin).

In the southern part of the San Mateo range, Oligocene volcanic rocks lie directly above Pennsylvanian Magdalena Group or Permian Abo Formation rocks (Farkas 1969). Drill hole data from areas near the range indicate that a large sedimentary basin existed beneath the area during Pennsylvanian time (Kottlowski 1965).

Lake sediments overlying volcaniclastic units are present in the lower or middle portions of the Red Rock Ranch Formation. This suggests the presence of depressions or basins in the region during the Oligocene, prior to deposition of the late Red Rock Ranch Formation lavas.

Two periods of faulting are apparent in the study area. Early volcano-tectonic structures and later extensional faulting. The Rock Spring fault and Priest Mine fault are apparently related to the formation of the Nogal Canyon Caldera. The Deep Canyon fault is and extensional basin and range type fault. Changes in thickness of several of the rock-stratigraphic units across the Rock Spring fault may indicate repeated movement along this fault and possibly with reversals of direction of movement at various periods. Several Rock Spring Formation members change thickness across the Rock Spring fault. The Priest Mine andesite thickens to the east across the fault. The Shipman Spring tuff thins to the

east across the fault. The Hump Mountain member thickens to the east across the Rock Spring fault. These relationships may suggest repeated movement along the Rock Spring fault. Thickness changes of the marker horizons and intervening units make displacement measurements approximate for most faults or fault zones exposed in pre-Vicks Peak Tuff deposits. The last major movement along the Rock Spring fault was apparently related to volcano-tectonic activity associated with the eruption of the Vicks Peak Tuff. The last apparent displacement along the Rock Spring fault was down to the northwest displacing the lower contact of the Vicks Peak tuff an estimated 500 ft, but this may be mis-leading as to the most recent movement along this fault. The greater thickness of the Vicks Peak tuff northwest of the Rock Spring fault, and the height at which the deposits rest may indicate that the latest movement may have been up to the northwest, not quite taking out the down to the northwest movement that may have occurred during collapse of the area during the Vicks Peak tuff eruption.

Basin and Range faults associated with the Alamosa and Muligan Gulch Grabens are generally high or moderate angle normal faults. They are northwest-southeast trending and down to west. These faults are later than much of the post Rock Spring Formation deposits, and cut earlier volcano-tectonic structures and extensional faulted zones. The

Deep Canyon fault, thought to be the youngest major extensional fault within the study area, is related to the formation of the Alamosa Graben to the west. The Deep Canyon fault cuts earlier faults that juxtapose Red Rock Ranch deposits and Rock Spring deposits in the southern part of the study area and displace the upper Vicks Peak Tuff against the lower Vicks Peak Tuff and underlying Rock Spring Formation deposits in the northern part of the map area.

The stratigraphic separation on the Deep Canyon fault in the northern part of the map area is estimated to be up to 4000 feet (1300 m). The displacement in the southern part of the study area could not be estimated with any degree of confidence due to extensive alluvial deposits. However, small isolated outcrops of altered moderately crystal-rich tuff (interpreted to be upper Vicks Peak tuff deposits) are found west of the fault near the Burma Road. If these are upper Vicks Peak Tuff the displacement may be greater in this area than to the north.

Isolated terrace deposits in high elevation areas indicate that alluvial fan material may have covered much of the pedimented bedrock within the mapped area at one time. Some movement along the Deep Canyon fault has occurred after deposition of the alluvial fan sediments because gouge zones separate Garcia Falls andesite and fan sediments (Figure 71). Evidence for the Deep Canyon fault

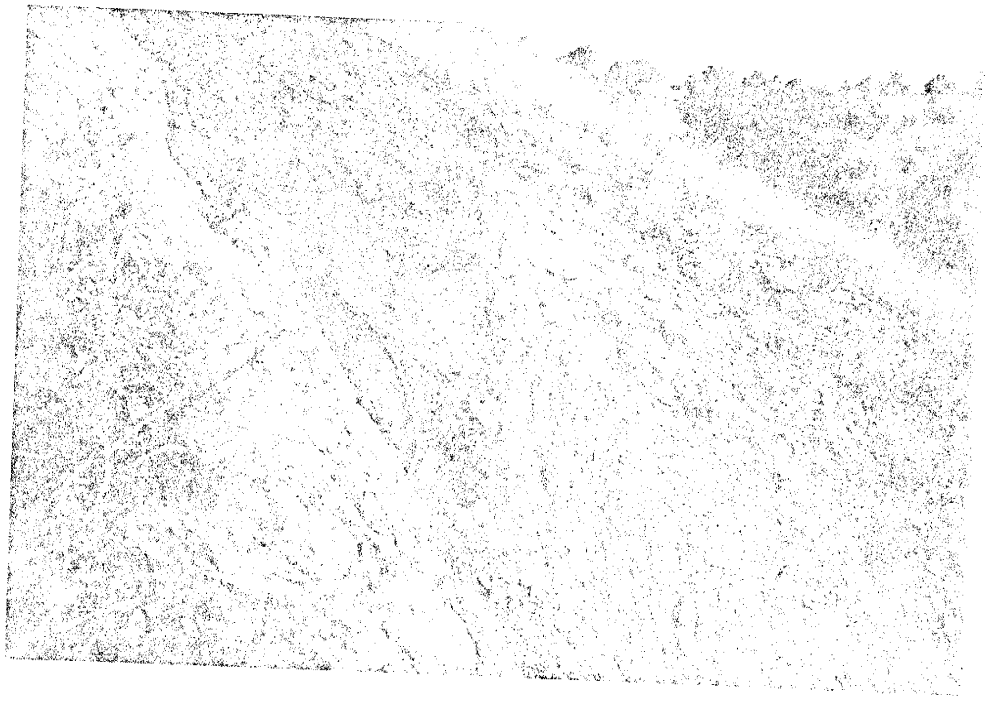

Figure 71. Garcia Falls Andesite (Red Rock Ranch Formation) against terrace gravels at the Deep Canyon fault.

cutting alluvial sediments can also be found near the Burma Road where fault gouge material occurs in the alluvial deposits.

# ECONOMIC GEOLOGY

Production of metals or mining of valuable minerals in the San Mateo Mountains has historically maintained a low level since gold was discovered by "modern" prospectors in 1883. Production of gold and silver ore has been reported from the San Jose Mining District west of the study area. Three historically relevant mining areas lie within the study area. These are the Nigger Diggins (hereafter referred to as the Diggins), the Victorio Mines and the Priest mine. No production data from mines in the mapped area was available. Descriptions of mining localities in the San Mateo Mountains have been given by Gordon (1910), Lasky (1932), Metzger (1938), Johnson (1972), and North (1983). Mineral investigations have been done by Griffits et al (1971), Neubert (1983), Foruria (1985), and Cox (1986).

Various prospect pits and minor workings can be found scattered throughout the study area fringing the known mining areas. Disseminated mineralization and alteration are evident in many areas, mainly concentrated along fault traces, along boundaries between rock types of differing permeability near fault zones, and around and within intrusive bodies and associated hydrothermal breccias. Although no clear evidence of order of intrusive activity as related to mineralization has been established,

a spatial relationship between the location of intrusive activity and mineralization seems apparent in the study area. The intrusive boundaries and surrounding fracture zones may have served as a plumbing system for mineralizing fluids.

The "major" workings within the study area lie on or near major fault zones, or near intrusive bodies. The Victorio mines are near the Rock Spring fault, above the lithic rich and andesite interval of the Vicks Peak Tuff, and near an eroded stock. The workings at the Diggins are along fault zones, stratigraphic contacts and intrusive contacts. The Priest Mine lies on the Priest Mine fault east of the intrusive complex at the Diggins.

Mineralized areas show a variety of alteration styles, including kaolinitization, pyritization, silicification, chloritization, albitization?, potassic alteration, and zeolitization (and combinations thereof). Oxidation of sulfide minerals is evident locally as limonite stainings along joints and partial replacements of pyrite by limonite.

Many of the rocks obtained from mineralized locations within the study area contain anomalous concentrations of precious and base metals. Some samples could be considered "ore grade" under ideal mining conditions. A list of the assays and sampling locations is presented in Table 3.

| SAMPLE | Ag | Au | As | Bi | Cu | Mo | Pb | Sb | Zn | ppm |
|---|---|---|---|---|---|---|---|---|---|---|
| ND-1-A | 329.80 | 1.43 | 107.10 | 116.50 | 800.00 | 108.40 | 800.00 | 9.14 | 195.70 | |
| ND-1-A-b | 283.80 | 1.37 | 81.30 | 103.40 | 800.00 | 111.40 | 800.00 | 9.85 | 210.40 | |
| ND-1-B | 113.00 | 1.37 | 7.30 | 77.41 | 800.00 | 83.28 | 800.00 | 1.61 | 380.90 | |
| F-62-A | 20.41 | 1.01 | 8.59 | 0.40 | 88.34 | 10.42 | 66.03 | 2.60 | 118.80 | |
| F-62-B | 19.91 | 0.82 | 6.25 | 0.61 | 82.80 | 10.56 | 53.07 | 2.61 | 73.26 | |
| F-1A-A | 0.54 | 0.10 | 25.17 | 1.63 | 140.70 | 17.73 | 31.71 | 6.67 | 31.87 | |
| F-1A-B | 1.58 | 0.18 | 26.54 | 1.87 | 142.60 | 17.16 | 32.47 | 6.67 | 49.87 | |
| SILL-2 | 28.18 | 0.73 | 0.00 | 0.38 | 80.66 | 3.17 | 25.67 | 0.77 | 41.22 | |
| ND-2-A | 3.95 | 0.18 | 0.00 | 0.00 | 76.82 | 1.88 | 9.34 | 0.00 | 14.82 | |
| ND-1-C | 104.20 | 0.06 | 0.00 | 10.86 | 1252.00 | 0.00 | 81.44 | 0.00 | 46.22 | |
| TI-1-C | 13.98 | 0.62 | 20.79 | 0.31 | 21.76 | 26.76 | 39.22 | 1.49 | 0.00 | |
| b | 5.95 | 0.11 | 0.00 | 0.00 | 17.32 | 18.16 | 35.62 | 0.00 | 11.20 | |
| TI-10-A | 0.97 | 0.19 | 13.83 | 0.10 | 27.39 | 2.41 | 6.65 | 0.43 | 20.84 | |
| TI-15 | 4.03 | 0.05 | 0.00 | 1.70 | 133.00 | 0.00 | 21.26 | 0.00 | 80.38 | |
| RSP-1 | 9.34 | 0.14 | 0.00 | 0.87 | 286.10 | 10.03 | 31.44 | 0.98 | 67.56 | |
| RSP-2 | 7.38 | 0.29 | 0.00 | 0.87 | 410.90 | 9.08 | 54.96 | 0.00 | 80.28 | |
| TI-10-SS2 | 577.40 | 1.81 | 109.60 | 241.90 | 800.00 | 556.00 | 800.00 | 10.09 | 110.40 | |
| RRR-4-19 | 7.32 | 0.07 | 1.31 | 0.77 | 67.10 | 10.95 | 49.49 | 1.30 | 83.09 | |
| C-DRAW-1 | 23.01 | 0.43 | 2.78 | 1.81 | 560.80 | 30.27 | 175.10 | 0.00 | 363.00 | |
| RRR-4 | 10.21 | 0.21 | 3.13 | 0.75 | 21.27 | 15.66 | 41.68 | 0.96 | 110.90 | |
| RRR-4-19 | 7.32 | 0.07 | 1.31 | 0.77 | 67.10 | 10.95 | 49.49 | 1.30 | 83.09 | |
| CQS-S-ND | 3.45 | 0.00 | 22.43 | 0.56 | 40.34 | 14.76 | 31.53 | 3.66 | 23.07 | |
| C-19 | 1.01 | 0.18 | 0.00 | 1.54 | 191.70 | 4.12 | 36.13 | 3.10 | 76.73 | |
| CQS-S-ND | 3.45 | 0.00 | 22.43 | 0.56 | 40.34 | 14.76 | 31.53 | 3.66 | 23.07 | |
| | | | | | | | | | | |
| WHC2-BZ | 1.30 | 0.08 | 19.79 | 0.38 | 160.80 | 12.61 | 31.15 | 3.74 | 30.77 | |
| BZ-W-MT | 8.59 | 0.02 | 0.00 | 0.34 | 159.50 | 1.31 | 62.04 | 0.00 | 51.31 | |
| C2-SINTER | 11.72 | 0.07 | 3.97 | 0.63 | 143.20 | 5.81 | 57.38 | 2.25 | 153.90 | |
| WHC-1 | 0.00 | 0.08 | 1.23 | 0.37 | 0.32 | 7.90 | 15.72 | 1.32 | 50.74 | |
| WHCTSC | 0.00 | 0.42 | 0.09 | 0.61 | 11.73 | 3.77 | 19.75 | 1.00 | 31.64 | |
| SMC-1 | 0.00 | 0.04 | 0.00 | 0.16 | 17.78 | 5.36 | 15.48 | 1.28 | 37.09 | |

Table 3. List of assays from mineralized areas in the study area. Samples ND-1-A through CQS-S-ND are from the "Diggins" area, in sections 14, 15, 22 and 23, T9S, R6W. Samples WHC2-BZ through SMC-1 are from the northwest part of the study area in sections 19, 20, 30 and 31, T8S, R6W, N.M.P.M.

The Priest Mine fault zone consists of altered fault gouge material near the surface and vein in-fillings of chrysocolla, malachite, azurite, and unidentified black silver minerals, with varying amounts of anglesite, cerussite and galena. Upper parts of exposed vein rocks show effects of oxidation and intense weathering and/or alteration.

Mineralized areas near the "Diggins" are very similar mineralogically to the Priest Mine area, but show evidence of stratigraphic control, and proximity to intrusive bodies in addition to fault control. Sparse hydrothermal brecciation and amethystine quartz veins are also found at various prospects in the area. Pyritization of wall rocks and intrusive bodies is also evident near mineralized veins around the Diggins. X-ray diffraction analyses of sample ND-1-B indicate the presence of quartz, calcite, potassium feldspar, plagioclase, illite or sericite, serpentine group minerals, kaolinite, galena, chalcopyrite, cuprite and argentite. The sample was taken from the dump near a shaft 2000 feet northeast of Villa Nerce Spring. The sample consisted of altered and, copper oxide-hydroxide stained andesite chips.

# DISCUSSION

Many of the volcanic deposits within the study area have characteristics similar to those of other volcanic centers described in the literature. Megacrystic flows of the Luna Peak andesite resemble pre-collapse rhomb-porphyry lavas described from alkaline volcanic complexes and calderas in the Oslo Rift region of Norway. In many Norwegian complexes, the large rhomb-shaped phenocrysts are calcic plagioclase rimmed by albite or potassium feldspar. Due to the alteration of the upper flows of the Luna Peak andesite it is not possible to determine if these rocks contained similar feldspars or were similar chemically to the rhomb porphyries of Norway or similar alkaline complexes. Altered rims surround many of the plagioclase megacrysts in the Luna Peak andesite. These rims conceivably were alkali-feldspar which altered more readily than plagioclase. If so, this suggests that the Luna Peak andesites may have had similar petrographic characteristics to voluminous lavas which predate major collapse in some alkaline caldera complexes.

A long lived intrusive center seems to be localized along the Rock Spring fault zone. Dome structures, and volcanic vents for some of the Rock Spring Formation flows are also localized along the fault. The similarities

of composition of intrusives with lavas indicates a possible genetic relationship between the rocks.

Many previously undocumented features of the Vicks Peak Tuff have been described. These include lithic-rich zones (mesobreccias) and andesite lavas within the Vicks Peak Tuff. Lithic fragments within the lithic-rich part of the Vicks Peak Tuff are progressively older higher in the unit. This relationship is consistent with deposition during progressive collapse of a caldera. Lithic fragments were apparently derived from progressively lower stratigraphic units on the caldera wall and incorporated into the cauldron fill deposits during eruption and synchronous collapse. This suggests strongly that the Rock Spring fault zone is a strand of the Nogal Canyon Cauldron structural margin. The small size (typically less than 10 cm) of the lithic fragments and the lack of internal stratification of the lithic-rich interval supports a caldera-collapse origin for the deposits (Lipman 1976, Walker, 1985). The angularity of the fragments of lower Vicks Peak Tuff within the lithic-rich interval indicate that welding and consolidation of the Vicks Peak Tuff had begun prior to caldera collapse.

The presence of intercalated andesite flows in the middle portion of the Vicks Peak Tuff west of the Rock Spring fault could be interpreted as evidence for a two-stage eruption consistent with a model proposed by Druitt

and Sparks (1984). Their model proposes that an initial voluminous eruption is followed by caldera collapse, and this is in turn followed by another energetic, voluminous ash-flow eruption. The andesites within the Vicks Peak Tuff may have been deposited as lava flows during a hiatus in the Vicks Peak Tuff eruption cycle. Alternately, this series of andesitic flow rocks could represent a large, lenticular, cohesive slab of Rock Spring Formation rocks that slid into a caldera during collapse (Bob Osburn Pers. comm.).

The presence of lithic fragments within the lower parts of the Vicks Peak Tuff have not been described previously. Lithic fragments encountered in the lower densely welded crystal-poor portions of the Vicks Peak Tuff are commonly of andesitic composition (similar to andesites of the Rock Spring and Red Rock Ranch Formations) and may have been ejected from the vent(s) during the eruptions of the Vicks Peak Tuff. Many of the larger clasts are somewhat rounded. Alternately they may be derived from a caldera wall. Walnut sized spherulites surround many of the smaller lithic fragments encountered in the lower welded parts of the Vicks Peak Tuff. The thick deposits northwest of the Rock Spring fault are obviously cauldron fill, whereas the thinner deposits southeast of the fault may be interpreted as proximal outflow deposits or as

deposits filling a shallower part of the Nogal Canyon Caldera.

The occurrence of hydrothermal vent breccias and hydrothermal alteration in the Vicks Peak tuff is apparently spatially related to the location of the alkali-granite intrusives (Ti4) and some of the smaller fine-grained rhyolitic intrusives bodies (Ti3). Pyritic and propylitic alteration of early intrusive bodies and volcanic rocks seems to be spatially related to locations of early and late-stage fine-grained and porphyritic intrusive bodies.

# CONCLUSIONS

Many of the goals set out in the beginning of the project have been accomplished. The probable source region for the Vicks Peak Tuff has been established and one cauldron related structure clearly documented.

A general understanding of the volcanic stratigraphy and tectonics have been established for the field area. Bracketing of the various rock-stratigraphic units within the paleomagnetic reversal time frame allowed a greater degree of confidence in correlating volcanic units (data courtesy Bill McIntosh). Vent locations for some of the pre-Vicks Peak Tuff units have been located. Possible ring-fracture intrusive rocks related to the Nogal Canyon Caldera and post-Vicks Peak Tuff intrusive bodies have been delineated.

A volumetric preponderance of lava flows over volcaniclastic sedimentary rocks and complex interfingering relationships of volcanic rocks in the study area probably indicate that the southern San Mateo Mountains were a site of continued and prolonged volcanic activity prior to the eruption of the Vicks Peak Tuff.

# FURTHER RESEARCH

Further subdivisions and petrographic studies of the Red Rock Ranch and Rock Spring Formation members and the Vicks Peak Tuff are possible and might expand on ideas set forth in this study. Detailed paleomagnetic studies of the volcanic rocks might make age correlations with rock suites in surrounding areas possible.

Detailed mapping of the shale horizons and underlying volcaniclastic rocks of the Red Rock Ranch Formation may be able to delineate ancient shorelines or indicate transport directions for sedimentary units. Extensive exposures of the Red Rock Ranch Formation exist south and southeast of the study area.

A diversity of rock types and intrusive bodies is found within the study area, as well as alteration and mineralization styles. This, combined with deep erosion of the area might make some areas good places for alteration studies.

Geochemical and petrographic studies of the intrusive bodies and volcanic units in the study area may determine if any genetic relationship exists between them. Further field investigations may also be able to establish better age relationships for the various intrusives and mineralization episodes.

Mapping of the high country north of the study area may establish the area of thick Vicks Peak Tuff, lithic-rich breccias and andesite units. Some well exposed, complete sections of relatively unaltered Vicks Peak tuff may exist north and northwest of the area and geochemical studies may be suitable. If the Rock Spring fault is a ring fracture of the Nogal Canyon Caldera, then a corresponding northwest boundary might be expected.

Reconnaissance indicates that post Vicks Peak Tuff deposits may thicken northwest of the study area. The lower volcaniclastic unit may represent Nogal Canyon Cauldron fill or moat fill deposits or be related to other volcanic or tectonic features. Circular features observable on Landsat images northwest of the study area might be interesting targets for future mapping investigations. The general eastward dip of the volcanic units in the mountain range should make the west face a good location for deep exposure of rock units.

## ACKNOWLEDGEMENTS

I wish to thank Clay T. Smith, Fredrick J. Kuellmer, and Glenn R. Osburn for critical reviews of the manuscript and technical assistance during the field study. Wolfgang E. Elston, Ted Eggleston, Eugene W. Cox, and Cortney E. Hesse provided stimulating discussion concerning geological problems associated with the study and/or assistance during the mapping phase of the project.

Bill McIntosh provided invaluable paleomagnetic data used in bracketing age relationships of various ash-flow tuffs and help in interpretation of the genesis of some of the mystery units within the area. Lynn Brandvold, John Husler, and Curtis Verpleogh, aided by providing geochemical analyses of various rock samples.

Raul Campos-Marquetti, Thomas K. Budge, Mike Inglis, and the staff of the Technology Application Center assisted in acquisition, interpretation, enhancement and reproduction of remotely sensed data used in the study. Larry Spear of the Office of Government Research provided the location map used to show quadrangle locations and landmarks in the region of the study area.

I also wish to thank Chris K. Mawer and David Johnson for providing assistance in the photo-microscopy of various thin-sections used in some of the illustrations and Brooke Bergeland for providing photographs used for illustrations

of hand specimens. Funding for the project was provided through capital generated by the Rift Rangers, the beneficial performance of the New York and American stock exchanges, and high interest rates during the period 1980-1986.

# Appendix 1

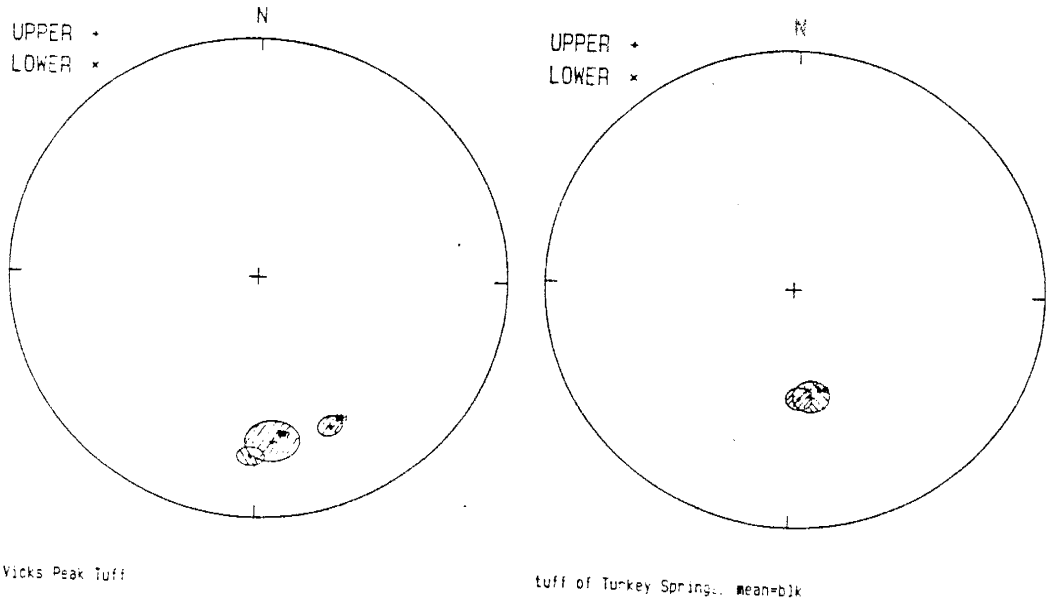


Paleomagnetic pole positions reported from ash-flow tuffs in the study area (courtesy Bill McIntosh). Upper (+) reversed polarity, lower (x) normal polarity. /// = Average in study area. \\\ = Average of eastern Mogollon-Datil Volcanic Field. For detailed data refer to McIntosh, et. al., 1986, and reports in preparation.

Appendix 1 continued

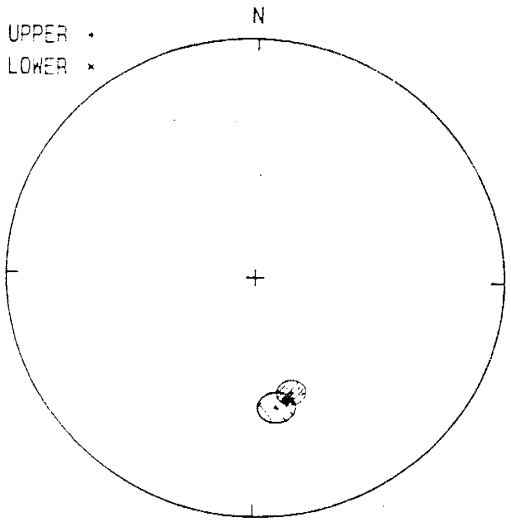


La Jencia Tuff

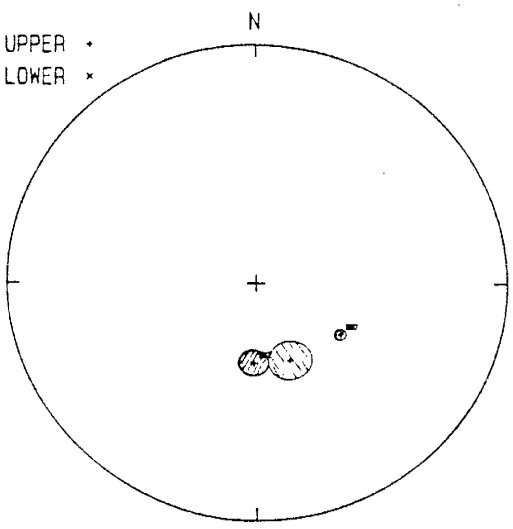


Hells Mesa Tuff

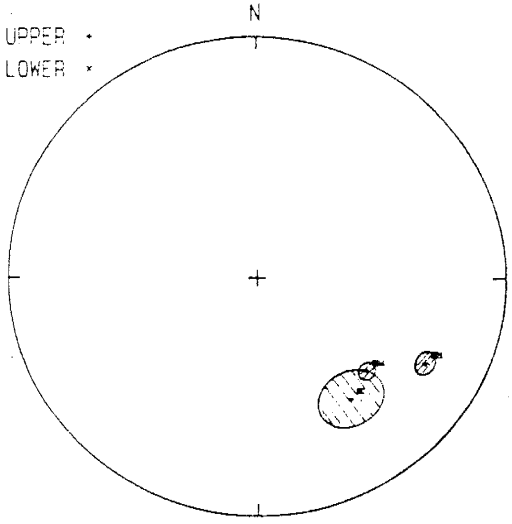


tuff of Shipman Springs

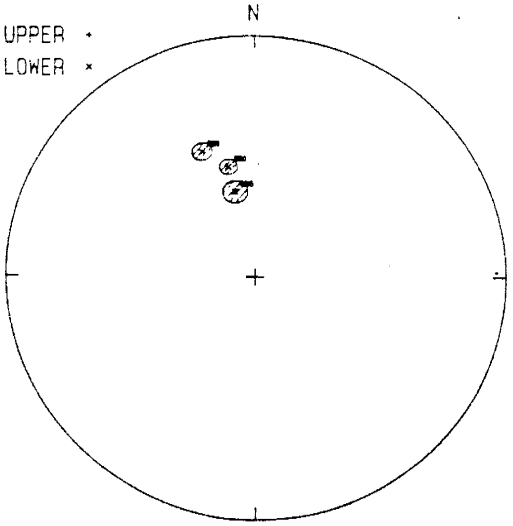


tuff of Luna Park

## REFERENCES CITED

Abrams, M., and Siegal, B. S., 1980, Lithologic Mapping in Remote Sensing in Geology, Siegal, B. S., and Gillespie, A. R., eds., John Wiley & Sons Inc., p. 381.

Atwood, G. W., 1982, Geology and geochemistry of the San Juan Peak area, San Mateo Mountains, Socorro County, New Mexico: with special reference to a riebeckite bearing rhyolite (M.S. Thesis): U.N.M., Albuquerque, N.M.

Cather, S. M., 1983, Laramide Sierra Uplift: Evidence for major pre-rift uplift in central and southern New Mexico in Chapin, C.E. editor, Socorro Region II, New Mexico Geological Society 34th Field Conference Guidebook, p. 99-101.

Chapin, C. E., and Cather, S. M., 1981 Eocene tectonics and sedimentation in the Colorado Plateau-Rocky Mountain area: Arizona Geological Society Digest, vol. 14, p.173-198.

Chapin, C. E., Chamberlin, R. M., Osburn, G. R., White, D. W., and Sanford, A. R., 1978, Exploration framework of the Socorro geothermal area, New Mexico: New Mexico Geological Society. Special Publication 7, p. 114-129.

Conradsen, K., and Harpoth, O., 1985, Use of Landsat Multispectral Scanner Data for Detection and Reconnaissance Mapping of Iron Oxide Staining in Mineral Exploration, Central East Greenland: Economic Geology, vol 79, no 6, p. 1229-1244.

Cox, E., 1986, Geology and Gold-Silver Deposits in the San Jose Mining District, Southern San Mateo Mountains, Socorro County, New Mexico (Unpuplished M.S. Thesis): New Mexico Institute of Mining and Technology. Socorro, N.M. --- p.

Deal, E. G., 1973, Geology of the northern part of the San Mateo Mountains, Socorro County, New Mexico: A study of a rhyolite ash-flow tuff cauldron and the role of laminar flow in ash-flow tuffs (Ph.D. dissert.): U.N.M., Albuquerque, N.M., 136 p.

Deal, E. G., and Rhodes, R. C., 1976, Volcano-tectonic structures in the San Mateo Mountains, Socorro County, New Mexico: in Elston, W. E., and Northrop, S. A., (eds.), Cenozoic Volcanism in Southwestern New Mexico: New Mexico Geological Society, Special Publication 5, p. 51-56.

Druitt, T. H., and Sparks, R. S. J., 1984, On the Formation of Calderas During Ignimbrite Eruptions: Nature, Vol. 310, p. 679-681.

Farkas, S. E., 1969, Geology of the southern San Mateo Mountains, Socorro and Sierra Counties, New Mexico (Ph.D. dissert.): U.N.M., Albuquerque, N.M., 137 p.

Ferguson, C., 1985, Geology of the central San Mateo Mountains, Socorro County, New Mexico (M.S. Thesis): New Mexico Institute of Mining and Technology. Socorro, N.M. --- p.

Ferguson, C., 1986, Geologic map of the east-central San Mateo Mountains, Socorro County, New Mexico: New Mexico Bureau of Mines and Mineral Resources Open-File Report 252.

Foruria, J., 1984, Geology of part of the southern San Mateo Mountains, Socorro and Sierra Counties, New Mexico (M.S. Thesis): C.S.U. Fort Collins, Colorado, ??? p.

Furlow, J. W., 1965, Geology of the San Mateo Peak area, Socorro County, New Mexico (M.S. Thesis): U.N.M. Albuquerque, N.M. 83 p.

Gordon, C. H., 1910, Sierra and central Socorro Counties in The Ore Deposits of New Mexico, U.S. Geological Survey Professional Paper 68, Lindgren, W., Graton, L. C., and Gordon, C. H., p. 240.

Griffits, W. R., Alminas, H. V., and Mosier, E. L., 1971, Pb, Sn, Sr, La, Ag, Be, Zn, Sb, Mo, Nb, & Au distribution in the Vicks Peak, Steel Hill, and Black Hill quadrangles, New Mexico: U.S Geological Survey. Open File Reports 71-129 through 71-137.

Kedzie, L. L., 1984, High-precision $^{40}Ar/^{39}Ar$ dating of major ash-flow tuff sheets, Socorro, New Mexico (M.S. Thesis): New Mexico Institute of Mining and Technology, Socorro, N.M., 95 p.

Keller, G. R., 1983, Bouger gravity anomaly map of the Socorro region, New Mexico: in Chapin, C. E. editor, Socorro Region II, New Mexico Geological Society 34th Field Conference Guidebook, p. 96.

Lasky, S. G., 1932, The Ore Deposits of Socorro County, New Mexico: New Mexico Bureau of Mines and Mineral Resources bull. 8, pp. 93-118.

Lipman, P. W., 1976, Caldera-Collapse Breccias in the Western San Juan Mountains, Colorado: Geological Society of America Bull., Vol. 87, p. 1397-1410.

Maldonado, F., 1974, Geology of the northern part of the Sierra Cuchillo, Socorro and Sierra Counties, New Mexico (M.S. Thesis): University of New Mexico, Albuquerque, N.M., 59 p.

McBirney, A. R., 1980, Mixing and Un-mixing of Magmas: Journal of Volcanology and Geothermal Research, vol. 7, p 357-371.

McIntosh, W. C., Sutter J. F., Chapin C. E., Osburn G. R., Ratte' J. C., 1986, A Stratigraphic Framework for the Eastern Mogollon-Datil Volcanic Field Based on Paleomagnetism and High-Precision $^{40}Ar/^{39}Ar$ Dating of Ignimbrites- A progress report: New Mexico Geological Society Guidebook, 37th Field Conference, Truth or Consequences Region, p 183-195.

Nelson, C. E., and Giles, D. L., 1985, Hydrothermal Eruption Mechanisms and Hot Spring Gold Deposits: Economic Geology, Vol 80, p. 1633-1639.

Neubert, J. T., 1983, Mineral Investigations of the Apache Kid and Withington Wilderness area: U.S Geological Survey Open File Report 5-83, 35 p.

Osburn, G. R., and Chapin, C. E., 1983a, Ash Flow Tuffs and Cauldrons in the Northeast Mogollon-Datil Volcanic Field: A Summary: New Mexico Geological Society Guidebook, 34th Field Conference, Socorro Region II, pp. 197-204.

_____, 1983b, Nomenclature for Cenozoic Rocks of the Northeast Mogollon-Datil Volcanic Field, New Mexico: New Mexico Bureau of Mines and Mineral Resources Stratigraphic Chart 1.

Segal, D. B., 1983, Use of Landsat Multispectral Scanner Data for the Definition of Limonitic Exposures in Heavily Vegetated Areas: Economic Geology, Vol. 78, no 4, p. 711-722.

Smith, R. L., 1960, Ash Flows: Geological Society of America Bull., vol 71, p. 795-842.

Smith, R. L., and Bailey, R. A., ???, Resurgent Cauldrons: U.S. Geological Survey Studies in Volcanology, ? p 613-662.

Sparks, R. S. J., Self, S., and Walker, G. P. L., 1973, Products of Ignimbrite Eruptions: Geology, Vol. 1, p. 115-118.

Walker, G. P. L., 1985, Origin of Coarse Lithic Breccias Near Ignimbrite Source Vents: Journal of Volcanology and Geothermal Research, Vol. 25, p. 157-171.

Williams, H., and McBirney, A. R., 1979, Volcanology: Freeman, Cooper and Company, San Francisco CA 94133, 397 p.

# BIBLIOGRAPHY

Abrams, M., and Siegal, B. S., Lithologic Mapping in Remote Sensing in Geology, Siegal, B. S., and Gillespie, A. R., eds., John Wiley & Sons Inc., p. 381.

Atwood, G. W., 1982, Geology and geochemistry of the San Juan Peak area, San Mateo Mountains, Socorro County, New Mexico: with special reference to a riebeckite bearing rhyolite (M.S. Thesis): U.N.M., Albuquerque, N.M.

Blagbrough, J. W. and Farkas, S. E., 1968, Rock glaciers in the San Mateo Mountains, south-central New Mexico: American Journal of Science, vol. 266, Nov. 1968, pp. 812-823.

Cather, S. M., 1983, Laramide Sierra Uplift: Evidence for major pre-rift uplift in central and southern New Mexico in Chapin, C.E. editor, Socorro Region II, New Mexico Geological Society 34th Field Conference Guidebook, p. 99-101.

Chapin, C. E., and Cather, S. M., 1981 Eocene tectonics and sedimentation in the Colorado Plateau-Rocky Mountain area: Arizona Geological Society Digest, vol. 14, p.173-198.

Chapin, C. E., Chamberlin, R. M., Osburn, G. R., White, D. W., and Sanford, A. R., 1978, Exploration framework of the Socorro geothermal area, New Mexico: New Mexico Geological Society. Special Publication 7, p. 114-129.

Conradsen, K., and Harpoth, O., 1985, Use of Landsat Multispectral Scanner Data for Detection and Reconnaissance Mapping of Iron Oxide Staining in Mineral Exploration, Central East Greenland: Economic Geology, vol 79, no 6, p. 1229-1244.

Cordell, L., 1983, Composite residual total intensity aeromagnetic map of the Socorro region, New Mexico: in Chapin, C.E. editor, Socorro Region II, New Mexico Geological Society 34th Field Conference Guidebook, p. 97.

Cox, E., 1986, Geology and Gold-Silver Deposits in the San Jose Mining District, Southern San Mateo Mountains, Socorro County, New Mexico (Unpublished M.S. Thesis): New Mexico Institute of Mining and Technology. Socorro, N.M. --- p.

Deal, E. G., 1973, Geology of the northern part of the San Mateo Mountains, Socorro County, New Mexico: A study of a rhyolite ash-flow tuff cauldron and the role of laminar flow in ash-flow tuffs (Ph.D. dissert.): U.N.M., Albuquerque, N.M., 136 p.

Deal, E. G., and Rhodes, R. C., 1976, Volcano-tectonic structures in the San Mateo Mountains, Socorro County, New Mexico: in Elston, W. E., and Northrop, S. A., (eds.), Cenozoic Volcanism in Southwestern New Mexico: New Mexico Geological Society, Special Publication 5, p. 51-56.

Druitt, T. H., and Sparks, R. S. J., 1984, On the Formation of Calderas During Ignimbrite Eruptions: Nature, Vol. 310, p. 679-681.

Eaton, G. P., 1984, Mineral abundance in the North American Cordillera: American Scientist, vol 72 pp 368-377.

Farkas, S. E., 1969, Geology of the southern San Mateo Mountains, Socorro and Sierra Counties, New Mexico (Ph.D. dissert.): U.N.M., Albuquerque, N.M., 137 p.

Ferguson, C., 1985, Geology of the central San Mateo Mountains, Socorro County, New Mexico (M.S. Thesis): New Mexico Institute of Mining and Technology. Socorro, N.M. --- p.

Foruria, J., 1984, Geology of part of the southern San Mateo Mountains, Socorro and Sierra Counties, New Mexico (M.S. Thesis): C.S.U. Fort Collins, Colorado, ??? p.

Furlow, J. W., 1965, Geology of the San Mateo Peak area, Socorro County, New Mexico (M.S. Thesis): U.N.M. Albuquerque, N.M. 83 p.

Gillespie, A. R., 1980, Digital Techniques of Image Enhancement in Remote Sensing in Geology, Siegal, B. S., and Gillespie, A. R., eds., John Wiley & Sons Inc., p. 139-226.

Gordon, C. H., 1910, Sierra and central Socorro Counties in The Ore Deposits of New Mexico, U.S. Geological Survey Professional Paper 68, Lindgren, W., Graton, L. C., and Gordon, C. H., p. 240.

Griffits, W. R., Alminas, H. V., and Mosier, E. L., 1971, Pb, Sn, Sr, La, Ag, Be, Zn, Sb, Mo, Nb, & Au distribution in the Vicks Peak, Steel Hill, and Black Hill quadrangles, New Mexico: U.S Geological Survey. Open File Reports 71-129 through 71-137.

Harley, G. T., 1934, The Geology and Ore Deposits of Sierra County, New Mexico: New Mexico Bureau of Mines and Mineral Resources Bull. 10, pp. 190-193.

Hildreth, W., and Mahood, G., 1985, Correlation of Ash-Flow Tuffs: Geological Society of America Bull., Vol. 96, p. 968-974.

Hillard, P. D., 1969, Geology and beryllium mineralization near Apache Warm Springs, Socorro County, New Mexico: New Mexico Bureau of Mines and Mineral Resources circular 103, 16 p.

Johnson, M. G., 1972, Placer Gold Deposits of New Mexico: U.S. Geological Survey bull. 1348, pp. 28-29.

Kedzie, L. L., 1984, High-precision $^{40}Ar/^{39}Ar$ dating of Major ash-flow tuff sheets, Socorro, New Mexico (M.S. Thesis): New Mexico Institute of Mining and Technology, Socorro, N.M., 95 p.

Keller, G. R., 1983, Bouger gravity anomaly map of the Socorro region, New Mexico: in Chapin, C. E. editor, Socorro Region II, New Mexico Geological Society 34th Field Conference Guidebook, p. 96.

Lasky, S. G., 1932, The Ore Deposits of Socorro County, New Mexico: New Mexico Bureau of Mines and Mineral Resources bull. 8, pp. 93-118.

Lipman, P. W., 1976, Caldera-Collapse Breccias in the Western San Juan Mountains, Colorado: Geological Society of America Bull., Vol. 87, p. 1397-1410.

Maldonado, F., 1974, Geology of the northern part of the Sierra Cuchillo, Socorro and Sierra Counties, New Mexico (M.S. Thesis): University of New Mexico, Albuquerque, N.M., 59 p.

McBirney, A. R., 1980, Mixing and Un-mixing of Magmas: Journal of Volcanology and Geothermal Research, vol. 7, p 357-371.

Metzger, O. H., 1938, Gold Mining in New Mexico: U.S. Bureau of Mines Information Circular 6987, pp.60-67.

McIntosh, W. C., Sutter J. F., Chapin C. E., Osburn G. R., Ratte' J. C., 1986, A Stratigraphic Framework for the Eastern Mogollon-Datil Volcanic Field Based on Paleomaggnetism and High-Precision $^{40}Ar/^{39}Ar$ Dating of Ignimbrites- A progress report: New Mexico Geological Society Guidebook, 37th Field Conference, Truth or Consequences Region, p 183-195.

Nelson, C. E., and Giles, D. L., 1985, Hydrothermal Eruption Mechanisms and Hot Spring Gold Deposits: Economic Geology, Vol 80, p. 1633-1639.

Neubert, J. T., 1983, Mineral Investigations of the Apache Kid and Withington Wilderness area: U.S Geological Survey Open File Report 5-83, 35 p.

North, R. M., 1983, History and Geology of the Precious Metal Occurrence in Socorro County, New Mexico: New Mexico Geological Society Guidebook 34th Field Conference, Socorro Region II, pp. 261-268.

North, R. M., and Mclemore, V. T., 1984, Silver and Gold Occurrence in New Mexico: New Mexico Bureau of Mines and Mineral Resources Open File Report 191, pp. 10-12.

Osburn, G. R., and Chapin, C. E., 1983a, Ash Flow Tuffs and Cauldrons in the Northeast Mogollon-Datil Volcanic Field: A Summary: New Mexico Geological Society Guidebook, 34th Field Conference, Socorro Region II, pp. 197-204.

_____, 1983b, Nomenclature for Cenozoic Rocks of the Northeast Mogollon-Datil Volcanic Field, New Mexico: New Mexico Bureau of Mines and Mineral Resources Stratigraphic Chart 1.

Osburn et. al 1986

Rowan, L. C., and Lathram, E. H., 1980, Mineral Exploration in Remote Sensing in Geology, Siegal, B. S., and Gillespie, A. R., eds., John Wiley & Sons Inc., p. 553-606.

Segal, D. B., 1983, Use of Landsat Multispectral Scanner Data for the Definition of Limonitic Exposures in Heavily Vegetated Areas: Economic Geology, Vol. 78, no 4, p. 711-722.

Sillitoe, R. H., and Bonham, H. F., Jr., 1984, Volcanic Landforms and Ore Deposits: Economic Geology, vol 79, no 6, p. 1286-1298.

Smith, R. L., 1960, Ash Flows: Geological Society of America Bull., vol 71, p. 795-842.

Smith, R. L., and Bailey, R. A., ???, Resurgent Cauldrons: U.S. Geological Survey Studies in Volcanology, ? p 613-662.

Snead, R. E., 1979, Landforms in New Mexico in Maps: Williams J. I., and McAllister, P. E., eds., Technology Application Center, U.N.M., p. 6-7.

Sparks, R. S. J., Self, S., and Walker, G. P. L., 1973, Products of Ignimbrite Eruptions: Geology, Vol. 1, p. 115-118.

Vincent, R. K., and Rouse, G., 1977, Landsat Detection of Hydrothermal Alteration in the Nogal Canyon Cauldron, New Mexico: International Symposium Remote Sensing Environment, 11th, Ann Arbor, April 25-29, 1977, Proc., p. 579-590.

Vink, G. E., Morgan, W. J., and Vogt, P. R., 1985, The Earths Hot Spots: Scientific American, vol 252, no 4, p. 550-57.

Walker, G. P. L., 1985, Origin of Coarse Lithic Breccias Near Ignimbrite Source Vents: Journal of Volcanology and Geothermal Research, Vol. 25, p. 157-171.

Willard, M. E., 1957, Reconnaissance geologic map of the Luera Spring thirty-minute quadrangle: New Mexico Bureau of Mines and Mineral Resources Geologic Map 2.

Williams, H., and McBirney, A. R., 1979, Volcanology: Freeman, Cooper and Company, San Francisco CA 94133, 397 p.

This thesis is accepted on behalf of the faculty of the Institute by the following committee:

Advisor

DEC 0 5 1986

Date